Dissertation

submitted to the
Combined Faculties for the Natural Sciences and for Mathematics
of the Ruperto-Carola University of Heidelberg, Germany
for the degree of
Doctor of Natural Sciences

Regulation of Telomere Length and Organisation in Human Skin Cells *in vitro* and *in vivo*

presented by
Graduated Engineer of Biology Damir Krunic
2008

Dissertation

submitted to the
Combined Faculties for the Natural Sciences and for Mathematics
of the Ruperto-Carola University of Heidelberg, Germany
for the degree of
Doctor of Natural Science

Presented by
Graduated Engineer of Biology Damir Krunic
Born in: Slavonski Brod, Croatia
Oral-examination: .....

2008

Regulation of Telomere Length and Organisation in Human Skin Cells *in vitro* and *in vivo*

Referees: Prof. Dr. Thomas Efferth
Prof. Dr. Petra Boukamp

The present doctoral thesis has been carried out in the Department “Genetics of Skin Carcinogenesis” at the German Cancer Research Center, Heidelberg, under supervision of Prof. Dr. Petra Boukamp.

Herewith, I declare that I am the sole author of the submitted dissertation and made no use of any sources or help apart from those specifically referred to.

_____ _____

(Date) (Signature)

Acknowledgements

There are too many people I would like to acknowledge, without their help and support this thesis would never come to exist.

First of all, I would like to thank to Prof. Dr. Thomas Efferth for supervising my thesis at the Ruperto Carola University of Heidelberg.

I especially want to thank to Prof. Dr. Petra Boukamp for being a great supervisor at the German Cancer Research Centre. It is not always possible to find a position in a good group that is working exactly on the subject you are interested in; thank to the fact that Petra gave me her trust - it was possible for me.

Each good group is, of course made out of good members, and I would like to thank those present and past, colleagues and friends, for their help and advice, as well as for the good working atmosphere that never lacked in the Boukamp´s lab, namely; to Sharareh Moshir for the help in my first steps in the lab, to Karin Greulich-Bode for being a great FISHing guide and proof-reader of the thesis, to Hans-Jürgen Stark for the help with immune staining and a healthy humour, to Hermann Stammer, Katrin Schmidt and Iris Martin for very professional technical assistance. Further thanks to Mara Amoros, Berit Falkowska-Hansen, Katrin Wischerman, Karston Böhnke, Sonja Muffler, Felix Bub, Sybille Ermler, Sabine Rosenberger, Susanne Buschke, Jutta Laykauf, Christine Baderschneider, Sabrina Gundermann, Pavle Krsmanovic, Petra Sanders, and Susanne Popp. Thanks also to Christa for beautiful immune stainings, to Melanie and to Dirk, and to Müller and Franke group for being good helping neighbours on the floor.

Special thanks to my colleagues and friends from the university in Croatia that were PhD students at DKFZ and EMBL, namely Alen, Josipa, Vibor, Ana, Moki, Kreso, Filip, and there associates; Andreas, Timo, Dilem, and to Jean, Zoran, Snjezana and others that were very helpful from the beginning, and made my living abroad much easier. Fruitful exchange of experience from our two institutes was often subject of our meetings in Untere Straße.

Finally, biggest thanks to my wife, first of all for deciding to became one, although she was fully aware of all the good and bad sides of the scientific career. She was and still is a great support, like she promised – in good and bad. Thanks also to my family, parents, brothers and friends in Croatia – it is always nice to know that even if no experiment works, and if everything goes wrong, at least vacation with all of them will be great.

To Roko,
my newborn son.

Abstract

Telomeres are specialized DNA-protein structures at the ends of the linear chromosomes that form protective caps. They are composed of multi-fold double-stranded 5'-TTAGGG-3' repeats and a 3' single stranded overhang that loops back and invades the duplex region. The so called T-loop structure is stabilized by a number of associated proteins that protect the DNA against degradation and hinders the cellular machinery to recognize the ends as broken DNA, thus being essential for chromosomal integrity. Investigating the three-dimensional (3D) telomere distribution we now show that telomeres of the immortal HaCaT keratinocytes are distributed in distinct non-overlapping territories within the inner third of the nuclear space in interphase cells and extend more widely during mitosis. This distinct localization is abrogated in a HaCaT variant that constitutively expresses the c-Myc onco-protein. Telomeres in HaCaT-myc cells form aggregates (TAs) that are accompanied by an overall irregular telomere distribution in interphase. Since this TA formation also leads to clustering of the respective chromosomes and TA formation is present during mitosis, TAs most likely contribute to genomic instability by forcing abnormal chromosome segregation. As a first step to approach the mechanism of TA formation we compared the difference in nuclear protein expression between HaCaT and HaCaT-myc cells by two-dimensional polyacrylamide gel electrophoresis. Out of 30 differentially expressed proteins, the most promising candidate was Matrin 3, a nuclear matrix protein that, being reduced in HaCaT-myc cells, suggests for a mechanism involving incorrect adhesion to the nuclear matrix.

The most essential function of the telomeres is their role as protective caps and thus their role in guaranteeing chromosomal integrity. Telomeres shorten with each replication cycle (end-replication-problem) and accordingly, telomere shortening is supposed to be a major cause of aging in proliferatively active tissues. To investigate the role of telomere loss for skin aging *in situ*, we developed a 3D deconvolution microscopy based Q-FISH/immunofluorescence technique on individual cells in tissue sections. When investigating skin from different-age donors, we found that similar as for dermal fibroblasts and another non-proliferative cell type in the epidermis, the melanocytes, also the epidermal keratinocytes only show a minimal age-dependent telomere decline. Thus age-dependent telomere loss appears largely neglectable. However, we found significant inter-personal differences and most strikingly, intra-personal variations in telomere lengths between similar sites of the epidermis. Moreover, in 10 of 30 samples of normal skin, preferentially from sun exposed sites of elderly donors, we identified regions within otherwise normal looking epidermis with significantly shorter telomeres. Though size and number of these micro-lesions as well as amount of telomere shortening varied, all enclosed various basal and suprabasal differentiated cells. Most importantly, they were all characterized by expression of the p53 tumour suppressor gene and 53BP1 foci co-localizing with telomeres. Since the latter are representative for DNA double strand breaks and when co-localized with telomeres represent critically short uncapped telomeres, these date demonstrate that in these micro-lesions the telomeres are dysfunctional and likely represent stages of genomic instability. Such distinct areas can only be maintained when damage has occurred in a stem cell. We, therefore, postulate that damage did not cause cell death but was repaired and lead to a decreased telomere length. This reduced telomere length was then transmitted to the daughter cells. Thus each micro-lesions most likely represents the space of one stem cell compartment.

We also identified shorter telomeres in skin from heavily sun-exposed individuals and in several skin sections in sites closer to the surface (outside) as compared to more protected areas of the epidermis (deeper parts of the rete ridges, deeper parts of the hair follicles). Since we further show that in skin from 16 volunteers irradiated with UVA, UVB, or a combination of UVA and UVB, distinct telomere shortening was visible already 3 days post irradiation, UV radiation is clearly a responsible factor for accelerated telomere loss in human skin. Another factor may be forced oxidative damage because also chronic and to a lesser extend acute wounds showed distinct telomere shortening.

Finally, we demonstrate for the first time a population of rare cells within the epidermis which have the "longest" telomeres and which likely represent the stem cells. These cells are distributed rather randomly throughout the basal layer. Furthermore, when cultured and replated in organotypic cultures they re-establish as stem cells in the newly developing epidermis. Thus, telomere length is a valuable marker for stem cells and it is damage rather than replication-dependent telomere shortening that leads to significant shortening and potential sites of genomic instability in human skin.

Zusammenfassung

Telomere sind spezialisierte DNA-Proteinstrukturen an den Enden der linearen Chromosomen, die aufgrund ihrer Länge und Struktur als schützende Endkappen die Chromosomenstabilität garantieren. In der vorliegenden Arbeit konnte nun gezeigt werden, dass in adherent wachsenden Zellen (Keratinotzyten und Fibroblasten der Haut) die Telomere in allen Phasen des Zellzyklus eine ganz spezifische Verteilung aufweisen. Die damit verglichenen HaCaT-myc Zellen, die aufgrund der konstitutiven Expression des c-Myc Onkogens sog. Telomer Aggregate (TAs) enthalten, zeigen dagegen eine generell veränderte Verteilung. Besonders bemerkenswert war, dass die TAs auch während der Mitose erhalten blieben und in Anaphase Zellen meist nur in einer der Tochterzellen nachweisbar waren oder dass das gesamte TA in Mikrokernen ausgeschleust wurde. Diese Befunde deuten darauf hin, dass TAs zu chromosomaler Missverteilung führen und damit ein möglicher Grund für die Entstehung numerischer Aberrationen sind.

In einem ersten Schritt den Mechanismus zu ermitteln, der zur TA Bildung führt, haben wir die Kernproteine der HaCaT und HaCaT-myc Zellen mit Hilfe der zweidimensionalen Polyacrylamidgel Elektrophorese verglichen. Von 30 unterschiedlich exprimierten Proteinen war das Zellmatrixprotein Matrin 3, der aussichtsreichste Kandidat, da es in den HaCaT-myc Zellen deutlich reduziert war und dies auf eine inkorrekte Adhesion der Telomere an die nukleäre Matrix hinweist.

Wie die Telomerorganisation so spielt auch die Telomerlänge für die chromosomale Stabilität eine wesentliche Rolle. Telomere werden mit jedem Replikationszyklus kürzer (Endreplikationsproblem) und deshalb geht man davon aus, dass Telomerverkürzung die Hauptursache für die Alterung von proliferativ aktiven Geweben ist. Zur Untersuchung der Rolle des Telomerverlustes bei der Alterung der Haut *in situ*, haben wir eine *3D Deconvolutionsmikroskopie-basierte Q-FISH/immunfluoreszenz Technik* entwickelt, die es erlaubt, die verschiedenen Zellen zu identifizieren und ihre Telomere individuell zu analysieren. Mit dieser Methode können wir nun zeigen, dass in der Haut von Spendern aus verschiedenen Altersgruppen die Telomere der dermalen Fibroblasten (teilen sich nur selten) aber gleichermaßen auch die Telomere der ständig proliferierenden epidermalen Keratinozyten eine nur minimale Verminderung der Telomerlänge zeigen. Somit scheint ein Alters-abhängiger Telomerverlust als Grund für die Hautalterung weitgehend vernachlässigbar. Dagegen zeigten unsere Untersuchungen aber signifikante Unterschiede zwischen Spendern gleichen Alters und unerwarteter Weise auch innerhalb eines Spenders. Besonders auffällig waren „Mikroläsionen“, Areale mit Zellen mit extrem kurzen Telomeren umgeben von Zellen mit normaler Telomerlänge. Interessanterweise waren diese Bereiche auch durch Expression des Tumorsuppressorgens p53 und durch 53BP1 Fozi charakterisiert, die mit den Telomeren ko-lokalisierten. Letzteres ist wiederum charakteristisch für ungeschützte Telomere (repräsentieren nun Doppelstrangbrüche), und weist auf stark geschädigte Zellen hin, die höchstwahrscheinlich aufgrund kritisch kurzer Telomere genomisch instabil geworden sind und so eine mögliche erst Vorstufen von Hautkrebs darstellen.

Da diese Bereiche häufig in Haut von stark Sonnen-exponierten Arealen nachweisbar waren, haben wir dann gezielt Haut nach definierter UV-Exposition untersucht: Hierbei zeigte sich, dass, wenn gleichzeitig mit UVA und UVB bestrahlt wurde, in der Tat bereits nach 3 Tagen eine deutliche Telomerverkürzung vorlag,. UVA oder UVB alleine waren dagegen deutlich weniger effektiv. D.h. UV Strahlung scheint ein wesentlicher Faktor für vorschnelle Telomerverkürzung in der Haut zu sein. Für diese Interpretation sprechen auch Befunde, dass die Telomere in Bereichen, die weiter entfernt von der Oberfläche lagen (im unteren Teil der Rete Ridges, oder im unteren Teil der Haarfollikel) und damit gegenüber Strahlung besser geschützt waren, deutlich länger waren. Ein weiterer Faktor für vorschnelle Telomerverkürzung könnte massive oxidative Schädigung sein. So fanden wir in chronischen Wunden eine massive Telomer-verkürzung, während akute Wunden eine deutlich geringere Verkürzung aufwiesen.

Obwohl die Größe der Mikroläsionen als auch der Umfang der Telomereverkürzungen variierte, waren in allen Fällen die basalen wie auch die suprabasalen, differenzierenden Zellen betroffen. Dies ist nur möglich, wenn die Schädigung (Telomerbruch) in einer Stammzelle erfolgt ist und diese die verkürzten Telomere nun an alle Tochterzellen weitergibt. Somit stellt jede Mikroläsion wahrscheinlich ein Stammzellkompartiment dar. Um die Rolle der Telomere in den Stammzellen noch weiter zu charakterisieren, haben wir schließlich die Basalschicht der Epidermis im Detail untersucht. Diese Studien zeigen nun zum ersten Mal, dass es einzelne Zellen gibt, die längere Telomere aufweisen und wahrscheinlich Stammzellen sind. Diese Zellen liegen „zufällig“ in der Basalschicht verstreut. Nach Kultivierung und Wiedereinsetzung in organotypische. Kulturen reetablieren sie sich als Stammzellen auch in der neu sich bildenden Epidermis. Damit ist die Telomerlänge ein neuer wertvoller Marker für die Identifizierung der Stammzellen und es ist ihre exogene Schädigung und nicht die Replikation, die zu einer signifikanten Telomerverkürzung und damit zu potentieller genomischer Instabilität in den humanen Keratinozyten führen kann.

List of abbreviations

%	Percent
°C	Celsius degree
µg, µm,	Micro-gram, -meter
µl, µM	Micro -litter, -molar
3D OTC	Three dimensional organotypic co-cultures
3D	Three-dimensional
A	Adenine
a.u.	Arbitrary units
A_{260}	Absorbance on Λ =260 nm
ALT	Alternative lengthening of telomeres
bp	base pairs
BrDu	Bromo-deoxyuridine
C	Cytosine
CA IX	Carbonic anhydrase IX
CCD	Charge-coupled device
CO_2	Carbon dioxide
CPD	Cyclobutane pyrimidine dimer
CRBCs	CPD retaining basal cells
Cy2	Cyanine fluorochrome
Cy3	Indocarbocyanin fluorochrome
Da	Dalton (molecular size U)
DAPI	4´-6-Diamidino-2-phenylindol
ddH_2O	Double-distilled water
DMEM	Dulbecco's modified Eagle's medium
DNA	Deoxyribonucleic acid
DSB	Double strand break
EDTA	Ethylene-diamine-tetra-acetat
FACS	Fluorescence activated cell sorting
FCS	Foetal calf serum
Fig.	Figure
FISH	Fluorescence *in situ* hybridization
FITC	Fluorescein isothiocyanate
g	Gram
G	Guanine
h	Hour
HaCaT	Human adult calcium temperature (keratinocyte cell line)
HaCaT-myc	myc transfected HaCaT
HCl	Hydrochloric acid
HF	Hair follicle
hTERT	Human telomerase catalytic subunit
hTR	Human telomerase RNA
ID	Identification number
IUdR	Iododeoxyuridine
IFE	Interfollicular epidermis
kb	Kilobase
LRC	Label retaining cell
M, N	Molar, normal
mA, mg, mm	Milli-ampere, -gramm, -meter
MCSP	Melanoma associated chondroitin sulphate proteoglycane
MEM	Modified Eagle's minimal essential medium
Mg^{2+}	Magnesium ions
min	Minute
ml, mM	milli-litres, -molar
Na	Sodium
NaCl	Sodium chloride
NaOH	Sodium hydroxide
ng, nm	Nano-gramm, -meter
No.	Number of
$ONOO^-$	Peroxynitrite
PBS	Phosphate buffered saline
PD	Population doubling
PD	Population doublings
pH	Measure of the acidity or alkalinity of a solution
RNA	Ribonucleic acid
RNase	Ribonuclease
RNP	Ribonucleoprotein
ROS	Reactive oxygen species
rpm	Rotation per minute
RR	Rete ridges
rt	Room temperature
SCC	Squamous cell carcinoma
SDS	Sodium dodecyl sulphate
SI	Signal intensity
T	Thymine
TA	Telomeric aggregate
TACs	Transit amplifying cells
TL	Telomere length
T-loop	Telomeric loop
TRF1,2	Telomeric repeat binding factor 1, 2
TRFL	Terminal restriction fragment length
Tris	Tris-(hydroxymethyl)-aminomethan
Triton X-100	Ocylphenol-polythylenglycol ether
TSI	Telomere signal intensity
TTS	Telomere territories
Tween 20	Polyoxyethylen-sorbitanmonolaurat
U	Unit
UV	Ultraviolet light
V	Volt
vs.	*Versus*
α	Level of significance
Λ	Wave length in nm
Q-FISH	Quantitative fluorescence *in situ* hybridization

TABLE OF CONTENTS

1. Introduction

1.1 The Telomere structure

Modern interest in telomeres has its roots in experiments carried out in the 1930s by Hermann J. Müller, and Barbara McClintock. Working separately and with different organisms, both investigators realized that chromosomes bore a special component at their ends that provided stability. Müller coined the term "telomere“, from the Greek for "end" (telos) and "part" (meros). He realized that upon X-ray irradiation, some structural chromosomal changes are possible, but the natural chromosome ends are never involved in these rearrangements (Müller, 1938). McClintock noted that without these end caps, chromosomes stick to one another, undergo structural changes and misbehave in other ways. “These activities threaten the survival and faithful replication of chromosomes and, consequently, of the cells housing them” (McClintock, 1941). It was not until 1978 however, that the precise makeup of the telomere was determined when it was found that the telomeres in *Tetrahymena thermophila* contained an extremely short, simple sequence of Thymines (T) and Guanines (G) -TTGGGG- repeated 20-70 times (Blackburn and Gall, 1978).

1.1.1 The Telomere sequence

Scientists have described the telomeres in different animals, plants and microorganisms, and similar as those of *Tetrahymena*, virtually all telomeres contain repeated short subunits rich in T and G nucleotides.

Telomeric repeats can be sorted into two basic groups; regular ones, consisting of perfect tandem repeats of a fixed repeat unit sequence, and irregular ones, consisting of length or sequence variations of a basic repeat unit (Table 1).

Table 1: Some examples of irregular and regular telomeric repeats

Organism	Irregular telomere repeat sequence (5´-3´)
Tomato	TT(T/A)GGG
Paramecium	TT(T/G)GGG
S. cerevisiae	$TG_{(1-3)}$
	Regular telomere repeat sequence (5´-3´)
Tetrahymena	TTGGGG
Arabidopsis	TTTAGGG
Homo sapiens	TTAGGG

However, regardless of regularity and the number of telomeric repeats, some characteristics are common for all telomeres; one strand of the tandemly repeated telomeric DNA sequence is characterized by containing clusters of guanine (G) residues, so called G-rich strand, and a complementary cytosine (C), C-rich strand. The G-rich strand is always found at the 3' end of each chromosomal DNA strand, and at each end it protrudes beyond the complementary C-rich strand (Klobutcher, 1981). There are few exceptions to this rule; *Drosophila melanogaster* for example has retrotransposons and mosquito *Anopheles gambiae* and onion *Allium cepa* contain complex-sequence tandem repeats instead of typical telomeric sequence (reviewed in McEachern *et al*., 2000).

In most species, telomeric sequences have changed very little over evolutionary time, which indicates the importance of the function, and possibly the most crucial function of telomeric repeats is to serve as binding sites for proteins that together with the telomeric DNA contribute to protective capping of the chromosomal ends.

1.1.2 Telomeric proteins

A number of proteins were identified that directly, or indirectly - via other proteins - interact with the telomeric DNA. Six of them are abundant at chromosome ends and do not accumulate elsewhere. They are present at telomeres throughout the cell cycle, and their known function is restricted to telomeres. These are double-stranded telomere repeat-binding factors TRF1 and TRF2, and a single-stranded binding POT1 that directly recognize TTAGGG repeats, and are interconnected with TIN2, TPP1, and Rap1, forming a large-molecular-mass complex that could be co-purified and is referred to as the mammalian telosome, or shelterin (Houghtaling *et al*., 2004; de Lange, 2005) (Figure 1).

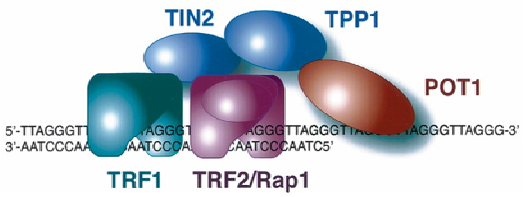

Telomere proteins	
Telomeric-repeat-binding factor	TRF1
Telomeric-repeat-binding factor 2	TRF2
TRF1-interacting nuclear factor 2	TIN2
TRF2-interacting telomeric RAP1	RAP1
Putative telomere-end-binding protein	POT1
Binding protein of POT1	TPP1

Figure 1: Schematic of telomere protein complex, so called telosome, or shelterin; Proteins that are always present at mammalian telomeres (taken from de Lange, 2005), and the list of their full names.

TRF1 and TRF2 form homo-dimers and are described as negative regulators of telomere length as shown by over-expressing TRF1 and TRF2 in various cell types. TRF2 is thought to be present predominantly at the loop junction and is now believed to be a key protein for remodelling telomeres into telomere-loop (T-loop), a higher order structure of telomeres (reviewed in de Lange, 2002).

1.1.3 Higher order telomere structure

Telomeres with associated proteins form a higher order structure. So fare two models are discussed; the T-loop model and the G-quadruplex structure.

By using electron microscopy Griffith *et al*. (1999) showed that artificial telomeric DNA with TRF2, as well as fixed, precipitated telomeric DNA from primary cultures, is able to form duplex loops, so called T-loops. According to the model, double stranded DNA is folded in the T-loop, while a single stranded 3'-overhang undergoes limited strand invasion to form a displacement loop (D-loop) (Figure 2).

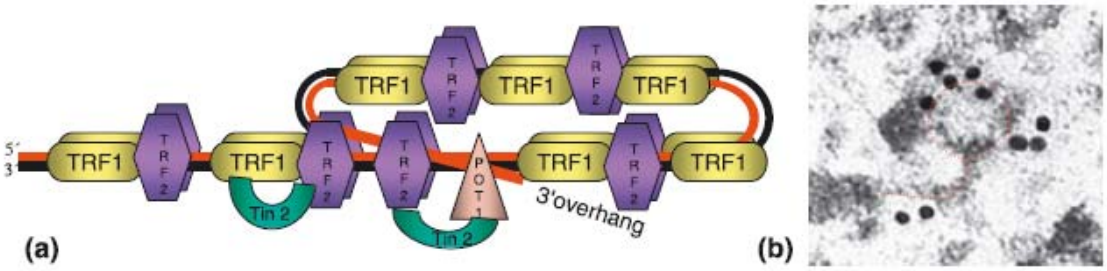

Figure 2: Telomere model of the: (a) T-loop structure occupied by some of telomeric protein components, **(b)** Immune electron micrograph of a telomere loaded with TRF2-tagged gold particles, resembling a T-loop structure (taken from Boukamp and Mirancea, 2007)

T-loops contain only telomeric sequences, and the loop size is proportional to the telomere length of human and mouse cells. From the studies on lower eukaryotes, as the yeasts and protozoan, up to vertebrates like chicken, mouse and human there is compiling evidence that chromatin looping is a common characteristic in most eukaryotes (reviewed in de Lange, 2002).

Crystal analysis of telomeres, however, resulted in an alternative model. This proposed the formation of four-stranded G-rich quadruplex structures of the telomeric sequence. This special type of DNA folding can be inter- , and intramolecular. Two (dimeric) or four (unimolecular) separate strands associate together and form intermolecular quadruplexes. Intramolecular quadruplexes are formed by the folding of either two or four consecutive repeats, such as the four repeats of human telomeric DNA in d[AGGG(TTAGGG)$_3$] (Smith, 1992; Parkinson, 2002).

It was shown that quadruplex structures could negatively influence recruitment of TRF2 and POT1 to the telomeric complex, and possibly cause dysfunctional telomeres (Yanez, 2005). Therefore, development of therapeutic strategies designed to stabilize telomeric ends as G-quadruplex structures using specific small molecules, appears to be a promising approach since it could destabilize telomere maintenance in tumour cells (reviewed in Raymond *et al*., 2000; Boukamp and Mirancea, 2007).

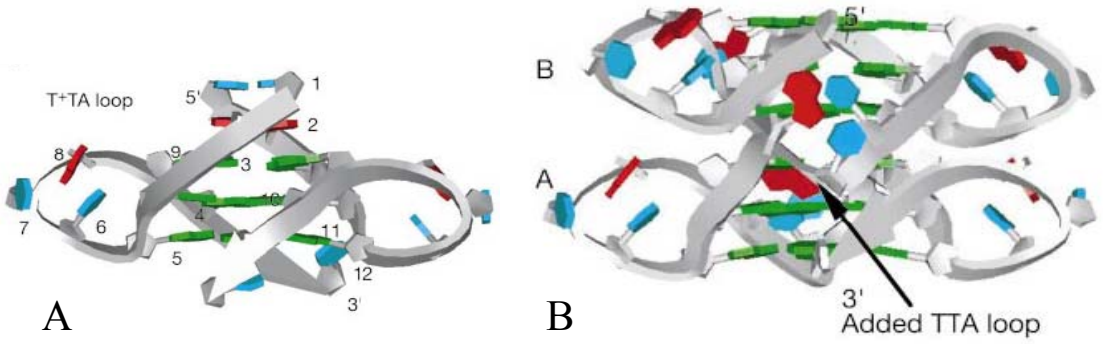

Figure 3: 3D models of G-quadruplex structure.
A) Side view of the quadruplex with the phosphate sugar backbone ribbon (gray) showing 5'–3' directionality. The guanines are green, thymines and modified uracils are blue, and adenines are red. **B)** Model showing how two (and possibly more) G-quadruplex repeats could be stacked 3' to 5'. The upper stack has been rotated relative to the lower quadruplex, with a TTA loop modelled between the two to link them (taken from Parkinson, 2002).

1.2 Three-dimensional distribution of telomeres in the nucleus

In addition to the telomere structure, spatial organization of telomeres may play a significant role in genomic integrity; however, their three-dimensional (3D) distribution within the nucleus is still controversially discussed. The first organization of telomere distribution was suggested by Rabl (1885), who proposed that the anaphase chromosome configuration would persist into the subsequent interphase. According to Rabl, centromeres are located at the nuclear envelope, the chromosome arms folded together, and the telomeres located at the opposite side of the nuclear envelope. *In situ* staining for centromeres and telomeres confirms that this arrangement is common to wheat and some other plants. The Rabl distribution was also found in some insects. However, non-Rabl chromosome topography was reported for mammalian cell types (Moroi *et al*., 1981; Brinkley *et al*., 1986).

In nuclei of murine Dorsal Root Ganglion cells more then 40% of telomeres were associated with the nucleolus. The remaining signals were localized between the nucleolus and the nuclear membrane (Billia and de Boni, 1991). In mouse lymphocytes telomeres were found throughout the entire nucleus (Vourc`h *et al*., 1993). In the human sperms the nuclear architecture is characterized by clustering of the 23 centromeres into a compact chromocenter positioned in the nuclear interior. The ends of the chromosomes are exposed to the nuclear periphery where telomere sequences of the chromosome arms are joined into dimers (Zalensky *et al*., 1995).

Weierich *et al*. (2003) reported on differences in telomere distribution in mouse and human lymphocytes; in mouse nuclei, the telomeres clustered preferentially at the nuclear periphery while in human lymphocytes most clusters were located in the nuclear interior.

So fare the reason for the observed differences in telomere organisation is unclear, and it remains to be seen weather the cell type, tissue-specific, and species-specific organization of the chromatin could be responsible for the observed differences between the normal cells. In addition to the normal cells, also tumour cells were analysed for their telomere distribution. In a study on glioma cells, it was proposed that positional changes for telomeres as well as other chromosome domains probably reflect fundamental molecular and structural alterations that create genomic instability. Interestingly, in the same study signals much larger than the individual telomeres were

identified obviously representing close apposition of several telomeres (Manuelidis, 1994).

1.2.1 Telomere interactions in the nucleus

1.2.1.1 Telomere clustering in meiosis

During meiosis chromosome ends attach to the inner nuclear envelope and cluster in almost all organisms studied, regardless of the size of their genomes (Scherthan, 2001). It was described for fission yeast that at the beginning of zygotene phase of meiosis, or just before, the chromosomes form the so-called "bouquet" and telomeres are clustered. In maize, bouquet formation is initiated during a conspicuous change in chromatin morphology at the leptotene-zygotene transition. The bouquet persists through zygotene in some organisms and through early pachytene in maize and certain other organisms. Telomere clustering correlates with the meiotic recombination between homologs, which is resolved by mid-pachytene (reviewed in Harper *et al*., 2004). After pachytene telomeres are no longer clustered therefore, this type of interactions is only transient and specific for meiosis.

1.2.1.2 Telomeric associations in normal and tumour cells

Another type of temporary interactions between telomeres was observed in slowly proliferating cells (i.e. a prolonged G1 phase), replicatively quiescent or terminally differentiated normal human cells. The number of telomeric associations in interphase nuclei was described to be more dependent on the cycling status of the cell, rather than on individual telomere length. Interestingly, end associations were only rarely present in the interphase nuclei of rapidly cycling, telomerase-positive immortalized human cells with shortened, but stable telomere lengths (Nagele *et al*., 2001).

Although telomere associations were observed in normal cells, translocations arising through apparent fusion of telomeres are rare in normal fibroblasts and lymphocytes. In contrast, telomere fusions can be detected in certain types of leukaemias and in some solid tumours where they correlate with translocations in neoplastic cells. The telomere fusions were not present in every cell but mostly observed in only 20-30% of the cells. Furthermore, it appeared to be at random, involving associations of a variety of chromosome pairs that were different in each cell (reviewed in Hastie and Allshire, 1989). However, what was not random was the role of telomere shortening in the

development of these telomeric associations and the subsequent genetic instability observed in a majority of tumour cells (Wan *et al*.,1999).

Therefore, due to shortening, the telomeres can become dysfunctional, two chromosomes fuse, they form end-to-end fusions, thus becoming dicentric chromosomes. If so, the two centromeres can be pulled to opposite spindle poles during mitosis, create an anaphase bridge that is resolved by chromosome breakage, which can cause loss of essential genes or loss of the entire chromosome (McClintock, 1941; Haber and Thorburn, 1984). The resulting broken ends can undergo subsequent fusions, perpetuating a breakage-fusion-bridge cycle (McClintock, 1941).

1.2.1.3 Telomeric aggregates

Finally, a telomere-dependant, but telomere-length-independent mechanism of genomic instability was proposed. Chuang *et al*. (2004) have observed that the telomeres are assembled in a highly defined position during the G2 phase, which they termed “telomeric disc”. This telomere distribution was distorted in some tumour cells due to the formation of large telomeric associations termed “telomeric aggregates” (TA). Different size, shape and number of this complex structure of telomeric DNA was found to be present in tumour cells with known deregulated c-Myc. Furthermore, it could be shown that a single transient induction of the c-Myc oncogene in immortalized mouse B lymphocyte cell lines resulted in the formation of TAs, which was followed by structural and numerical chromosomal aberrations (Louis *et al*., 2005). As a potential mechanism the authors proposed that because of the TA formation also the chromosomes have altered their normal location. In fact, an overlap of chromosomal territories and finally translocations upon TA induction can easily occur since different chromosomes now come into such close vicinity that they intermingle and if breakage occurs can now exchange chromosomal material (reviewed in Boukamp *et al*., 2005).

1.3 Telomere length regulation

3D distribution and telomere-length-independent interactions of telomeres may play a significant role in genomic integrity; however, further analysis is required to determine precisely the mechanism responsible for the formation of telomere aggregates. Telomere-length-dependent interactions were studied more extensively, and it is widely accepted that critical shortening of telomeres can cause genomic instability.

How does it come to critically short telomeres? Until the 1960s, it was believed that all cultured cells were potentially immortal, as it was the case for several populations of apparently immortal cancer cell populations – best exemplified by HeLa. It was then that Hayflick and Moorhead (1961) observed that cultured normal cells have a limited replication capacity. Human fibroblasts from different embryonic donors underwent a finite number of population doublings (PDs) - between 40 and 60. Also frozen cells at any PD level from 1 to 50 retained memory, so that the total number of PDs including those before and after freezing was in average 50, the so called Hayflick limit (reviewed in Hayflick, 2000). “Mitotic clock” which could be responsible for the Hayflick limit was not known until it was shown that telomere length decrease *in vitro* with each PD (Harley *et al*., 1990).

1.3.1 Telomere shortening *in vitro*

As proposed independently by Olovnikov (1971, 1973) and Watson (1972), DNA polymerase is not able to fully replicate the linear ends of DNA, and therefore with each replication cycle, a number of telomeric base pairs are lost. Indeed, as it was later confirmed on the same normal human diploid fibroblasts that Hayflick was using in his studies, mean telomere length decreased by 2 to 3 kilobase pairs during the entire *in vitro* lifetime (Harley *et al*., 1990). Telomere length progressively shortened due to the end replication problem and the cells finally arrest in a stage called replicative senescence.

Normal culture conditions gave a linear correlation of replicative history and telomere length, but mild oxidative stress on the other hand gave somehow different results. As exerted by culturing human WI-38 fibroblasts under 40% oxygen partial pressure, cell proliferation was irreversibly blocked in G1 phase of the cell cycle after one to three PDs with a clearly senescent phenotype. Southern blotting revealed an

increased telomere shortening rate from 90 bp per PD under normoxia to more than 500 bp per PD under hyperoxia. There are also indications for accumulation of single-strand breaks in the telomeres of nondividing fibroblasts irrespectively of culturing condition, although more pronounced under conditions of higher oxidative stress. From all of this it was concluded that oxidative stress is a major cause of telomere shortening, possibly more important than incomplete replication (von Zglinicki *et al*., 1995).

What ever the cause fore telomere shortening is, there is accumulating evidence when only a few telomeres tend to be short, these form end-associations (end to end fusions), leading to DNA damage signalling, which finally results in replicative senescence, a cellular growth arrest, also called the M1 stage (reviewed in Shay and Wright, 2005).

While *in vitro* culturing of human fibroblasts and lymphocytes resulted in a clear telomere length shortening due to the end replication problem, or factors such as oxidative stress, *in vivo* the rate of telomere loss with age is less clear (reviewed in Hodes *et al*., 1999).

1.3.2 Telomere length regulation *in vivo*

There are two mechanism identified that are capable of lengthening telomeres, and thus to compensate for the telomere shortening that would otherwise occur as a consequence of cell division; the telomere lengthening mediated by telomerase, and by Alternative Lengthening of Telomeres (ALT).

While telomerase is the dominant mechanism of the telomere length maintenance, ALT was found in some *in vitro* immortalized cells, as well as in 15% of all tumours, most of them of mesenchymal origin. It was not clear which mechanism is behind ALT until it was found that in *S. cerevisiae* the homologues recombination based pathway was involved in telomere length maintenance in rare survivors when telomerase was inactivated (Lundblad and Blackburn, 1993). This finding helped to reveal the recombination mechanism that is now accepted for the ALT mechanism in mammalian cells as well (reviewed in Neumann and Reddel, 2002).

1.3.2.1 Telomerase activity in somatic cells

Telomerase, a unique ribonucleoprotein polymerase is responsible for synthesising telomeric repeats and thus for telomere length maintenance. Telomerase can be classified as a reverse transcriptase, because its mechanism of action involves the copying an RNA template into DNA. It is an unusual reverse transcriptase, however, since it contains its own template RNA (TR) that together with a protein component (TERT) makes the core enzyme. Telomeric DNA is synthesized *de novo* in 5' to 3' direction by copying an RNA template sequence within the RNA moiety of telomerase. A multi-component ''telomere homeostasis'' system prevents the over-extension of telomeres. Protein–protein interactions among the telomere-associated proteins are important for this function (reviewed in Blackburn, 1992; 2005) (Figure 4).

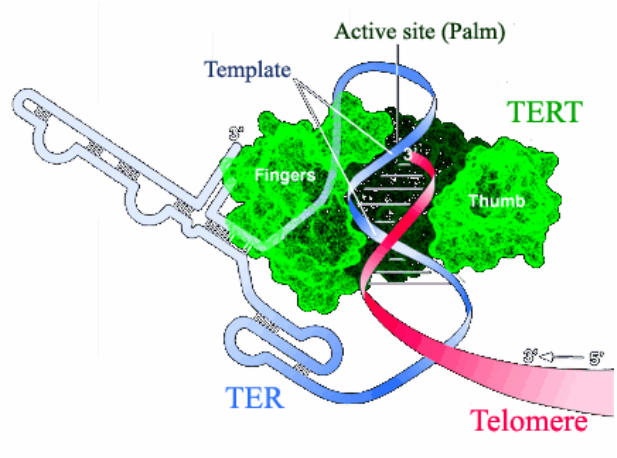

Figure 4: Schematic of telomerase structure at work; the telomerase enzyme complex contains an RNA template (TER, blue) and the catalytic protein component (TERT, green) which ads telomeric repeat sequences to the telomere DNA strand (red) (taken from http://en.wikipedia.org/wiki/).

High levels of telomerase activity are expressed in cells of the germ line. In these cells it is critical to maintain stable telomere length as this ensures the capacity for limitless replication. In somatic cells on the other hand, telomerase activity was not initially detected. More recently, a number of reports demonstrated that some somatic cells express high levels of telomerase under certain conditions (reviewed in Hodes *et al*., 1999). Lymphocytes express telomerase during development and retain the ability to express telomerase after maturation in response to antigenic challenges (Broccoli *et al*., 1995; Weng, 2002). B cells, for example undergo somatic hypermutation, followed by multiple cycles of clonal expansion. It might have been expected that the

differentiation of naive B cells would, therefore, be accompanied by progressive telomere shortening, reflecting the cell division that occurs. However, it was in fact observed that during differentiation telomeres were consistently longer than those of either precursor naive or finally differentiated B cells. Therefore, depending on the physiologic conditions, telomere length can actually increase during a period of active cell division (Wenig, 1995).

Besides the lymphopoietic tissue, regenerative epithelia were also found to be telomerase positive. Telomerase activity was found in all epithelia along the gastrointestinal tract (Bachor *et al*., 1999) as well as in the epidermis (Harle-Bachor and Boukamp, 1996; Taylor *et al*., 1996). Telomerase activity, therefore, may play an important role in the lifetime regenerative capacity of normal epithelium *in vivo*.

1.3.2.2 Telomeres and Telomerase in immortalized cell lines and tumours

Despite the compensating mechanisms for telomere shortening, it is nevertheless clear that telomeres shorten as a function of age (Rufer *et al*., 1999).

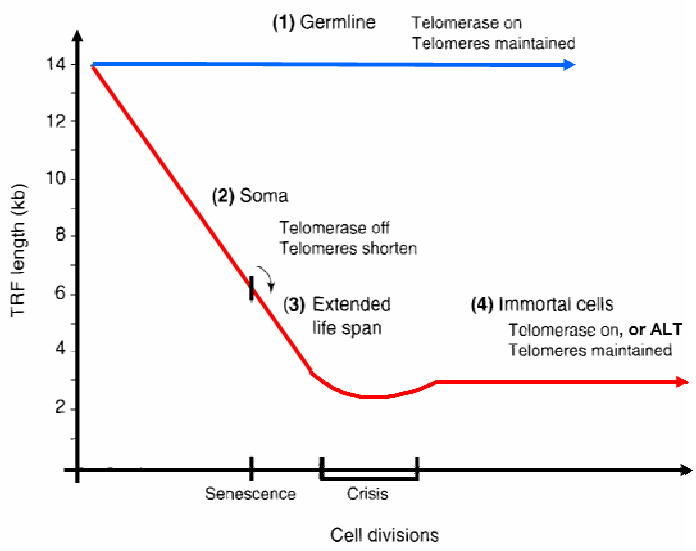

Figure 5: Simplified model of the telomere length regulation hypothesis.
(1) Telomerase is active in germline cells and required for telomere length maintenance. **(2)** Cells that lack telomerase activity shorten their telomeres with each cell division. **(3)** Viral oncogenes allow the bypass of senescence; further telomere shortening. The culture soon reaches crisis where most of the cells die. **(4)** Immortal clones that survive crisis reactivate telomerase, or ALT in ~15%, and telomere length is maintained (adapted from Autexier and Greider, 1996).

When cells reach the Hayflick limit and one or more telomeres become critically short this is proposed to trigger a p53 dependent DNA damage response and finally

cause senescence (M1 stage). Some viruses, like human papillomavirus 16 or 18, can extend the life span of cultured cells by binding to p53 and pRB and block the M1 mechanism. In the absence of cell-cycle checkpoint pathways cells bypass M1 senescence and telomeres continue to shorten eventually resulting in crisis (also called the M2 stage). Chromosome ends are 'uncapped', and chromosome breakage-fusion-bridge cycles can occur followed by mitotic catastrophe and a high fraction of apoptotic cells. In a rare M2 cell, telomere erosion is stopped by reactivation or up-regulation of telomerase, resulting in indefinite cell proliferation and immortalization (Autexier and Greider, 1996; reviewed in Shay and Wright, 2005).

1.4 Telomeres in human skin

The skin, larges human organ covering the entire body, is composed of different tissues; the epidermis that protects the body as an outermost barrier rests upon the basement membrane that joins the epidermis to the connective tissue – the dermis and the underlying subcutaneous fat. In contrast to the dermis, which mostly consists of extracellular matrix and quiescent fibroblasts, the epidermis is a multilayered, well-organised and constantly proliferative epithelium.

What is known about telomere length regulation in the skin?

1.4.1 Constant proliferation in epidermis requires telomere length maintenance by telomerase

The epidermis is a self-renewing tissue that remains proliferative throughout the human lifetime with a complete turnover of 26–42 days. Proliferation takes place in the basal layer. From there the keratinocytes migrate through several suprabasal layers where they undergo a continuous process of differentiation terminated in the formation of dead horn squames. These provide an efficient barrier to prevent water loss as well as to protect the body against insults such as bacterial infiltration or damage by UV-radiation (Leigh, 1994).

The high rate of proliferation necessary for the life long regeneration can result in a steady replication-dependent loss of telomeric DNA, and finally senescence-dependant growth arrest. Interestingly, this does not happen in the skin and in other regenerative epithelia. They retain their replicative capacity, therefore, telomere length has to be

maintained which is normally accomplished by telomerase. Accordingly, it was demonstrated that telomerase activity is detectable in the epidermis of the skin; it is highest in the basal layer of the epidermis and little or none was present in suprabasal layers (Harle-Bachor and Boukamp, 1996). As the premature loss of proliferative capacity in the epidermis would be fatal, the basic telomerase activity was proposed to be involved in maintaining – not just the tissue's regenerative potential – but the tissue's integrity in total. Further support came from a number of later studies that confirmed similar telomerase activity in the renewable epithelia (Yokoyama *et al*., 1997; Nakayama, 1998; Bachor *et al*., 1999).

1.4.2 Telomere length in the skin

Despite telomerase activity, early studies demonstrated a statistically significant age-dependant telomere length decline. This was described for the total skin, and also separately for epidermis, and dermis. Nevertheless, in most studies the reported telomere loss per year was relatively low (ranging from 9 to 75 bp/year).

In the first report 21 skin samples of donors aged between 0 and 92 years were analysed and reported on an average shortening of 19.8 bp/years (Lindsey *et al*., 1991).

A second study investigated telomere length in three unrelated tissues of nine elderly patients (age range 73–95 years old) and found the most drastic shorting in leukocytes, but also in the skin, and in synovial tissue. Again, inverse relationship between donor age and telomere length was obtained with a shortening of 75 bp/year for the skin. Interestingly, comparing the telomere length in the different tissues from the same donor, suggested a strong genetically inherited determination of the telomere length regulation (Friedrich *et al*., 2000).

In both studies, by Lindsey *et al*. (1991) and Friedrich *et al*. (2000), the whole skin was analyzed, and only few samples were included. As the skin is composed of different tissues, and there could be large interpersonal differences in telomere length, it was necessary to analyse separately epidermis from dermis, and to include more samples. In a recent study, Nakamura *et al*. (2002) investigated 52 specimens and thus all were isolated epidermis only, collected at autopsy from subjects who died at ages between 0 and 101 years revealed an average reduction rate of 36 bp/year.

The largest and probably the most precise study so fare, with seventy-six specimens of epidermis from sun-protected sites and 24 specimens of epidermis from sun-exposed

sites, did not showed significant difference between two groups, but the aging associated significant telomere shortening of epidermis and dermis of 9 and 11 bp/year respectively, was found in the same samples. In six cases, epidermal specimens from sun-protected and from sun-exposed sites of the same individual were analyzed and the result showed unexpectedly longer telomeres in the epidermis of exposed skin which did not correlate with the proposed photo-aging of the skin (Sugimoto *et al*., 2006).

1.4.3 Damage on telomeres in the skin

As a major interface between the environment and the internal milieu, our skin is constantly exposed to exogenous and endogenous insults that threaten its genomic integrity and that can lead to changes at the molecular, biochemical, and cellular levels. Common insults on the skin include infectious agents, environmental pollutions and toxins, carcinogens, and ultraviolet (UV) irradiation (Goukassian and Gilchrest, 2004) and all of them can cause genetic damage, therefore, damage on telomeres as well.

1.4.3.1 UV damage on telomeres

It is known for 30 years now, that UV can form cyclobutane pyrimidine dimers (CPDs) as a direct damage on DNA, which is preferentially at dithymidine (TT) sites but can also be thymine-cytosine (TC) and cytosine- cytosine (CC) sites, and (6-4) photoproducts (Patrick and Snow, 1977). In early 90s it was shown that in addition to CPDs UV can also induce indirect, so called oxidative damage. UV causes the release of free radicals that result in perturbations of the cellular redox-equilibrium (Bose *et al*., 1990; Konishi *et al*., 1991). Hydroxyl radicals (·OH) have been found to be the main reactive oxygen species causing the formation of lipid radicals (Ogura *et al*., 1991), which is finally believed to be the principle source of oxidative stress *in vivo* (Renzing *et al*., 1996; reviewed in Ichihashi, 2003).

Interestingly, oxidants like H_2O_2, or UVA radiation plus riboflavin (photosensitizer), *in vitro* caused the damage on a DNA fragment containing the telomere sequence. Damage was specifically at the GGG in the telomere sequence, and included 8-oxodG formation. Human 8-oxodG-DNA glycosylase introduces a chain break in a double-stranded oligonucleotide specifically at an 8-oxodG residue. Therefore, the formation of 8-oxodG at the GGG triplet in the telomere sequence induced by oxidative stress could

participate in the accelerated telomere shortening, and potentially aging or even cancer (Fig. 6) (Oikawa and Kawanishi, 1999).

One third of the telomere single stranded overhang sequence TTAGGG is dithymidine, and half is triple guanine (G) residues, therefore, exposure to UV and/or to oxidative damage would be expected to introduce extensive damage into telomeres. This could destabilize the telomere loop structure and uncap the telomere, and finally activate a pathway common in DNA repair and apoptosis that is centrally involving the tumour suppressor protein and transcription factor p53 (Zhan *et al*., 1993), also known to be induced after experimental disruption of the telomere loop (Karlseder *et al*., 1999).

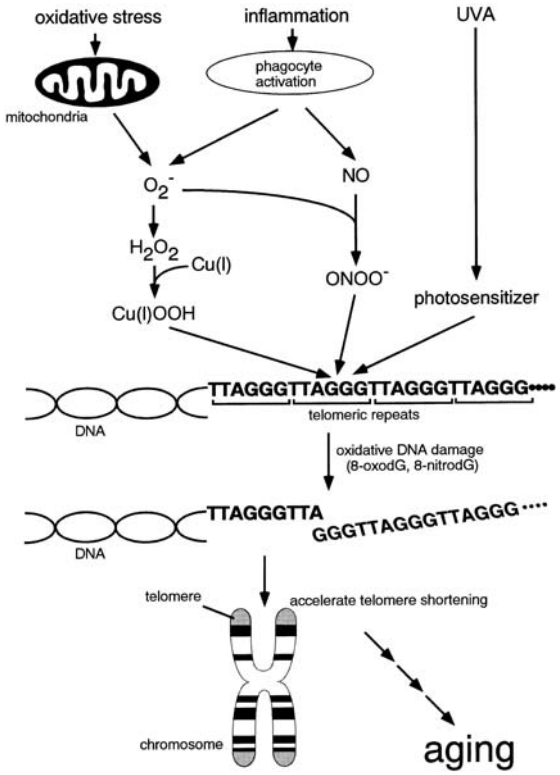

Figure 6: Schematic of mechanism of accelerated telomere shortening by oxidative stress. Taken from (Oikawa and Kawanishi, 2000).

1.4.3.2 Chronic inflammation and damage on telomeres

Inflamed tissue is havely populated with activated phagocytes which are important component of the immune protection, but they also cause some negative side-effects for the surrounding tissue. They produce reactive nitrogen NO and oxygen O_2^- species (ROS), which interact with each other, resulting in the formation of a highly reactive species, peroxynitrite ($ONOO^-$), at a very fast rate. It was demonstrated that $ONOO^-$

and 3-morpholinosydnonimine-*N*-ethylcarbamide (SIN-1), which generates NO and O_2^- simultaneously and continuously, caused DNA cleavage at every nucleotide even with a little dominance of guanines. The mechanism is again the same as previously described, and includes the formation of 8-oxodG, an oxidative product of guanine, with the only difference that it is this time not produced via UVA, but with $ONOO^-$ and SIN-1 (Figure 6) (Oikawa and Kawanishi, 1999).

Increased oxygen free radical generation is reported in chronic skin wounds; age related disorders in the heeling capacity of the skin, often characterized with the chronic inflammation. The available evidence suggests that the major impact of aging in the skin is in the dermal tissues, and it is know that fibroblasts within the dermis play a pivotal role in controlling wound healing responses. Therefore, it was suggested that chronic wound fibroblasts could demonstrate signs of senescence. On the contrary, there are studies that prove quite opposite; no signs of senescence, including no telomere shortening in fibroblasts originating from chronic wounds when compared to healthy ones from the same patient (Stephens *et al*., 2003).

1.4.4 p53 signalling and damage in the skin

Damage signalling through the p53 tumour suppressor protein pathway is known to occur after exposure to UV, or due to oxidative DNA damage. Experimental disruption of the telomere loop structure, the presence of T-oligos which are proposed to mimic exposure of the 3' telomere overhang, as well as entry into senescence also involve p53 signalling (reviewed in Kosmadaki and Gilchrest, 2004). Numbers of studies proposed the correlation of telomere shortening and p53 expression, however, very few actually show that cells with short telomeres *in vivo* are the ones that express higher amounts of p53. One report on the insulin-dependent diabetes mellitus that is known to generate reactive oxygen species (ROS), for example clearly shows that telomeres are shorter in cells expressing the p53 which, as suggested, impaired the growth reserve of the heart and can finally cause the heart failure (Rota *et al*., 2006).

There is also evidence on the presence of p53, and co-localization of p53 binding protein 1 (53BP1) foci with telomeres in baboon skin biopsies originating from older animals, but not in the post mitotic skeletal muscle where only a small fraction of myonuclei displayed coolocalization in both young and old animals (Jeyapalan *et al*., 2007).

53BP1 was described to be important part of a DNA damage repair, it becomes hyperphosphorylated after radiation and colocalizes with phosphorylated γH2AX in megabase regions surrounding the sites of DNA double strand breaks (DSB) (Ward *et al*., 2003).

A DNA damage response was also observed in the skin dysplastic nevi and in human lung hyperplasia, which included p53 accumulation, focal staining of p53 binding protein (53BP1) and histone γH2AX, as well as apoptosis. It was proposed that from its earliest stages, cancer development is associated with DNA replication stress (as occurs in preneoplastic lesions), which leads to DNA double-strand breaks, genomic instability and selective pressure for p53 mutations. Telomere attrition is hypothesised to contribute to DNA DSB formation, activation of the checkpoint and genomic instability (Gorgoulis *et al*., 2005)

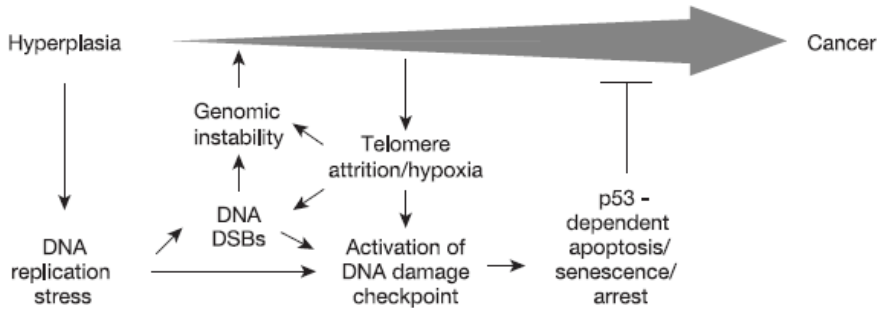

Figure 7: Model of aberrant stimulation of cell proliferation that leads to DNA replication stress, DNA DSBs, genomic instability, activation of the DNA damage checkpoint, and p53-dependent apoptosis. p53-dependent apoptosis suppresses expansion of the precancerous lesion (p53 tumour suppressor function) and provides selective pressure for p53 inactivation. Telomere attrition and hypoxia can also contribute to DNA DSB formation, activation of the checkpoint and genomic instability (adapted from Gorgoulis *et al*., 2005).

1.4.5 Search for stem cells in the human skin

When the skin becomes exposed to the insult, as it is UV irradiation or wounding, it has to regenerate the damaged regions. The epidermis maintains its life-long regenerative potential through a subpopulation of cells in the basal layer, known as epidermal stem cells. It is a small population of cells, 2 to 5 % of the basal cells, with unlimited capacity for self-renewal, which give rise to the rapidly proliferating transit

amplifying cells that after a number of divisions are destined to differentiate. Thus, in steady state epidermis the stem cells, although they have a large capacity for proliferation, actually divide infrequently (reviewed in Watt, 2002).

In search for new stem cell markers, a number of potential proteins were proposed. Some of them are protein markers as melanoma chondroitin sulphate proteoglycan (MCSP), β1 integrins, and carbonic anhydrase IX (CA-IX). In addition, as the stem cells are slow-cycling, they retain the radioactive label over a long period of time, which can be used as a marker in a mouse model (Bickenbach, 1981). Since *in vivo* radioactive labelling of human cells is not possible, alternatively long-term human skin equivalents are recently described as an alternative approach for searching the epidermal stem cells.

1.4.5.1 Label retaining cells in three-dimensional organotypic cocultures (3D-OTCs)

3D-OTCs are developed as *in vitro* skin equivalents to represent the major principles of skin biology, as they consist of epidermal keratinocytes growing on dermal equivalents (DEs). DEs are collagen hydrogels that are recently reinforced by modified hyaluronic acid fibers (Hyalograft-3D) and colonized with skin fibroblasts, producing genuine dermis-type matrix. This recent modification allowed formation of epidermal homeostasis in the long-term culturing of skin equivalents and for the first time provided proper experimental conditions for mechanistic studies of skin regeneration and homeostasis, as well as establishing a stem cell niche *in vitro* (Stark *et. al*., 2006). The protocol for labelling of the cells with 5-Iodo-2'-deoxyuridin (IUdR) and long-term culturing in 3D-OTCs was recently developed in our laboratory by Sonja Muffler *et al*. (personal comunication). It is a novel tool that enables us to further characterise label-retaining cells in the basal layer of human skin equivalents.

1.4.5.2 Melanoma chondroitin sulphate proteoglycan (MCSP) and carbonic anhydrase IX (CA-IX) as a potentional stem cell markers

There are reports that stem cells in the interfollicular epidermis are distinguished from other keratinocytes by high expression of β1 integrins and lack of expression of terminal differentiation markers. They divide infrequently *in vivo* but form actively growing colonies in culture. It was shown that those non-cycling, clonigenic keratinocytes with the highest β1 integrin levels in the interfollicular epidermis, also express MCSP. Therefore, it was proposed that MCSP could be a novel marker for

epidermal stem cells, which contribute to their patterned distribution by promoting stem cell clustering (Legg *et al*., 2003).

There is evidence that hypoxia promotes stem cell renewal *in vitro* as well as *in vivo*. It therefore seems reasonable that stem cell survival and hypoxia response are strictly connected at the molecular level. Hypoxia survival is characterized by induction of the hypoxia-survival gene CA-IX; therefore, localization of CA-IX expression in the skin may indicate position of the stem cells (Sansone *et al*., 2007).

1.4.5.3 Telomere length in stem cells

There are some reports on telomere length in a most naïve subpopulation of hematopoietic stem cells proposing that stem cells have in average one kb increased telomere length (Van Ziffle *et al*., 2003). They proposed that the telomere length could be used for enrichment of very rare precursors of hematopoietic and probably other tissues as well. There are other studies indicating the low level of telomerase activity or even absents in the majority of $CD34^{+}CD38^{lo}$ hematopoietic stem cells (Engelhardt, 1997; Yui, 1998). Thus, even stem cells, except for embryonal or germ stem cells, could have their telomere shortened during replicative ageing (Vaziri, 1994; Notaro, 1997), but possibly at a slower rate than in other somatic cells (reviewed in Hiyama and Hiyama, 2007). Nevertheless, there are very few studies of telomere length in tissues other than embryonic, germ or hematopoietic, and so fare there are no reports on telomere length in human interfollicular epidermal stem cells.

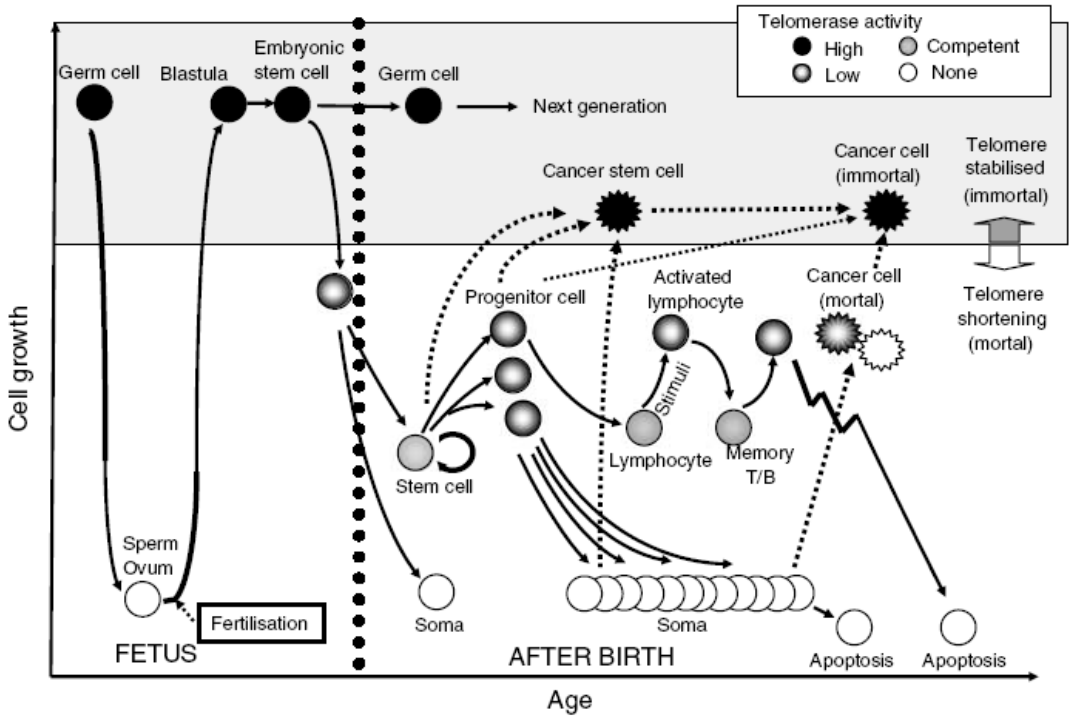

Figure 8: Model of telomere and telomerase dynamics in human stem cells. Telomerase is highly active in germ cells, but inactive in non-proliferating sperms and ova. It is then highly activated, but gradually decreases and diminishes in many cells after birth. In adult stem cells, the level of telomerase activity is low or undetectable, and upregulated in committed progenitor cells which have high reproducible activity in each tissue. Cancer stem cells can be derived from normal stem cells, progenitor cells, or possibly somatic cells and might be immortal, having the capacity of indefinite self-renewal and proliferation (taken from Hiyama and Hiyama, 2007).

1.5 Objectives

Chromosomal stability depends on stable telomeres and their normal distribution in the nucleus. Thus, critical telomere shortening and/or changes in telomere organisation are known to cause genomic instability. Due to the crucial importance of telomeres, therapeutic strategies that target telomeres and telomerase in tumour cells have recently been developed and first compounds entered clinical trials. Despite all this, knowledge on telomere distribution in tumor cells and telomere length regulation in some normal tissues is still insufficient and needs to be addressed in order to consider side effects and aspects that could interfere.

We recently showed that in certain hematopoietic cells telomeres can cluster,. i.e. form telomeric aggregates (TAs) and that this is correlated with genomic instability. We now aimed to elucidate the telomere organisation in adherently growing cells (human skin keratinocytes) in order to understand cell cycle-dependent movements in normal cells and to compare this with cells that exhibit TAs due to constitutive overexpression of the *c-myc* oncogene. This study should elucidate how TAs are processed during the cell cycle and whether they contribute to an uneven chromosomal distribution thus, play a role in generating numerical chromosomal aberrations.

Similar as telomere organisation, also telomere length regulation is still poorly understood. This is particularly true for human skin, an organ that is composed of two different tissues – the constantly regenerating epidermis and the resting matrix rich dermis - and that is exposed to various insults throughout life-time. Having developed a new technique to study telomere length *in situ* on tissue sections we aimed to use this technique to unravel telomere length regulation during physiological processes such as the aging process *in vivo* (skin from different-age donors), epidermal differentiation and wound healing and to explore the role of UV radiation as the major insult causing skin aging and skin cancer.

Despite the fact that the stem cells are not only the basis for a developing epidermis but also the target cells for developing tumors, still little is known about their regulation in particular about their telomere length regulation. It is thought that stem cells only proliferate rarely and we, therefore, hypothesized that these cells should have particularly long telomeres. Thus, the final aim was to determine how telomere length would compare with known stem cell markers and whether telomere length could serve as a new stem cell marker helping to identify epidermal stem cell in the intact tissue.

2. Materials and Methods

2.1 Materials

2.1.1 List of Chemicals

Acetic acid	Merck
Acetone	J. T. Baker
Agarose	Roche Diagnostics
Bromo-phenol blue	Sigma
Citric acid	Merck
Ethylenediaminetetraacetic acid (EDTA)	Sigma
Ethanol	Merck
Ethidium bromide	Sigma
Formaldehyde 37%	AppliChem
Formamide	Merck
Glycerol	Roth
Glycine	AppliChem
Hydrochloric acid (HCl)	Riedel de Haen
Laurylsarcosine	Serva
Maleic acid	Merck
Methanol	J.T. Baker
Magnesium chloride ($MgCl_2$)	Neolab
Natriumazid (NaN_3)	Merck
Natrium hydroxid (NaOH)	Merck
N-lauryl sarkosin (35%)	Serva
Phenol/Chloroform/Isoamylalcohol (25:24:1)	Roth
Potassium chloride (KCl)	Merk
Sodium acetate	Merck
Sodium chloride (NaCl)	Fluka
Sodium Dodecyl Sulphate (SDS)	Roth
Sodium hydroxide (NaOH)	Fluka
Sodium citrate	Fluka
TRIS base	AppliChem
Triton X-100	Sigma
Tween 20	Sigma
Xylene-cyanol blue FF	Sigma

2.1.2 DNA and PNA probes, DNA-counterstains and length-markers

Telomeric DNA probe; Digoxygenin-labelled	Oncor Appligene
Telomeric PNA-probe; Cy3-labelled	DakoCytomation
Centromeric PNA-probe 7; FITC-labelled	DakoCytomation
Centromeric PNA-probe 17; FITC-labelled	DakoCytomation
All-Centromere PNA-probe; FITC-labelled	DakoCytomation
Ethidium Bromide	Sigma
DAPI (4',6-Diamidino-2-phenylindol)	Sigma
Lambda *Hind*III Digoxigenin-conjugated	Roche Diagnostics
Lambda *Hind*III marker	Boehringer

2.1.3 Enzymes and antibodies

2.1.3.1 Enzymes

Proteinase K	Quiagen
RNase A	Roche
*Rsa*I	Fermentas
Hinf I	Fermentas
*Bst*NI	BioLabs
*Alu*I	Fermentas

2.1.3.2 Primary Antibodies

Specificity:	**Origin:**	**Supplier:**
Dig-AP-Fab	Sheep polyclonal	Roche Diagnostics, Mannheim
TRF2	Mouse monoclonal	Oncogene
γH2AX	Mouse monoclonal	Upstate Technology
p53, Clone 1801	Mouse monoclonal	D. Lane, Oncogene
NG-2/CSPG (MCSP)	Rabbit polyclonal	Chemikon (AB 5320)
Pan-Keratin	Rabbit polyclonal	Dako (Z 0622)
h-TERT	Mouse monoclonal	Novocastra
Vimentin	Guinea Pig polyclonal	Progen
53BP1	Rabbit polyclonal	Novus Biologicals, Inc. (N3 100-904)
CA IX	Mouse monoclonal	

2.1.3.3 Secondary Antibodies

Specificity:	Conjugated	Origin:	Supplier (Cat. No.):
Mouse, IgG	Cy3	Donkey	Dianova(715-166-151)
Mouse, IgG	Alexa488	Goat	Invitrogen (A11029)
Mouse, IgG	Cy5	Donkey	Dianova(715-177-003)
Rabbit, IgG	Cy3	Donkey	Dianova(711-166-152)
Rabbit, IgG	Cy2	Donkey	Dianova(712-226-152)
Guinea Pig, IgG	AMCA	Donkey	Dianova(706-156-148)
Guinea Pig, IgG	DTAF	Donkey	Dianova(706-015-148)
Guinea Pig, IgG	Cy5	Donkey	Dianova(706-175-148)

2.1.4 Other solutions and reagents

Blocking Reagent	Roche Diagnostics, Mannheim
BSA (Bovine Serum Albumin)	Sigma, Steinheim
CDP-STAR	Roche Diagnostics, Mannheim
Immersol™	Zeiss
Permafluor	Beckman Coulter
VectaShield	Vector Laboratories Inc., Burlingame, CA

2.1.5 Cell lines, cell culture medias and solutions

2.1.5.1 Cell lines

HaCaT	Spontaneously immortalized human keratinocytes (human adult, low calcium, high temperature), hypotetraploid (Boukamp et al., 1988)
HaCaT-myc	HaCaT cells continuously expressing c-myc oncogene, stabile transfected with pMSc-myc (Cerezo et al., 2002)
VH7 Fibroblast	Primary human foreskin fibroblast
Keratinocytes	Primary cultures of human epidermal keratinocytes

2.1.5.2 Cell culture medias and solutions

4xMEM	Modified Eagle's Minimal Essential Medium (Fusenig and Worst, 1975) (four times concentrated aminoacids and vitamins and 2 mM L-Glutamine) with 100U/ml Penicillin (Sigma) and 50 µg /ml Streptomycin (Sigma).
DMEM	Dulbecco's Modified Eagle's Medium (Cambrex) with 100U/ml Penicillin and 50 µg /ml Streptomycin.
EDTA	0.05% EDTA (Serva) in 1x PBS with 1µl/ml of Phenol-Red
Foetal Calf Serum (FCS)	Heat inactivated at 56°C for 30 min (Biochrom)
Freezing medium	4×MEM or DMEM with 20% FCS and 10% Glycerol
Geneticin (G418)	100mg/ml in H2O
Penicillin	Sigma, Deisenhofen
Streptomycin	Sigma, Deisenhofen
Trypsin / EDTA	0.05% Trypsin (Roche), 0.025% EDTA (Serva) and 1µl/ml Phenol-Red in 1x PBS
10×PBS buffer (pH 7.4)	1.4 M NaCl, 27 mM KCl, 15 mM KH_2P0_4, 65 mM Na_2HP0_4

2.1.6 Laboratory equipment and software

2.1.6.1 Equipment

Autoradiography film	Bio Max MR-1, Kodak
	Fuji, Super RX
Casy cell counter	Schaerfe System
CCD camera	Hamamatsu
CCD-Camera (Kodak KAF 1400 Chip)	Photometrics,Tuscon, AZ, U.S.A.
Centrifuge (5415C)	Eppendorf, Hamburg
Centrifuge (Biofuge 15)	Heraeus, SEPATECH GmbH, Hanau
Chemiluminescence film	Fuji, Super RX
Electrophoreses device	Pharmacia, Freiburg

Fixogum	MARABU Werke, Tamm
Florescence Microscope	Leica DMXRA RF8, Leica, Wetzlar
Fluorescence Microscope	Zeiss, Axiovert S100 TV
Gel Imager (UV transilluminator)	Fisher Brand
Hybrite™	Vysis
Incubator with CO_2	Heraeus Spatech, Osterode
Minifuge centrifuge	Heraeus, SEPATECH GmbH, Hanau
Nitrocellulose membrane	Roche Diagnostics, Mannheim
pH Meter pH95	Wissenschaftlich-Technisch-Werkstätten
Pipet Eppendorf Research	Eppendorf, Hamburg
Pipetboy	IBS Integra Bioscience, Fernwald
Shaker	JKA Labortechnik
UV Stratalinker® 2400	Stratagene
Water bath	Grant
Whatman 3 MM paper	Roth

2.1.6.2 Software

Amira 3.1	Mercury computer systems
Argus X1 3.3.0	Biostep
AxioVision 4.2	Zeiss
GraphPad Prism 4	GraphPad Software Inc.
ImageJ 1.37	Wayne Rasband
Openlab 3.1.4	Improvision
Smart Capture	Digital scientific

2.2 Methods

2.2.1 Cell culture

2.2.1.1 Maintenance of cell cultures

HaCaT cells were cultured in 4×MEM medium with 10% FCS, in an incubator at 37°C with 95% humidity and 5% CO_2 pressure. Fibroblasts and other cell lines were grown in DMEM medium with 10% FCS (with 400 µg/ml Geneticin (G418) for HaCaT-myc). The cells were passaged at a ratio of 1:10, every 10 days (HaCaT), or depending on their proliferative capacity and passage number (primary cultures).

To passage HaCaT cells, media was removed and cells incubated with EDTA for 10 min in the incubator. EDTA was then removed and the cells incubated in Trypsin / EDTA for 2-5 min at 37°C. The activity of trypsin was stopped with 2 volumes of 10% FCS containing medium. The cells were sub-cultured, the medium was changed 24 h after trypsinisation and then three times a week The same protocol was used to passage fibroblasts, but the incubation in EDTA was not required.

2.2.1.2 Preparing frozen stocks of cultured cells

To prepare frozen cell stocks, cells were first trypsinised, resuspend in the medium and transferred in a 50 ml Falcon tube. The cells were counted with a CASY counter, centrifuged at 300 g for 5min, and resuspended in the freezing media to a final concentration of $2x10^6$ cells/ml. The aliquots of 1 ml were distributed into cryotubes, pre-cooled at 4°C for 1 h, frozen gradually (1°C/min) in an automatic cell freezer (Nalgene), and finally stored in liquid nitrogen.

2.2.1.3 Preparation of cell pellets for DNA extraction

To prepare cell pellets for DNA extraction, cells were first trypsinised, resuspended in the medium, and transferred in a 50 ml Falcon tube. The cells were centrifuged at 360 g for 5 min, the supernatant was discarded, and the cell pellet washed two times with PBS. After the second wash, PBS was completely removed and the pellet frozen at -80°C.

2.2.2 Isolation of genomic DNA

Pellets containing at least $1x10^6$ cells were resuspended in 2 ml 1 x PBS and 1 ml 3×lysis buffer (3 % N-Lauroyl-sarcosine, 0.07 M Tris/HCl (pH 8.5), 0.025 M EDTA), and incubated with RNase (0.33 mg/ml) for one h at 37°C. Proteinase K was then added (0.133 mg/ml) and incubation continued at 56°C for at least 2 h or overnight. The solution was cooled to RT and 3ml of phenol was added and mixed for 20 min. To separate upper watery layer from the denatured proteins and lower phenol layer, the solution was centrifuged for 10 min and 3000 rpm. The watery layer was transferred into a new 15 ml Falcon tube and the same volume of Phenol/Chloroform/Isoamylalcohol (25:24:1) was added, again mixed and centrifuged as described. The upper watery layer was transferred to a new tube containing 2 volumes of the ice-cold ethanol, and the solution was mixed by inversion until DNA strands precipitated. Optionally, if the number of cells was less then $1x10^6$, 0.1 Volumes of 3M Na-Acetate was added and the solution centrifuged at 5000 rpm for 10 min.

Precipitated DNA was transferred to a 1.5 ml Eppendorf tube, air dried, and dissolved in 100 – 200 µl of ddH_20 by gently shaking at 37°C overnight. The DNA concentration and purity were measured in a spectrophotometer by determining the absorbance of the DNA at 260 nm (A_{260}) and 280 nm (A_{280}), and further following the rule that 1 A_{260} is equal to 50µg/ml, and that the optimal purity is when the ratio A_{260}/A_{280} is 1.7-1.9. Samples were stored at 4°C until use.

2.2.3 Southern blotting

2.2.3.1 Digestion of genomic DNA

7µg of genomic DNA was digest over night at 37°C with *Rsa*I restriction enzyme (3 U/µg DNA) in 25 µl of 1x Y^+/TANGO™ buffer. The restriction was stopped by placing the tube at 65°C for 15 min, and samples were prepared for gel electrophoresis by addition of 10x Loading buffer (0.25% Bromophenolblue, 0.25% Xylencyanol, 50% Glycerol in H_2O).

2.2.3.2 Agarose gel electrophoresis

Agarose gels used for southern blotting were made with agarose concentration of 0.7% in 1×TAE (0.04 M Tris, 0.019 M acetic acid, 1 mM EDTA) which allows efficient separation and transfer of DNA fragments of 1-10 kb. To achieve better resolution of fragments larger then 10 kb, gels were run at low electric field strength (2V/cm) for 20 h. In addition to analysed samples, the control HaCaT 2n restricted genomic DNA and the molecular weight marker λ/*Hind*III were always loaded on the gel. EtBr (0.5µg/ml) was included in the gel to allow visualization of the separated DNA fragments with the UV-transilluminator.

2.2.3.3 DNA denaturation and transfer

The gel was soaked in HCl (0.25 M) with mild shaking for 20 min to partially depurinate the DNA. To remove HCl, the gel was rinsed 2x in distilled water, and further incubated in denaturing buffer (1.5 M NaCl, 0.5 M NaOH) for 2× 20 min. In the mean time a positively charged nylon membrane and 3 Whatman papers were cut in a size of 5 mm larger then the gel, and the membrane was immersed for 10 min in ddH_20. The paper towels were folded to a stack of 10 cm height, and the top 2 cm were soaked with denaturing buffer. Whatman papers were soaked in denaturing buffer and placed on the stack, and the membrane was placed on the top. The trapped air-bubbles between the Whatman paper and the membrane were removed by rolling a sterile pipette over the surface of the membrane. The gel was carefully placed on the membrane, and the whole stack was covered with a saran wrap. A glass plate and a weight of all together 500 g were placed on top of the gel. During this – so called “dry transfer” denatured DNA fragments were driven by the capillary forces from the gel on the membrane during 12 h. The membrane was labelled at the gel slots, removed from the stack and rinsed in neutralization solution (1.5 M NaCl, 0.5 M Tris, 1 mM EDTA, pH 7.2) for 30 min. The membrane was air-dried for 1 h and DNA crosslinked to the membrane at 260 nm and 1200 J/m^2 in a Stratalinker®.

2.2.3.4 Hybridization on the membrane

The membrane was placed in the hybridization tube, the tube was filled with 25 ml of pre-hybridization solution (5×SSC, 0.1% Laurylsarcosine, 0.02% SDS, 1× Blocking reagent) and rotated in the oven for 6 h at 68°C. The telomere specific Digoxygenin-labelled DNA probe (Oncor) was denatured at 95°C for 5 min and added to 30 ml of pre-hybridization solution to a final of 50 ng/ml and hybridized for the next 15 h at 68°C.

2.2.3.5 Stringency washing and detection

The membrane was washed for 3 × 10 min with washing buffer 1 (2×SSC, 1%SDS), and for 10 min in washing buffer 2 (0.2×SSC, 0.1%SDS), both with the rotation in the oven at 66°C. The membrane was taken out of the tube and additionally washed for 5 min in Wash buffer (0.3 % Tween 20 in Maleic acid buffer (0.1 M Maleic acid, 0.15 M NaCl, pH 7.2)) and incubated for 30 min in 1 × blocking solution (10x blocking reagent diluted in Maleic acid buffer). The membrane was then incubated for 30 min in 40 ml of antibody solution (alkaline phosphatase coupled anti-dig Fab (Roche) in 1 × blocking solution), and washed 2 x 15 min in wash buffer. The membrane was then equilibrated for 5 min in 20 ml detection buffer (0.1 M Tris/HCl, 0.1 M NaCl), placed on a hybridization bag, and covered with 3 ml CDP-STAR working solution (CDP-STAR (Roche) deluted 1:100 in detection buffer). The membrane was covered with the second sheet of the folder to spread the substrate evenly and without air-bubbles over the membrane. Excess liquid was squeezed out, and chemiluminescence film (Fuji, Super RX) was exposed for 5-20 in the dark room.

2.2.4 3D Fluorescence *In Situ* Hybridisation (FISH)

To determine the 3D distribution of telomeres during the cell cycle, and to quantify telomere signal intensities, cells were grown for 2-3 days on glass slides untill they were subconfluent, or 5µm skin cryostat sections were used. The cells grown on glass slides were washed with PBS for 5 min and fixed for 15 min in 3.7% formaldehyde buffered in PBS, washed with PBS for additional 3x5 min, and rinsed in double-distilled water (ddH_2O). Slides were shortly air-dried and 5µl of Cy3-labeled PNA probe (PNA

Telomere FISH Kit K5326; DAKO A/S, Lustrum, Denmark) was added on the cells and covered with 18x18 mm glass coverslip. The DNA was co-denatured for 3 min at 80°C and hybridized for 2 h at 30°C. The slides were washed with 70% formamide/10 mM Tris-HCl, pH 7.2, for 2x15 min, rinsed in PBS for 1 min, and stringency wash with 0.1xSSC for 5 min at 55°C. Slides were finally washed with PBS containing 0.05% Tween-20 for 2x5 min at rt, rinsed in ddH_2O, shortly air dried, and covered with 20µl of antifade solution (VectaShield, Vector Laboratories Inc., Burlingame, CA) containing 0.3 µg/ml of DAPI.

2.2.5 Simultaneous immunofluorescence/FISH staining

For simultaneous staining of telomeric DNA by *in situ* hybridization and proteins by indirect immunofluorescence, cells grown on glass slides or 5µm skin cryostat sections were first formaldehyde fixed and 3D FISH performed according to the previously described protocol. Instead of adding the antifade solution at the end, cells were first incubated in serum blocking solution for 30 min (2% goat, donkey, or sheep serum (depending on the species where the secondary antibody was produced), 1% BSA, 0.1% Triton X-100, 0.05% Tween 20, 0.05% sodium azide (NaN_3), all in 1x PBS). Cells were shortly rinsed in ddH2O and incubated for 1 h 30 min at rt with primary antibodies diluted in 1x PBS containing 3% BSA. Cells were washed for 3x5 min with 1x PBS, rinsed with ddH_2O and incubated with secondary antibodies diluted in 1x PBS for 45 min at rt. Cells were washed with 1x PBS for 3x 5 min , and covered with 20µl of antifade solution (VectaShield, Vector Laboratories Inc., Burlingame, CA) containing 0.3 µg of DAPI.

2.2.5.1 Optimisation of simultaneous immunofluorescence/FISH staining

Most of the antibodies perform and stain well when the immune staining is performed after FISH (antibodies against pan-keratin, vimentin, 53BP1, TRF2 and others), nevertheless some antibodies did not give staining at all (CA-IX, MCSP, and p53), or the staining pattern was not comparable to the immune staining only, when performed without FISH (hTERT, γH2AX). Therefore, optimisation of the previously described protocol was necessary in some experiments.

As the most aggressive step during FISH is the denaturation at 80°C in 70% formamid in which the PNA probe is provided, it is possible that some epitopes get masked during the treatment and became inaccessible. Another possibility is that some proteins, other than the protein of interest, change their conformation and get non-specifically recognised. Therefore, the optional techniques included the formaldehyde or methanol:acetic acid (1:1) fixation, and immunofluorescence before FISH (as it was used to visualize p53, CA-IX, and MCSP), followed by imaging, and then re-staining for telomeres, and finally after FISH again imaging of the same regions. In those experiments, if the fixation was not used after immune staining, and the staining is not strongly nuclear, FISH can easily be performed after imaging of immune staining, as the immune signals will be lost during FISH.

Nevertheless, if it was necessary to have immune staining until the end, to check for the coo-localization with telomeres for example, it was beneficial to perform another 5 min in 3.7% formaldehyde fixation step after immune staining, and then proceed with FISH. This optional technique was useful in case where the immune signals were stronger (hTERT), but was not appropriate for weaker staining (some weakly p53 stained regions) as a lot of immunostaining is lost during the FISH procedure, despite the stabilisation by the additional fixation step.

2.2.6 3D Image acquisition and Deconvolution microscopy

To obtain a 3D data set, 100 or optionally 50 sections of two-dimensional 1024x1022, or 1280x1022, 8-bit greyscale images (0.2 µm or optionally 0.3 µm z-axis distance) were recorded for the Cy3 fluorescent dye (telomeres), DAPI (nuclei), and for other immune fluorescent stains if present (Cy2, Cy5, DTAF, AMCA, and Alexa488). Precise z-axis distance was controlled by the motorized (a piezo-mover, PhysikInstrumente, Waldbronn, Germany) inverted epifluorescence microscope (Axiovert S100 TV; Carl Zeiss MicroImaging, Inc., Germany) equipped with a digital CCD camera (C4742 – 95 - 12NRB, Hamamatsu, Japan), a Plan-neofluar objective lens (63x magnification and NA 1.4; Zeiss, Oberkochen, Germany), and Chroma HQCy3 (Ex:545/30; DiM 570 LP; Em: 610/75), Omega XF02 (Ex: 340/40; DiM 390; Em: 400 LP), Omega XF22 (Ex: 485-22; DiM: 510; Em: 530-30), and Cy5 (Ex: 620/60;DiM 660

LPXR; Em: 700/75) filters. Image acquisition and analysis was driven by the OpenLab software (version 3.1.4, Improvision, Tübingen, Germany).

To obtain a detailed 3D image and accurate determination of telomere signal intensities within skin sections, the 6 nearest neighbour algorithm of OpenLab`s deconvolution module was used. The image stacks were processed and saved on an attached Power Macintosh G4 1.42 GHz CTO (Apple Computer Inc., Cupertino, CA). To perform deconvolution more independently, the automation program provided with the OpenLab software package was modified allowing deconvolution of >30 image stacks over night. Deconvolution of Cy3, Cy2, DAPI, AMCA and other signals were always performed individually with the same conditions for a given fluorochrome. Deconvolved images were stored as a stack of TIFF images on CD-ROM and further used for 3D reconstruction with Amira 3D visualization software (version 3.0, Indeed-Visual ConceptsGmbH, Berlin). Telomeric signal intensity determination was performed using ImageJ software (version 1.37u, Wayne Rasband, National Institutes of Health, USA).

2.2.7 3D Reconstruction of telomeres

For 3D visualization of telomeric and centromeric DNA and various immunostainings, the Amira`s module that computes an isosurface within a 3Dscalar field was used that pseudo-coloured 8-bit images of telomeres in red, and other staining depending on the emission wavelength in blue (in most cases DAPI nuclear counter-staining), green (Cy2, Alexa488 and others), and gray (Cy5).

Optionally, signals were visualized using Amira`s ProjectionView module that computes a shadow projection of a 3D image onto the three major planes (xy, xz, yz), or using maximum Z-axis projection of ImageJ software.

2.2.8 Quantification of the digitized telomere fluorescent signals

Images used for quantification of telomere and other signals were always ImageJ's maximum Z Projections of 3D image stacks. Projected telomeric signal intensities

having sizes greater than the threshold (background noise) were measured on the marked region of interest (ROI), tabulated and exported to Microsoft Excel (Microsoft Corp.). GraphPad Prism (GraphPad Software, San Diego California, USA) was used for further data processing and statistical analysis. To determine statistical significance of differences in mean telomere signal intensities t test was used with a significance level $p=0.05$ (* $0.01<p<0.05$, ** $p<0.01$, or *** $p<0.001$). Optionally, Mann-Whitney test was used if the data sets were asymmetrically distributed, and F-test was used to check for different variances between data sets. The linear regression and the significance of deviation from zero were used in studies on age dependant telomere decline. To obtain comparable signal intensity measurements between different experiments, a control skin with known telomere signal intensities, or HaCaT cells grown on glass slide were included in each experiment. Analysis of the same regions on serial skin sections as well as co-hybridization with a centromere 7, 17, or all centromere-specific PNA probes was used to confirm hybridization efficiency. All experiments were at least performed twice.

To recalculate telomere signal intensity into telomere length in kb telomeric signal intensities of HaCaT, HaCaT-myc, cultured dermal fibroblasts and A9 immortal mouse fibroblasts were calculated and plotted against the telomere length (terminal restriction fragment length (TRFL)) values determined separately by Southern analysis on these same cell populations. Optionally, 50µm thick skin cryo-sections and leftovers from standard cryo-sectioning were collected; genomic DNA was isolated and used for Southern blotting (TRFL). Calibration curves obtained there from were used for the absolute telomere length determination (in kb) in skin sections out of fluorescence signal intensities obtained by FISH. For the Southern Blot quantification, chemi-lumi image exposures of telomere-probed blots were digitised and transferred to Microsoft Excel, and were the basis for calculating quartiles and mean of TRF length using the formula:

$$TRFL = \Sigma(ODi)/ \Sigma(ODi/Li)$$

where ODi is integrated signal intensity at a position i, and Li - length of DNA fragment at the position i.

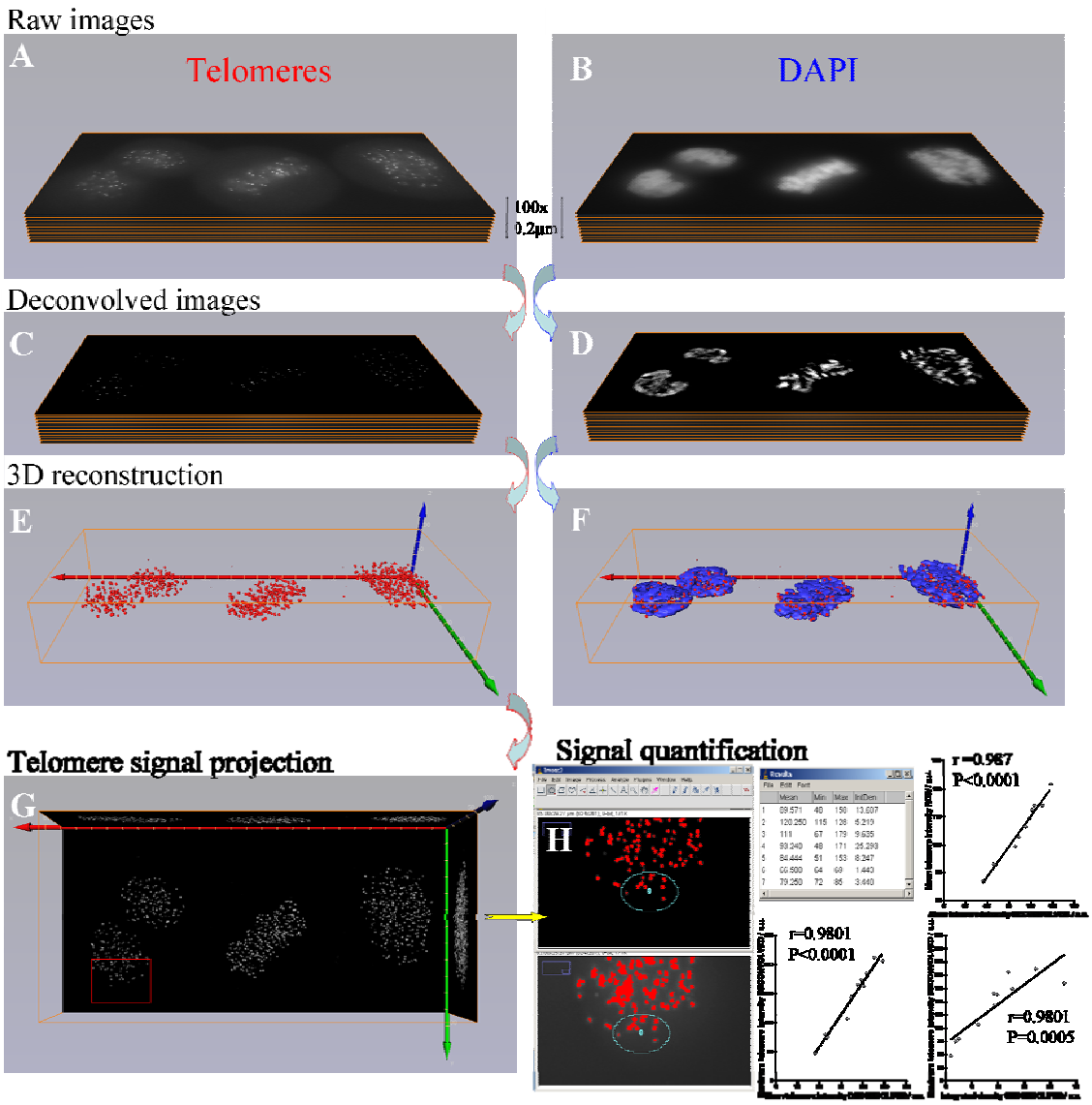

Figure 9: Schematic of image acquisition, deconvolution, 3D reconstruction and telomere signal quantification. Images of 3 mitotic HaCaT cells (telophase, metaphase, and early anaphase from left to right) are captured separately; red channel for telomeres **A)**, and blue **B)** for DAPI DNA counterstaining. 100 raw 2d optical sections were taken for each channel in the serial focal planes with the Z-axis distance of 0.2µm. Images of telomeres **C)** and chromosomes **D)** are deconvolved; out of focus light was removed, background subtracted and the resolution increased. Improved quality of the resulting image allowed 3D reconstruction of individual channels separately (only telomeres in **E)**), or overlapped in 3D (telomeres and chromosomes in **F)**). In addition, the same data set used for analysis of 3D distribution is used for quantification. 3D image of telomeres is projected **G)** using ImageJ's maximum Z-projection. Red square indicates region that is magnified in **H)** where the threshold (in red) is applied on the deconvolved image (upper) and on the same region of the non-deconvolved image (lower). The same region of interest (ROI) on both images marks the group of telomeres that will be quantified. Note the increased resolution and no background of the deconvolved image. Mean, maximum intensities and integrated densities of telomere signals are tabulated (list), and presented in graphical form. Upper graph in H) indicate the good linear correlation of mean deconvolved and non-deconvolved signal intensities, and lowers indicate good correlation of mean, maximum and integrated density, showing that all can be used as they are all finally comparable to the telomere length. Pearson correlation coefficient r and p value indicating significance of correlation are shown in the graphs.

3. Results

3.1 3D distribution of telomeres in immortalised HaCaT and HaCaT-myc keratinocytes

3.1.1 Cell cycle dependent 3D distribution of telomeres in HaCaT cells

The first studies on the three-dimensional (3D) telomere organization were performed on mouse and human lymphocytes, and demonstrated a well ordered cell cycle-dependent nuclear distribution. Telomeres were regularly distributed in G1, but aligned in a so-called telomeric disc late in G2 phase, i.e. prior to mitosis (Chuang et al., 2004). To investigate whether and how the cell cycle dependent distribution of the telomeres would differ in adherently growing cells, we analysed HaCaT keratinocytes with particular emphasis on the different stages of mitosis. To obtain a maximal number of mitoses, the cells were arrested in G1 and analysed 36 h and 48 h post G1 release. The cells were hybridized with a telomeric PNA probe, and studied for telomere and chromatin distribution by deconvolution microscopy and 3D reconstruction.

As shown in figure 10A, telomeres were rather evenly distributed in their x, y-axis (front view) throughout the nucleus of interphase of HaCaT cells. However, when looking from the z-axis most of the signals were located in the inner third of the nucleus (side view). Thus, different from lymphocytes the distribution in interphase nuclei was more restrictive most likely due to the flattened nature of the nuclei.

During mitosis, starting with pro-metaphase, telomere distribution changed. Cells acquired a more rounded shape and the telomeres occupied a wider space when viewed along the z-axis (figure 10B and 10E). This distribution was also seen throughout ana- and telophase (figure 10F, 10G, and 10K). The typical condensed distribution (inner third) was again visible in the interphase of new daughter cells (figure 10H). 3D reconstruction of the chromosomes confirmed that the telomeres are more widely distributed in mitotic cells than interphase cells demonstrating an active movement not only of the chromosomes but of the telomeres as well. To verify that this is not exclusive for HaCaT cells, other immortal and tumour-derived epidermal cell lines and normal fibroblasts and keratinocytes were analysed. Since they established the same distribution pattern (not shown) these data suggest that this cell cycle-dependent distribution accounts for all adherently growing cells.

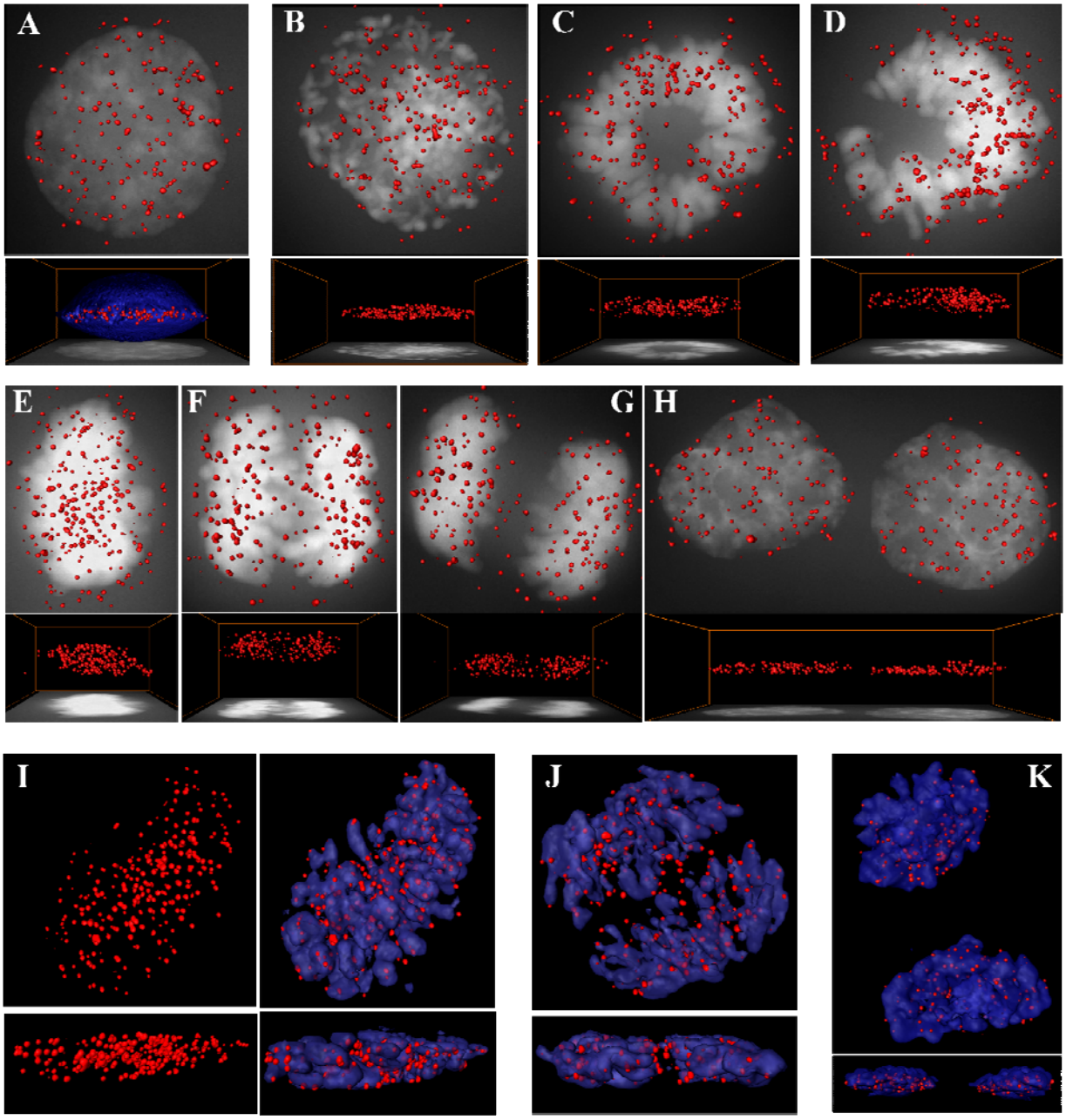

Figure 10: The 3D organization of telomeres in HaCaT cells is cell cycle-dependent.
A-H) 3D reconstructed images of HaCaT cells after FISH with a telomere-specific PNA probe (DAKO) and deconvolution microscopy shows telomeres pseudo-colored in red, combined with the images of nuclei and chromosomes (DAPI) pseudo-colored in blue (A, I, J, K), or projected as a shadow projection of a 3D image volume (A-H). Note that the projection view is at a different level and therefore appears smaller than the 3D reconstruction. The individual cells represent **A)** interphase, **B)** prophase, **C, D)** pro-metaphase, **E)** metaphase, **F)** early and **G)** late anaphase, and **H)** two daughter cells. Cells are shown from the front (x, y-axis; upper panel) and side view (x, z-axis; lower panel). Panel A additionally shows a merged side view of the 3D reconstructed image of the telomeres and the nucleus to demonstrate that the telomeres are localized in the inner third of the nucleus of interphase cells. **I-K)** 3D reconstructed images of chromosomes (DAPI) combined with the 3D images of the telomeres in **I)** metaphase, **J)** anaphase, and **K)** telophase to demonstrate telomere localization during mitosis. Panel **I)** contains a 3D reconstruction image of the telomeres only. Note the regular telomere distribution also in metaphase cells.

3.1.2 Constitutive expression of c-Myc correlates with the presence of telomeric aggregates (TAs)

It was also shown by Chuang et al., (2004) that c-Myc can contribute to a distorted telomere distribution, i.e. telomere aggregation, in lymphocytes. To examine whether this would be a more general characteristic of the c-Myc protein, we analysed HaCaT cells that constitutively expressed the c-myc oncogene, and compared them with the parental HaCaT cells. Indeed, in four independent experiments interphase nuclei of the HaCaT-myc cells showed telomeric aggregation, while the so called telomeric aggregates (TAs) were absent in parental HaCaT cells (figure 10A). In addition to the TAs, also the distribution of the other telomeres appeared more clustered than in the parental HaCaT cells thus making also this a very characteristic sign of aberrant nuclei.

3.1.3 Telomere aggregates are present during mitosis

It is well accepted that dysregulation of the c-Myc oncogene can contribute to genomic instability. Furthermore, since c-Myc obviously causes TA formation and this in turn causes “clumping” of a number of chromosomes, one potential consequence of TA formation could be that the chromosomes also remain associated with each other during mitosis, and thus lead to the uneven distribution of the chromosomes to the daughter cells during mitosis. For this purpose, it is necessary that the TAs would persist also throughout the mitotic phase. To test this, we analysed the 3D telomeric configuration of HaCaT-myc cells during the different phases of mitosis, and compared them with those of the parental HaCaT cells. As described above, HaCaT cells showed non-overlapping telomeric territories which were evenly spread in the x, y-axis formation. A similar well organized distribution was maintained in meta-, ana- and telophase cells (see figure 10). In contrast, about 60% of HaCaT-myc cells showed TAs. Most importantly and as demonstrated in figure 11A -G, TAs were present at all stages of mitosis and led to an uneven telomere distribution as demonstrated representatively for late telophase cells as well as two daughter cells that had already established a G1 distribution (see figure 11F, G).

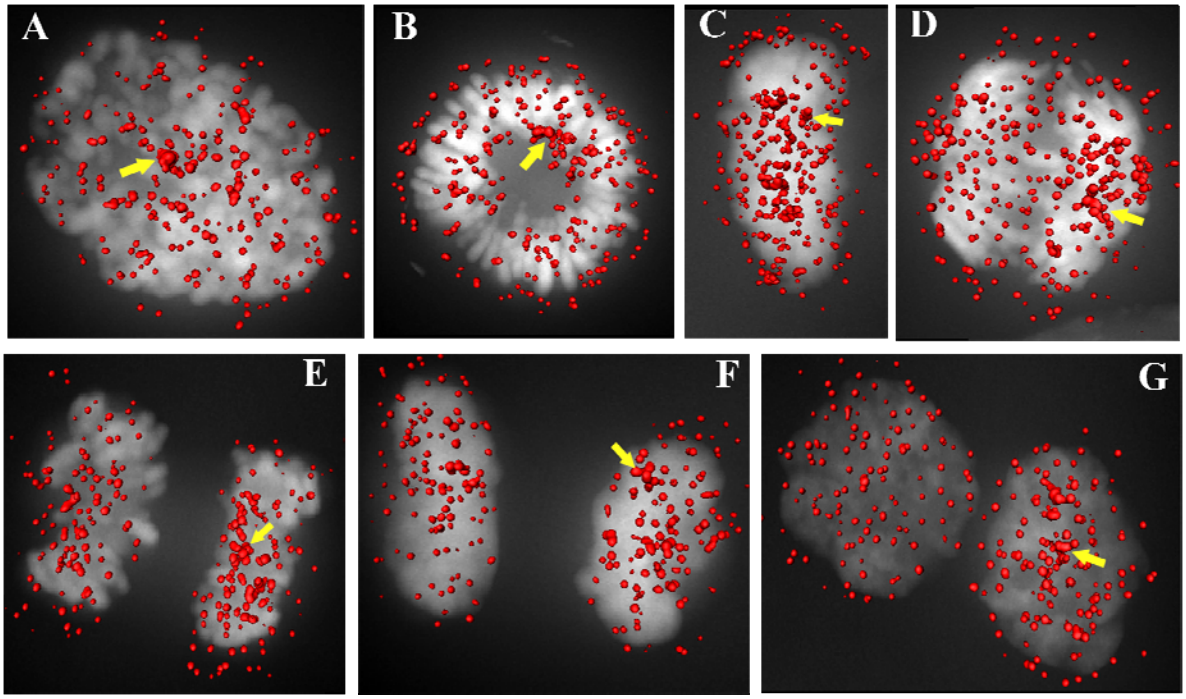

Figure 11: Telomere aggregates (TAs) are present during mitosis in HaCaT-myc cells.
A-G) 3D reconstructed image of the telomeres pseudo-coloured in red in **A)** prophase, **B)** pro-metaphase, **C)** metaphase, **D)** early and **E)** late anaphase, **F)** telophase, and **G)** early interphase of daughter cells, shown from the front (x, y-axis) and combined with the shadow projection of DAPI stained chromosomes/nuclei. The aggregates present in each mitotic stage are indicated by an arrow.

3.1.4 Identification of proteins potentially involved in the formation of telomere aggregates

In the first approach to determine the mechanisms of TA formation we aimed to analyse the difference in the nuclear protein expression pattern between HaCaT and HaCaT-myc cells, i.e. cells with and without aggregates. For this approach nuclear extracts were made from both cell types (in collaboration with Dr. Sabine Rosenberger) and in collaboration with Stefanie Winter-Simanowski analysed by two-dimensional polyacrylamide gel electrophoresis (2-D PAGE). 2-D PAGE allows resolution of proteins according to their isoelectric point (pI) in one dimension and according to their molecular mass (Mw) and by SDS-PAGE in the second dimension. Proteins that were differently expressed in HaCaT compared to HaCaT-myc cells were identified by 2-D PAGE (figure 12) and further analysed by Matrix-assisted laser desorption/ionization used in mass spectrometry (MALDI-MS) by Dr. Martina Schnölzer (all collaborators are from German Cancer Research Center, Heidelberg).

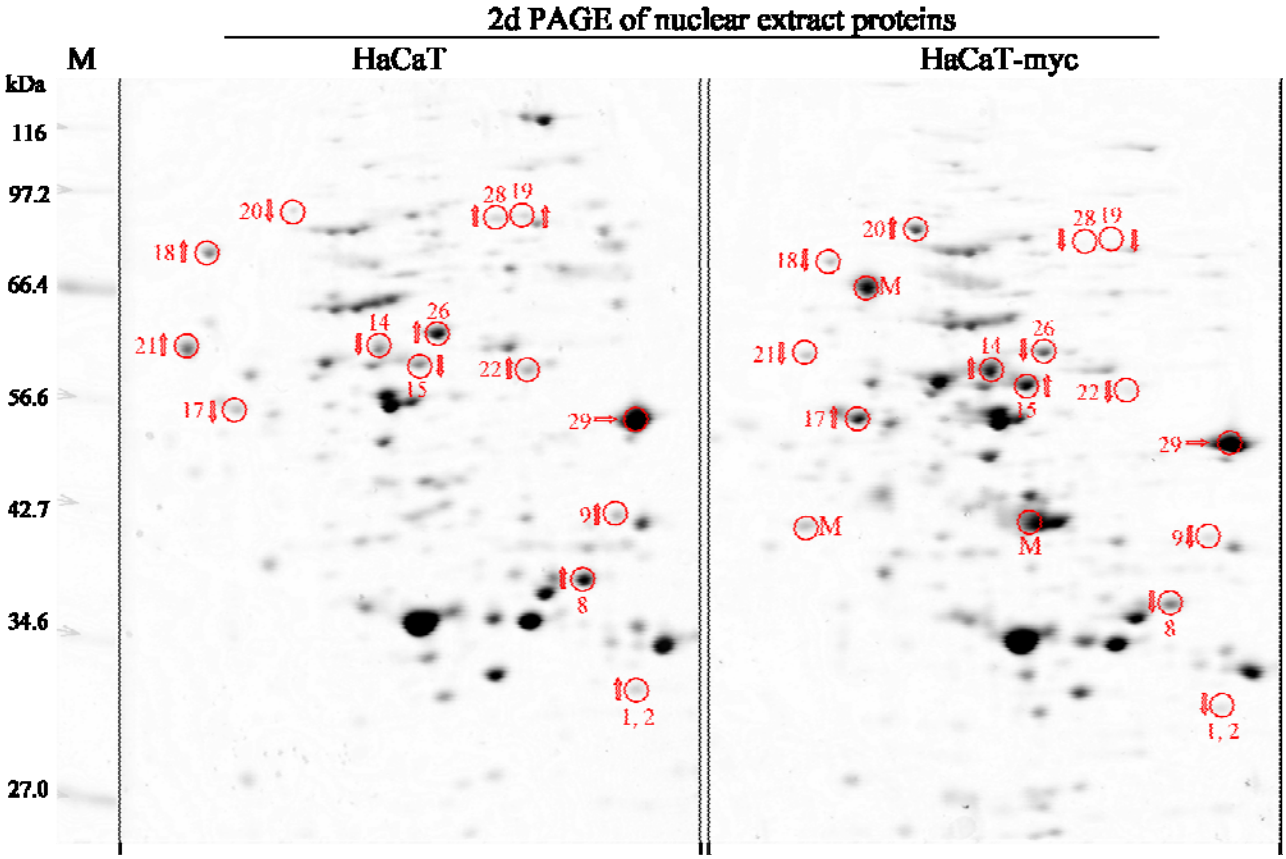

Figure 12: Identification of differences in the protein expression of HaCaT and HaCaT-myc cell lines by 2d PAGE. Proteins were isolated from the nuclear extracts of HaCaT and HaCaT-myc cells and separated according to charge (pI) in the first dimension and according to size in kDa by SDS-PAGE in the second dimension. Difference in the protein expression pattern were identified according to reduced (↓) or increased (↑) density of the signals as indicated on the 2d-gel. Some of the analysed proteins are indicated with a circle, and labelled with the same number as it is used in the table 2. Molecular weight marker is indicated in kDa (M), as well as an internal protein marker (M).

Table 2: Proteins that are differentially expressed in HaCaT versus HaCaT-myc are identified by MALDI-MS.

		Protein Expression*			
No.	**Protein**	**In HaCaT**	**In HaCaT-myc**	**pI**	**Mw / kDa**
1	39S Ribosomal protein (Mrp-L45)	↑	↓	9.4	36
2	40S ribosomal protein S3a	↑	↓	9.9	30
3	ATP synthase	↑	↓	5.3	57
4	Cytokeratin 1	↑	↓	8.3	66
5	Cytokeratin 19	↓	↑	5.0	44
6	Cytokeratin 2	↑	↓	8.3	66
7	ErbB3 binding protein (pa2g4)	↑	↓	7.2	38
8	Heterogeneous nuclear ribonucleoprotein A2/B1	↑	↓	9.0	37
9	Heterogeneous nuclear ribonucleoprotein A3	↑	↓	9.3	40
10	Hspa1l (ATP synthase)	↑	↓	5.3	57
11	Keratin 10	↑	↓	5.2	60
12	Keratin 13	→	→	4.9	50
13	Keratin 14	→	→	5.1	52
14	Keratin 5	↓	↑	7.7	63
15	Keratin 6A	↓	↑	8.3	60
16	Keratin 7	↓	↑	5.5	51
17	Keratin 8	→	→	5.6	54
18	Matrin 3	↑	↓	5.9	95
19	mll septin-like fusion	↑	↓	7.2	65
20	Mortalin-2 (Heat Shock 70 kDa protein)	↓	↑	5.4	70
21	P60 lymphocyte protein (Chaperonin)	↑	↓	5.7	61
22	PAI-1 mRNA-binding protein	↑	↓	8.4	42
23	Plakophilin 3	↑	↓	9.7	88
24	PRPF4	↑	↓	7.1	59
25	ptb-associated splicing factor	↑	↓	9.5	76
26	Pyruvat Kinase 3	↑	↓	8.4	59
27	RAB1B	↓	↑	5.6	22
28	SYNCRIP	↑	↓	5.9	47
29	Translation elongation factor 1 alpha 1-like 14	→	→	9.1	43
30	Villin 2	↓	↑	5.9	69

* Arrows indicate higher (↑), lower (↓), or the same (→) level of protein expression
** Isoelectric point (pI) and molecular weight (Mw) are theoretical values obtained from the NCBI database

We identified 30 proteins that are differentially expressed due to constitutive expression of c-Myc oncogene in HaCaT cells (table 2). The most promising candidate that could be involved in the formation of telomere aggregates is Matrin 3 (Belgrader et al., 1990). It is a part of the nuclear matrix – a salt-resistant proteinaceous nuclear structure – that could be isolated from interphase cell (Berezney and Coffey, 1974) and which is involved in the chromatin organization (reviewed in Berezney, 2002). Therefore, destabilised expression of Matrin 3 could have important influence on telomere distribution. Further analysis will elucidate the role of Matrin 3, and other differentially expressed proteins in the formation of telomere aggregates in HaCaT-myc cells.

3.1.5 Telomere length measurement in interphase cells

In a length-independent manner telomeres can contribute to genomic instability by forming telomeric aggregates. However, if telomeres become critically short they can be also responsible for the onset of genomic instability as they become sticky and prone to chromosome end-to-end fusions. Chromosome fusions can result in translocations, deletions, and amplifications, therefore, urging to determine potential telomere-length-dependent mechanisms of genomic instability (reviewed in Boukamp *et al*., 2005).

Besides telomere organisation, 3D microscopy also allows to determine for the size of the telomeres, as the fluorescent signal intensity is proportional to the telomere length determined by Southern blotting. Southern blotting is a well accepted technique used to get an insight into overall telomere length distribution, but it has certain limitations: it requires a lot of genomic DNA (>10^6 cells) and it does not give any information on telomere length of individual cells. By establishing a method to combine the Q-FISH technique on interphase cells with the 3D deconvolution microscopy it was possible to overcame these limitations (figure 13).

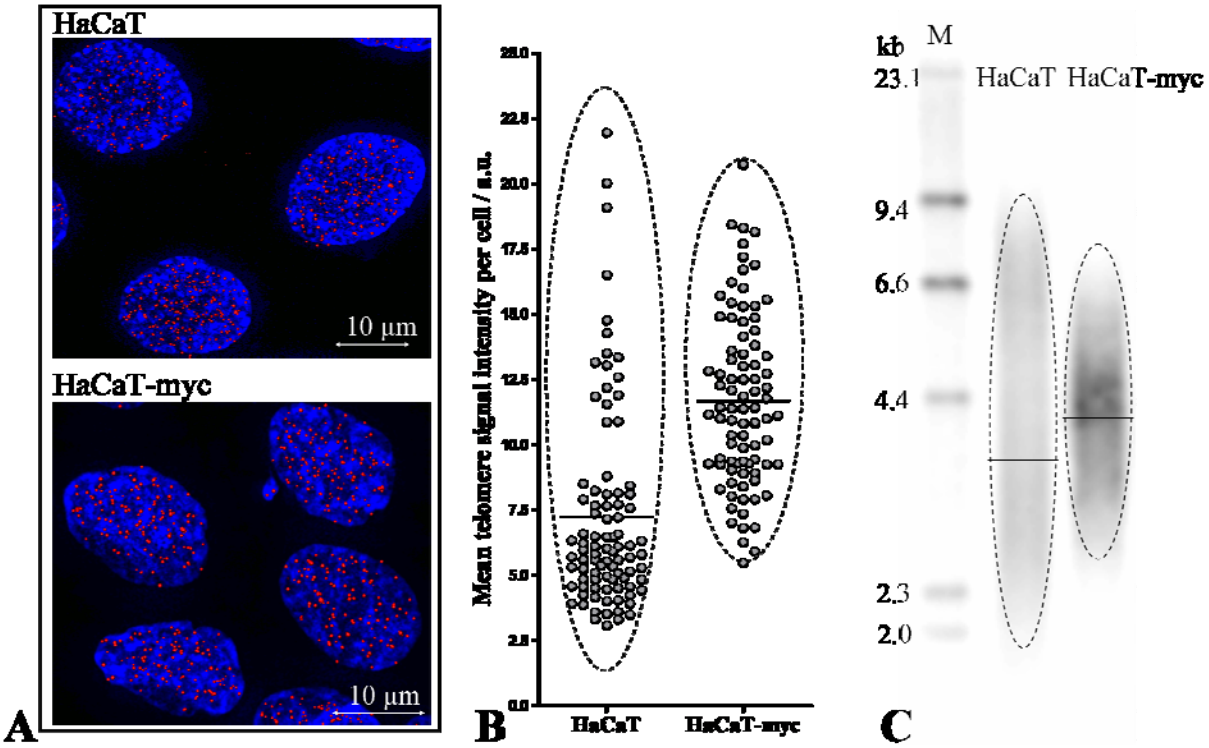

Figure 13: Telomere length in HaCaT versus HaCaT-myc cells can be measured by 3D deconvolution microscopy based Q-FISH on interphase cells. The same images used for the 3D visualisation in **A)** were quantified for telomere signals. Mean telomere signal intensity in the each cell is shown as a dot in **B)**. Results obtained by Q-FISH were clearly comparable to those obtained by Southern blotting in **C)**.

3.2 Telomere length in intact skin sections

Since 3D deconvolution microscopy based Q-FISH analysis on interphase cells allowed to measure telomere length in HaCaT cells, HaCaT-myc cells and a number of other cell lines, the next question was whether the same technique could be used to measure telomere length in tissues. We, therefore, modified the technique and measured mean telomere signal intensities in skin sections from 9 different skin samples of different age, body part and gender. Telomere length was also measured in the same samples by Southern blotting, and correlated with the Q-FISH signal intensities. Correlation of the two techniques was significant (figure 14C) indicating we can use the novel technique to address other important questions on telomere-length-dependant genomic stability in the skin *in situ*.

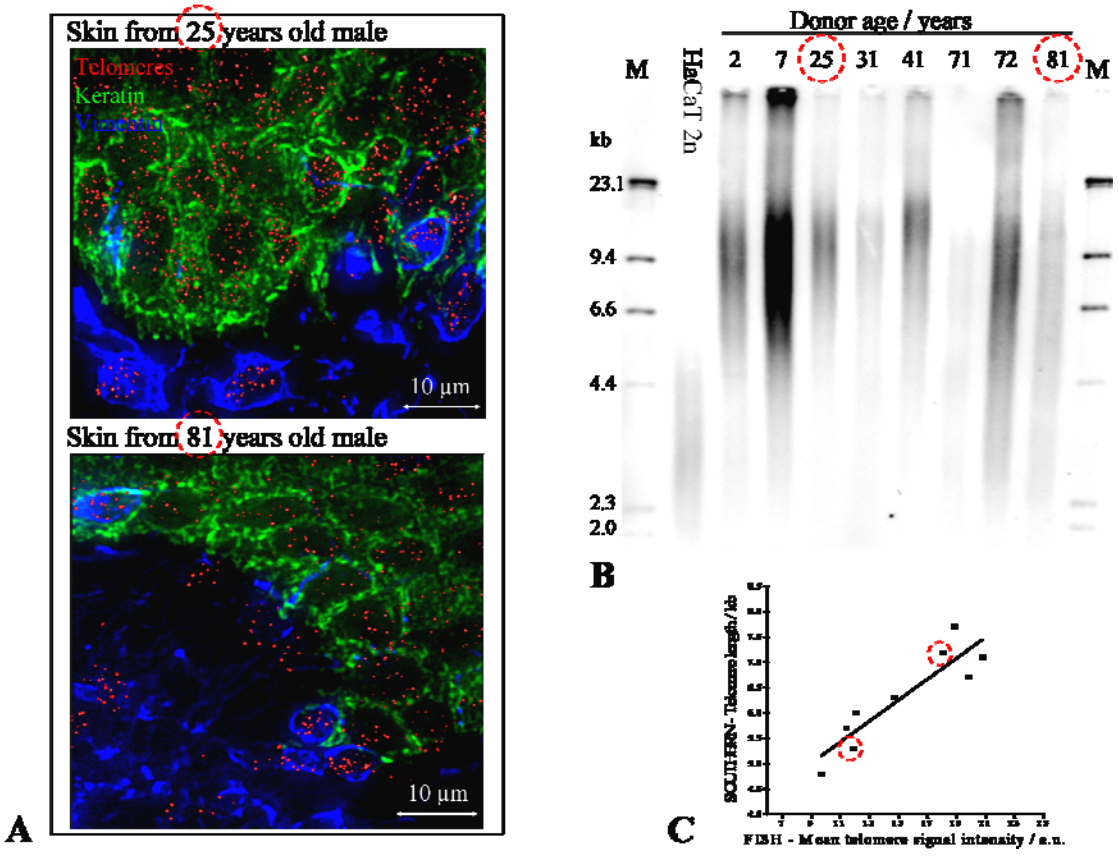

Figure 14: Telomere length in the skin measured by 3D deconvolution microscopy based Q-FISH on interphase cells gives comparable results to Southern blotting. A) An example of two skins of different age stained for telomeres in red, keratin (green) and vimentin (blue). The telomere length was measured in these 2 samples and 7 others by Southern blotting in **B)**, and correlated with the mean telomere signal intensity measured by 3D Q-FISH on interphase cells in **C)**. Correlation of two techniques was significant (p=0.0008), with the satisfying line fitting (r^2=0.817), indicate that two techniques are measuring the same, namely – telomere length. Marker (M): λ*Hind*III is indicated, as well as HaCaT 2n cell line with a constant TRFL of ~ 4 kb used as an internal control.

3.2.1 Minimal age-dependent telomere length decline

Previous studies based on the Southern blotting technique for telomere length measurement (terminal restriction fragment length – TRFL) suggested significant age-dependent telomere shortening in the skin (Lindsey et al., 1991; Friedrich et al., 2000; Sugimoto et al., 2006). Nevertheless, reports were somehow contradictory as large variations were observed within each study as well as between them (shortening of 9 bp/year up to 75 bp/year). Our Southern blotting measurements so fare indicated strong individual variability rather than a correlation of telomere shortening and age in the skin (figure 14B) (based on a study performed by Sharareh Moshir on 31 skin sample). We now demonstrate with a novel *in situ* telomere length measurement on 15 different donors ranging from 2 to 90 years that their mean telomere lengths correlate well with the pattern established by Southern blot analysis (figure 14C). Thus with a second independent technique we are able to confirm an only minimal overall age-dependent telomere loss (figure 15B).

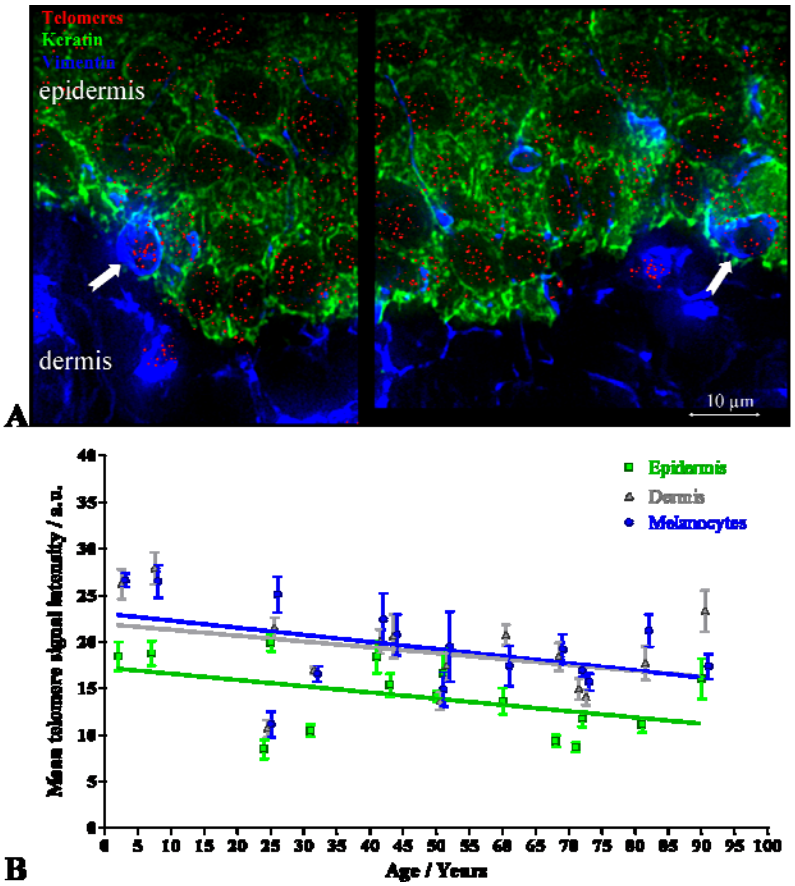

Figure 15: Minimal age-dependent decline determined by Q-FISH on interphase cells combined with 3D deconvolution microscopy and immune labelling. A) Human skin section stained for keratin (green) marking the epidermal keratinocytes and vimentin (blue) marking the fibroblasts in the dermis as well as melanocytes (marked with arrows) in the basal layer of the epidermis. The telomeres, hybridized with a telomere-specific PNA probe, are presented in red. Epidermis and dermis are indicated. **B)** Graphic presentation of the mean telomere signal intensities of keratinocytes (green), melanocytes (blue), and dermal fibroblasts (grey) in skins from different-age donors, demonstrating that telomeres in the proliferating keratinocytes are generally shorter than in the non-proliferating melanocytes or dermal fibroblasts. The respective donor age is indicated (X-axis).

3.2.2 Differentiation does not contribute to telomere loss

If proliferation-dependent telomere erosion occurs, it should be seen within the basal layer where the proliferatively active cells are located but not in the suprabasal layers where the cells no longer proliferate but are replication-arrested and differentiate. To test this hypothesis we studied the role of differentiation. In the epidermis, keratinocytes proliferate in the basal layer and after 4 to 6 divisions move upwards and pass through defined stages of differentiation. Most keratinocytes in the epidermis are, therefore, in a non-proliferative differentiating stage where telomerase is inhibited (Rosenberger, 2007). The epidermis of 14 different donors was divided into basal, suprabasal, and upper part (figure 16A) and at least 5 individual areas were analyzed for each specimen (figure B). We found one sample with both the suprabasal und the upper part containing shorter telomeres than the basal layer, one sample with the upper layers containing shorter and two containing slightly longer telomeres. In most (10/14) samples, however, telomere quantification revealed highly comparable values, thus demonstrating that epidermal differentiation does not contribute to telomere loss in a significant manner.

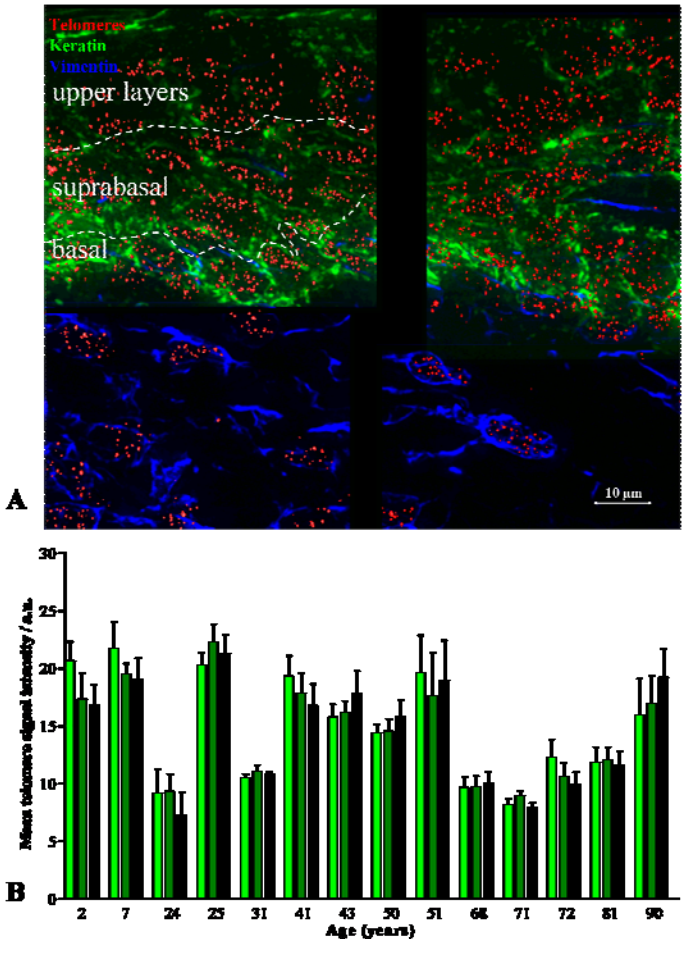

Figure 16:
Epidermal differentiation does not contribute to telomere loss.
A) Human skin stained for keratin (epidermis in green), vimentin (dermis in blue) and telomeres (telomere-specific PNA probe in red). The epidermis is divided by dotted lines into basal, suprabasal, and upper layers (as indicated). **B)** Graphic presentation of the mean telomere signal intensities and standard error of the mean in basal (light green), suprabasal (dark green), and upper layers (black) of the epidermis of different age donors.

3.2.3 Telomere length in keratinocytes versus melanocytes and fibroblasts

Combination of the 3D Q-FISH on interphase cells with the immune labelling enabled us to distinguish between different cell-types present in the skin. We measured telomere length in the epidermal keratinocytes representing the predominant cell type of the epidermis, in the melanocytes, which make ~10% of the cells in the basal layer of the epidermis, and in the dermal fibroblasts. Immune staining for vimentin was usually sufficient to distinguish between those three cell types as the epidermis can be differentiated morphologically from the dermis and vimentin clearly labels all nonkeratinocytes. Investigating different skin samples, it became obvious that in most samples telomeres were longest in the dermal fibroblasts and in the melanocytes, and were often significantly shorter in the keratinocytes. Determining the age-dependent telomere shortening separately for each cell type, we now show that no statistically significant decline is present in neither melanocytes nor fibroblasts (figure 15B). Thus, despite the fact that only keratinocytes are telomerase-positive and that telomeres may counteract telomere loss also the telomerase-negative melanocytes and fibroblasts only loose little telomeric DNA during aging, suggesting that telomere loss is not a major mechanism of skin aging. Moreover, we determined that telomere length in melanocytes, dermal fibroblasts and keratinocytes correlated to each other better than to age of different samples, thus if telomeres were shorter in one cell type, they were usually proportionally shorter in the others as well (figure 17).

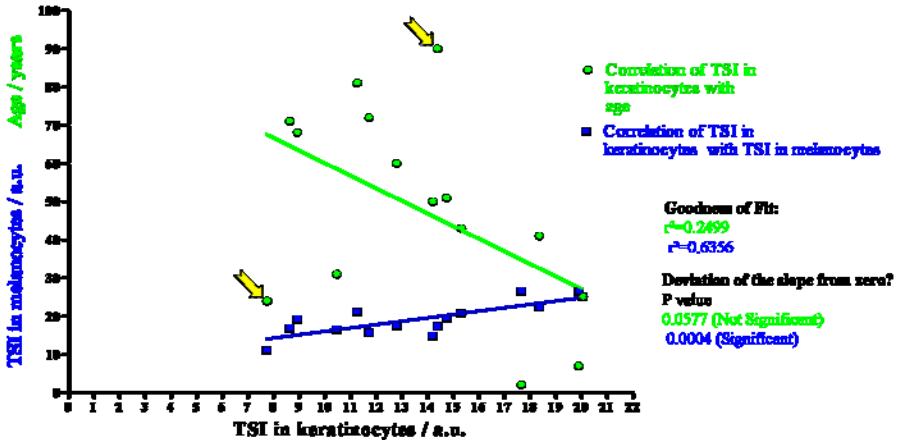

Figure 17: Correlation of mean telomere signal intensities (TSI) measured in keratinocytes with: the mean TSI in melanocytes (in blue), and with the age (in green): Both data sets are shown on the same y-axe to indicate in the same graph an obvious correlation of the telomere length between two different cell types (significant slope, and better r^2 goodness of fit), unlike the weak correlation of telomere length and age (non-significant slope, and less good fit of data with some extreme outliers indicated with yellow arrows). For the simplicity only correlation of keratinocytes with melanocytes is shown in this example, although even better correlation was observed between mean TSI of dermis and melanocytes ($P<0.0001$, $r^2=0.7185$).

3.2.4 Inter-personal telomere length variations

Despite the fact that overall telomeric DNA was hardly lost while aging we had observed a large telomere length variation between different donors of similar age. To examine this in more details and to exclude that the observed inter-personal heterogeneity was due to sample selection from different body sites, we next compared skin samples from 9 different donors (from the age of 32 to 77) which all derived from the upper side of the hand. Calculating the mean from 5 to 9 individual areas per section and verifying the reproducibility on consecutive sections in a second hybridization experiment, these samples confirmed the above results (figure 18A and 18B). In all specimens, the telomeres of the epidermis were shorter than those of the dermis and in both cases we did not find a statistically significant age-dependent decline neither for the epidermis (p value 0.5169) nor for the dermis (p value 0.5042).

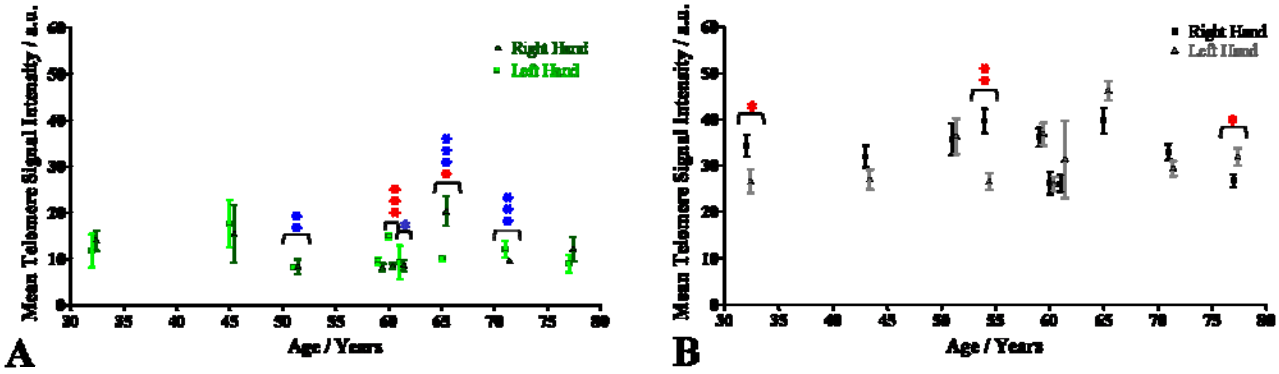

Figure 18: Graphic presentation of the mean telomere signal intensities in skin samples from the upper part of the right and left hand of: A) epidermal keratinocytes and **B)** dermal fibroblasts. Note that the differences between telomere lengths (signal intensities) in samples from the left and right hand of the same donor are statistically significant (*p<0.05, **p<0.01, ***p<0.001, *different variances – F test, *different length – T test). Donor age is indicated in the X-axis.

From all 9 donors biopsy samples from both hands were available. When comparing telomere lengths in the epidermis of skin biopsies from the left and right hand of the same donor only 4 showed comparable values while clear differences existed for the other 5 samples (two samples with significantly different mean telomere signal intensities, and three additional with significantly different variances) (see figure 18A). Similar results were obtained for the dermis (see figure 18B). Here only 3 samples showed very similar values while 6 differed (three samples with significantly different mean telomere signal intensities). Thus, besides an inter-personal heterogeneity,

telomere length in the epidermis and dermis in some samples varied strongly between different though largely equivalent sites of the same person.

3.2.5 Intra-personal telomere length variations

While analyzing telomere length in the skin from the two hands, intra-personal telomere length heterogeneity became evident even within different areas of the same section. To investigate whether this was a more common phenomenon and whether this may be age-related, 15 skin samples from additional donors were analysed. On average 8 areas per section were analyzed, and as summarized in figure 19, slight differences, were common to all individuals (in most cases the coefficient of variation of telomere signal intensities in the epidermis was 0.16-0.21). However, in some skin samples, we found differences largely exceeding this normal variation (variation coefficient of a 24-, 51-, and 90-year-old donors was 0.27, 0.37, and 0.33 respectively). To exclude staining variations, we re-verified the results by analyzing the same regions on serial sections.

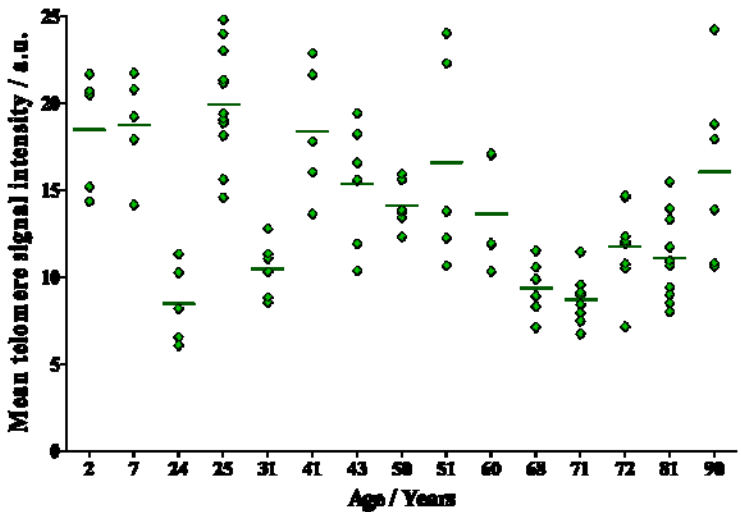

Figure 19: Graphical presentation of intrapersonal differences in telomere length in keratinocytes from 15 donors. Each rhombus represents the mean of an individual area on the section, and the mean of all areas is indicated with a line. Note the high variations in most of the samples, as well as extreme difference in some.

In 6 samples of different-age donors we even identified small areas within the epidermis where different-size groups consisted of basal keratinocytes as well as the corresponding suprabasal differentiated cells, that showed significantly reduced signal intensities in direct neighbourhood to cells with strong signal intensities. One of the most drastic examples is presented in figure 20. Interestingly, the reduced telomere length was restricted to the keratinocytes while the melanocytes (identified as vimentin-

positive cell within the basal layer of the epidermis) and the dermal fibroblasts (underneath the epidermis) showed similarly strong signal intensities in both areas.

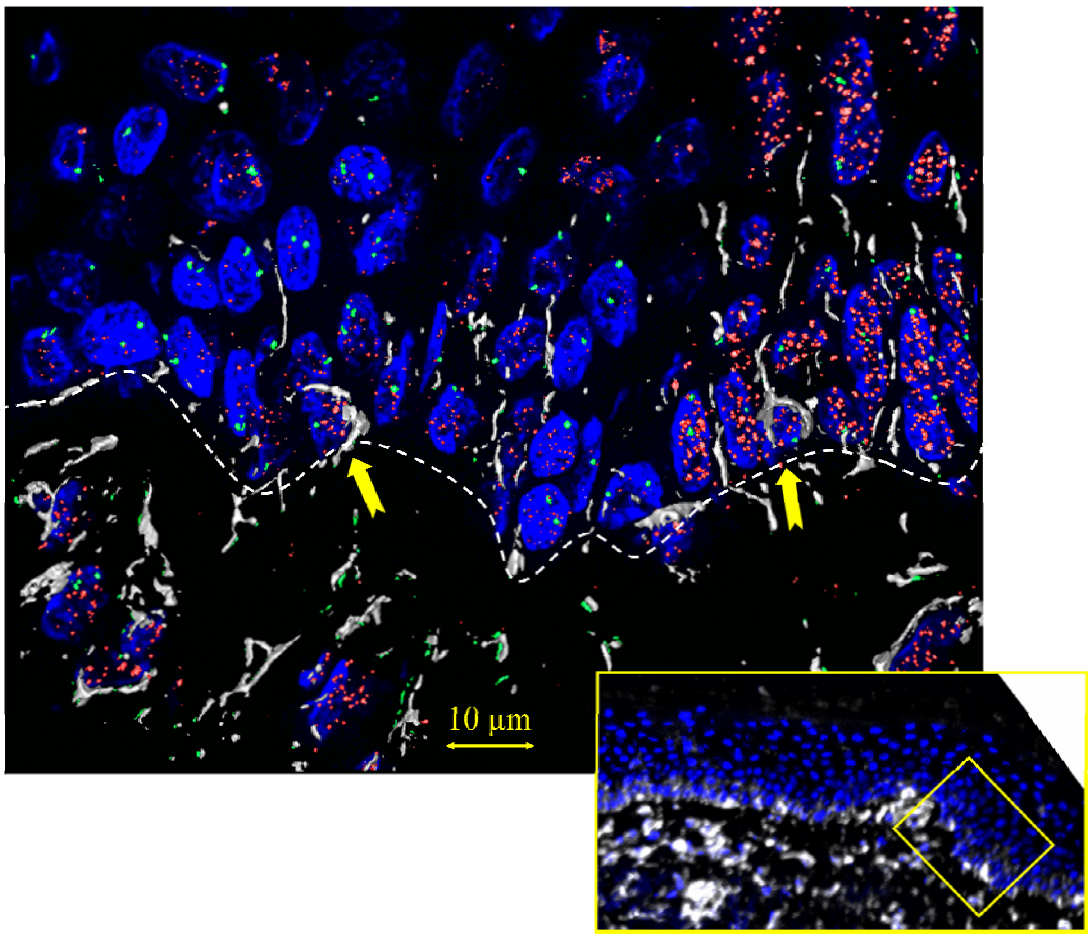

Figure 20: Accelerated telomere erosion in discrete area of human epidermis.
Human skin stained for vimentin (gray), DAPI (nuclei in blue), telomeres (red), and centromeres (green). The basement membrane zone is indicated with the white dashed line. Melanocytes are pointed out by yellow arrows. Note the extreme difference in telomere signals in the two areas and that differences in telomere length are restricted on epidermal keratinocytes. Image is acquired at high magnification (63x objective), and the scale bar is indicated. Insert below right shows the larger region of the skin with normal morphology as it is visualized at low magnification (10x objective). Yellow square on the insert shows the position of the image taken at higher magnification.

To exclude that this was a staining artefact the same sections were re-hybridized for centromeric DNA. This clearly demonstrated that centromeres in all cells (with short and long telomeres) stained equally strong. In addition, to determine whether all telomeres were still present, although shortened, were counted telomeres in all cells. The number of counted telomeric signals did not differ, the average was 20 signals per cell in nuclei with short as well as nuclei with long telomeres (figure 21). This verified

that the telomere length is the only difference between two areas. Thus, accelerated telomere loss occurs and is maintained in discrete areas of the epidermis.

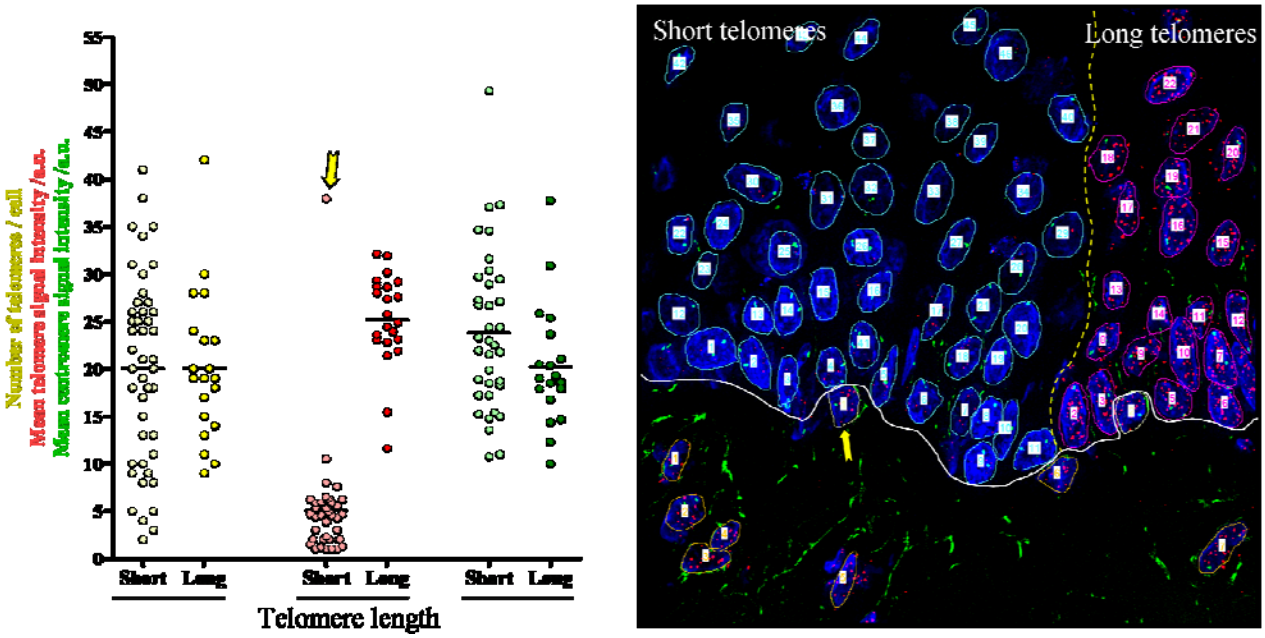

Figure 21: Additional characterisation of region with accelerated telomere shortening indicates the same number of telomeres and good centromere hybridisation efficiency.
A) Dot plot where each dot represents one nucleus from the left (short telomeres) and from the right side of the image in B) (normal, long telomeres). Quantified numbers of telomeres per nucleus (in yellow), mean telomere staining intensity (in red), and mean centromere 7 staining intensity per cell (in green) show that the two regions significantly differ only in telomere length demonstrating that this is not a staining artefact. **B)** Human skin stained for telomeres (red), centromeres (green), and DAPI (nuclei, in blue). The basement membrane zone is marked by a straight line. Note the extreme difference in telomere signals in the two areas (yellow dotted line separates the two groups of cells); and that telomere lengths differences are restricted to the epidermal keratinocytes. The melanocytes that were analysed in addition to the keratinocytes with short telomeres, still exhibit long telomeres (pointed out by the yellow arrow on the graph and on the image).

3.2.6 Correlation of accelerated telomere erosion, p53 and 53BP1

To further characterise regions with significantly reduced telomere length, we asked whether these areas would also be characterised by other changes, i.e. whether damage-dependent proteins would be expressed. Damage signalling through the p53 tumour suppressor protein pathway is known to occur due to experimental disruption of the telomere loop structure (reviewed in Kosmadaki and Gilchrest, 2004). Extremely shortened telomeres could be dysfunctional and therefore cause the G1 cell cycle arrest mediated by p53. Moreover, p53 binding protein (53BP1) was described to recognize regions of DNA double strand breaks (DSB) as well as dysfunctional telomeres (Ward et al., 2003). To visualize locations of DSB we stained for 53BP1, and to check whether signalling for the G1 arrest was activated, we stained for the product of the p53 gene.

As exemplified in figure 22A, p53 is strongly expressed and localised in nuclei with an accelerated telomere erosion (right side of the image). Also 53BP1 was concentrated in stronger foci in the same region (figure 22B). Since some foci were present in few keratinocytes with normal telomeres, we quantified telomeres, p53, and 53BP1 staining intensities within each nucleus. For this, nuclei were divided in two groups: those on the left side of the figure 22A and 22B and of the graph (figure 22D) with normal telomere length, and those on the right side with extremely shortened telomeres. This quantification confirmed that the difference in intensity of 53BP1 foci, and p53 expression was significantly different between the two groups. In addition, we compared telomere length of each cell with the presence of 53BP1 foci (figure 22E), and the p53 status (figure 22F). This comparison demonstrated an inverse correlation or telomere length and the presence of 53BP1 foci as well as p53 staining intensity. Actually - the shorter the telomeres – the stronger was the p53 staining, and the number and intensity of p53BP1 stained foci. Thus, staining of both proteins was strongest in cells with shortest telomeres (~20% of cells indicated with the red rectangle in images 22E and 22F).

Most importantly, 3D visualization of the region with accelerated telomere shortening revealed strong co-localization of 53BP1 foci with the short telomeres (marked with white arrows on the figure 22H). This strongly indicates that at least some of the telomeres in these cells are uncapped and carry on behave like DSB.

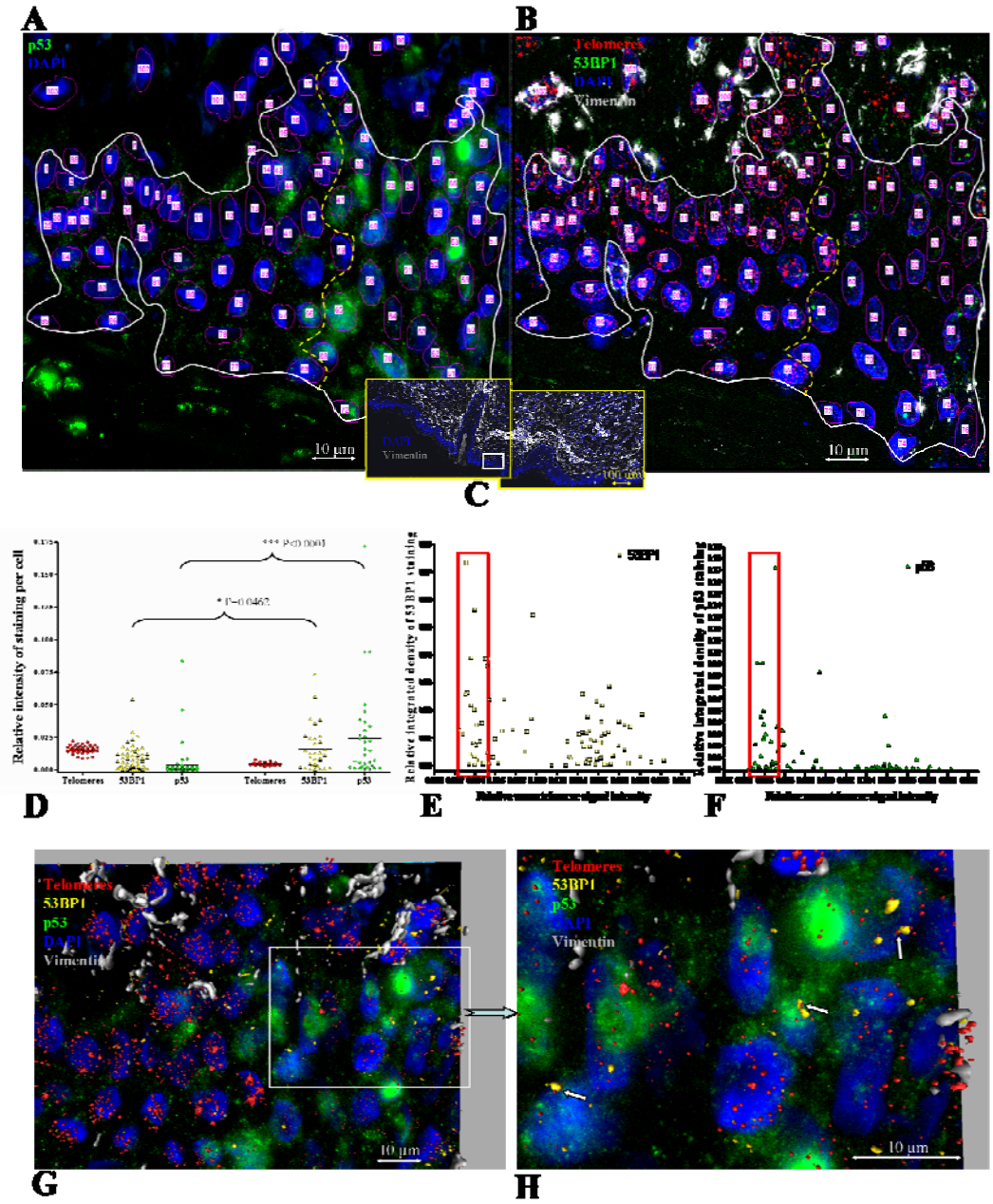

Figure 22: Correlation of accelerated telomere erosion with p53 and 53BP1.
A) p53 stained region (pseudo colored in green) of the epidermis with an accelerated telomere erosion **B)** The same skin section is restained for telomeres (red), 53BP1 (green foci), vimentin (dermis and all non-keratinocytes in gray), and DAPI (nuclei in blue). White line marks those keratinocytes that were further analyzed. The yellow dotted line separates the two groups of cells: those with normal telomere length (left side) and those with short telomeres (right side). **C)** Low magnification (10x objective) of the analysed skin. The marked area indicates the position of the p53 stained region with short telomeres from A) and B). **D)** Dot plot of the quantified telomeres, p53, and 53BP1 staining intensities. Each dot represents one nucleus from A) and B). The left side of the plot represents cells with longer telomeres, significantly less 53BP1 foci, and much weaker p53 expression (on the left side of the image A) and B) also) when compared with cells from the right side of the plot (Mann Whitney test determined significance for the difference between medians) **E)** Dot plot representing the correlation of telomere and 53BP1 staining, and **F)** telomere and p53 staining. Note that the cells with shortest telomeres (marked with the red rectangle) are the ones with strongest 53BP1 foci and p53 expression. **G)** 3D visualization of the region with accelerated telomere shortening; telomeres (red), 53BP1 (yellow) and vimentin (gray) are visualized in 3D in front of projected image of p53 staining (green), and DAPI (blue). White rectangle indicates the region presented at higher magnification in image **H)** showing that the strong 53BP1 foci co-localize with the short telomeres (marked with white arrows).

Since we observed a correlation between intensity of p53 staining and telomere length, i.e. in the regions with accelerated telomere erosion, we used p53 immunostaining to screen through a larger number of samples to address whether the number of regions and intensities of p53 staining may be increased with age, and whether it may be increased at certain body sites, i.e. may correlate with sun exposure. We analysed 30 normal skin samples originating from different age donors, and different body sites as well as 3 different Squamous Cell Carcinoma (SCC) samples (all presented in the table 3).

Table 3: Distribution of p53 stained regions in the epidermis of different donors

No. Donor	Age (y)	p53 staining intensity*	Gender	Site of the skin sample	Potential sun exposure
1	7	0	m	Foreskin	rare
2	24	0	f	Breast	rare
3	25	0	m	Buttock	rare
4	31	0	f	Stomach	intermittent
5	32	0	f	Genital	rare
6	38	0	m	Foreskin	rare
7	41	0	f	Head	continuous
8	41	0	m	Thigh	rare
9	49	2	f	Head	continuous
10	50	0	m	Back	intermittent
11	58	1	f	Back	intermittent
12	60	1	f	Cheek	continuous
13	66	0	m	Breast	intermittent
14	67	0	f	Stomach	intermittent
15	67	3	f	Back	intermittent
16	68	4	m	Shoulder	intermittent
17	69	0	m	unknown	unknown
18	70	3	m	Thigh	rare
19	70	2	f	Upper arm	intermittent
20	71	4	m	Temple	continuous
21	71	0	m	Back	intermittent
22	72	0	unknown	Neck	continuous
23	72	3	m	Nose	continuous
24	75	1	f	Back	intermittent
25	77	0	m	Shoulder	intermittent
26	81	2	m	Back	intermittent
27	83	0	f	Cheek	continuous
28	84	4	f	unknown	unknown
29	84	0	f	Head	continuous
30	90	2	m	unknown	unknown
SSC, 31	84	3	f	unknown	unknown
SSC, 32	91	4	f	unknown	unknown
SSC, 33	67	4	m	Ear	continuous

*** 0** demarcates no p53 stained regions in the skin section of a certain patient, **1** is very weak staining of one region, **2** is clear staining of one up to 2 smaller regions, **3** is strong staining of two to three larger regions (20-30 cells in the basal layer), and **4** is a strong staining of 3 and more large parts of the skin section

Since the size of the p53 positive regions, as well as the intensity of p53 staining differed between samples, a semi quantitative validation was carried out using a quantification scheme as outlined in table 3. In 17 out of 30 skin samples there were no p53 positive regions, and 3 of 30 samples contained one weakly stained region per section. In 4 samples there was a clear staining in one to 2 regions of less than 20 cells in diameter (number of cells in the basal layer). In 3 samples the strong staining of two to three larger regions (20-30 cells in diameter), and in other 3 skin samples a strong staining of 3 and more larger parts of the skin section was identified (up to 100 cells in diameter).

The same values are presented in the figure 23A demonstrating correlation of the number of regions and intensity of p53 staining with age. Note that the each patient is presented as a dot in the graph. Interestingly, up the age of 67 there was an only one out of 14 analysed skin samples with the stronger p53 stained regions. Those regions occurred much more frequently in samples from older donors, which suggested accumulation of genetic damage with age. As the sun exposure could be a source of damage, we analysed whether there was a correlation of p53 stained regions and the potential sun exposure (figure 23B). When the skin samples are grouped in 3 groups according to their potential sun exposure, it appeared that the p53 stained regions occurred mostly in intermittently and continuously exposed skin. In the rarely sun exposed group only one out of 7 skin samples had detectable p53 stained regions.

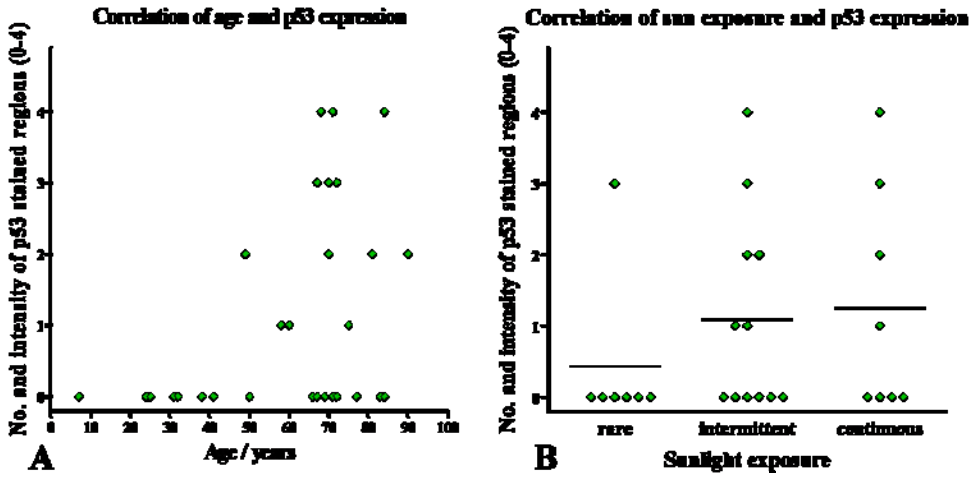

Figure 23: The number and intensity of p53 stained regions with accelerated telomere shortening in the epidermis is increased in older patients, and is also proportional to the increased sunlight exposure. A) Dot plot represents the number and intensity of p53 stained regions of different age donors **B)** Dot plot of p53 staining in three groups of skin samples sorted according to the potential sunlight exposure. Note that each dot represents one skin sample, and the line in B) indicates mean p53 staining of each group.

3.2.7 Damage as a major contributor to accelerated telomere loss

Since the above studies demonstrated that telomere shortening had occurred at distinct sites and correlated with defined signs of damage (p53 up-regulation, 53BP1 foci), we hypothesised that also the telomere length heterogeneity seen in the different age donors may in part be due to damage-dependent accelerated telomere erosion – damage telomere length maintenance. To test this we searched our samples for skin from chronically UV-exposed donors, i.e. a sailor and a farmer. Both donors became conspicuous because of skin carcinomas. Comparing their epidermis with that from the buttock of a inconspicuous donor, we found significantly shorter telomeres in their epidermis, but not necessarily in their dermal fibroblasts (figure 24A). Most interestingly, in a hair follicle present in the skin section from the sailor, telomere length increased with increasing distance from the surface (figure 24B and 24C).

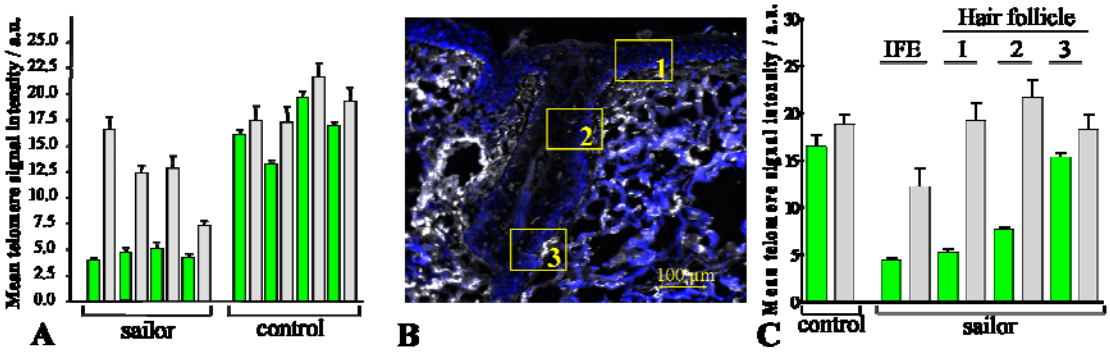

Figure 24: A) Graphic presentation of telomere signal intensities in sections from skin derived from a sailor and from the buttock of a 44 y-old control donor (epidermis in green and dermis in grey) 4 different areas were analyzed independently. Note that the telomeres in different areas of the sailor's epidermis are generally very short while the dermis is less affected. **B)** Skin from the sailor showing a hair follicle (vimentin in grey, telomeres in red and nuclei in blue). The numbered boxes mark the three areas measured for telomere signal intensities. **C)** Graphic presentation of the telomere signal intensities in control skin (as in A but mean value of the different areas), the interfollicular epidermis (IFE) and the three areas (1 to 3) of the sailor's hair follicle indicated in B.

3.2.8 Damage on telomeres is less pronounced in deeper parts of epidermis

3.2.8.1 Telomeres are longer in hair follicles then in interfollicular epidermis

As the above results suggested that UV radiation may contribute to telomere shortening by affecting particularly the most exposed (outer) parts of the epidermis, we reasoned that this should be more frequent. Therefore, we next searched for properly preserved hair follicles (HFs) in different skin samples. We identified 21 HF (from 15 different donors) that could be analyzed for signal intensities at different depths from the surface. In none of the samples were telomeres significantly longer in the outermost interfollicular epidermis (IFE) as compared to different depth into the HF. 7 of them showed a similar telomere length throughout. In 14 of the 21 HF, however, we found an increase in telomere length with distance from the surface. Linear regression and the significance of deviation from zero confirmed significant telomere shortening in the keratinocytes closer to the outer surface in all 14 HFs (representative example of the HF and appropriate regression is presented in the figure 25).

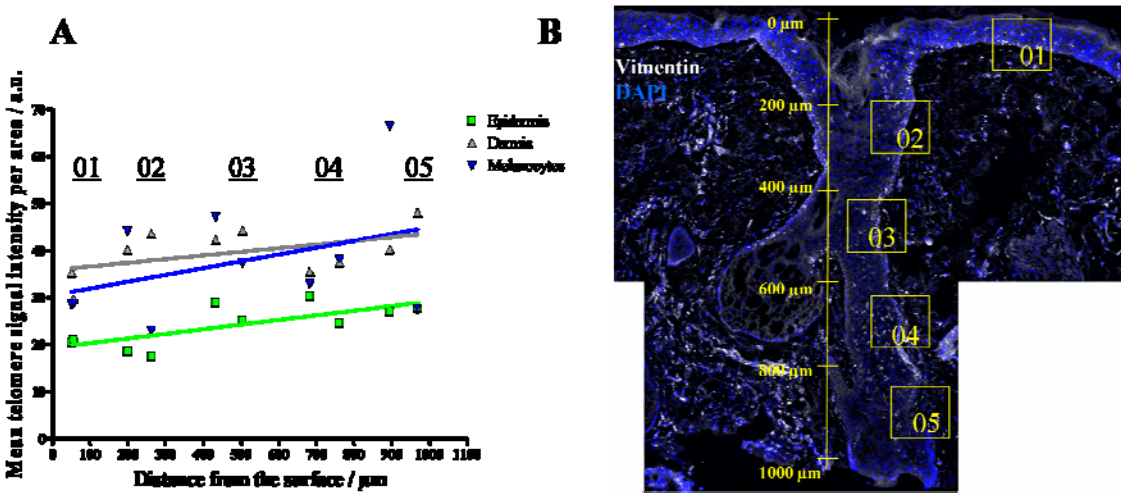

Figure 25: Increase in the telomere signal intensity with distance from the skin surface in 5 regions of the hair follicle's (HF) epidermis, dermis and melanocytes.
A) Graphical presentation; telomeres were measured twice in each region; in the part of the region that is closer, and in the part distant from the surface. Linear regression confirms the tendency to have longer telomeres deeper in the skin (the slope for keratinocytes – green regression - is significantly non-zero, p=0.0153). **B)** Mosaic image of the HF analyzed in A). Images were captured with the 10x objective, composed into a mosaic, and marked with rectangles that indicate positions of 5 regions where telomere signals were analysed in the HF by capturing images at high resolution (63x objective, images not shown). Distance from the surface is indicated (vertical scale bar).

Taken together, two thirds of the samples showed a positive correlation between telomere signal intensity and distance from the surface. Even in the dermal fibroblasts and melanocytes, although both have in general longer telomeres than the keratinocytes, we observed a similar increase in telomere length with distance from the surface. This indicated that if telomere erosion is due to UV radiation it occurs in both epidermis and the dermal compartment.

3.2.8.2 Telomeres are frequently longer deeper in rete ridges

Human skin does not contain many hair follicles but is often characterized by a significant interdigitation of the epidermis and the dermis, the so-called rete ridges. Since some of the rete ridges deeply invaginate into the dermis, we reasoned that also the lower parts of these rete ridges may be protected from extensive UV radiation and, therefore, exhibit longer telomeres than the upper parts. From 12 different skin samples at least 4 but in general 7 to 8 rete ridges per sample were analyzed and the mean of the different areas is presented in figure 26. In 5 of these 12 samples the telomere intensity measures at the lower and upper part of the rete ridges were highly comparable. In the other 7 samples there was indeed tendency towards longer telomeres in the lower parts of the rete ridges. Actually, 3 samples showed statistical significance, thus, accelerated telomere erosion does not necessarily affect the overall epidermis but individual areas and particularly those most exposed to UV radiation.

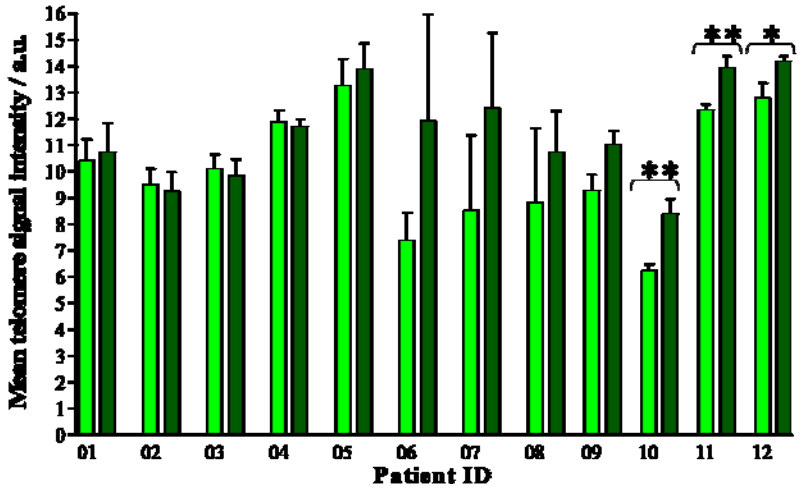

Figure 26: Telomeres are longer deeper in rete ridges. Graphic presentation of the mean telomere length in the upper (light green) and lower (dark green) part of rete ridges found in skin samples from 12 different donors. Note that three samples (No.10-12) show a statistically significant difference in telomere signal intensities.

3.2.9 Influence of the chronic UV exposure on telomere length

From the above result it was suggested that UV irradiation might play an important role in accelerated telomere erosion. To test this further, we analysed skin from 5 donors who had a history of chronic exposure to UV radiation. The affect of UV irradiation was confirmed by the presence of cyclobutane pyrimidine dimers (CPDs). CPD-retaining basal cells (CRBCs) were counted in each of five samples to determine the average level of UV damage. These samples derived from different regions of the head: two from cheeks, two from ears, and one sample from the scalp. They were compared with samples from donors without history of massive UV exposure and without detected CRBCs. In addition, these samples derived from sites generally protected from UV exposure: four from groin and one from the buttock. Samples were collected by Dr. R.Greinert, and Dr. B.Volkmer Dermatology Center, Elbeklinikum, Buxtehude, and provided as sections with and without CPD staining.

Telomere length measurements determined higher intrapersonal variations in the epidermis of the sun exposed donors as compared to the control. Moreover, regions with accelerated telomere shortening, i.e. very short telomeres were identified in two samples (number 1, and 3 in figure 27A and 27C). One region with shortened telomeres from the sun-exposed skin is shown in figure 27A (sample number 1 in figure 27C). Figure 27B presents one of the regions from the sun-protected skin where we did not locate larger variations in telomere length (sample number 6 in figure 27C).

Telomeres were on average longer in the rarely sun exposed skins in all cell types, and the difference was significant for fibroblasts as summarised in figure 28.

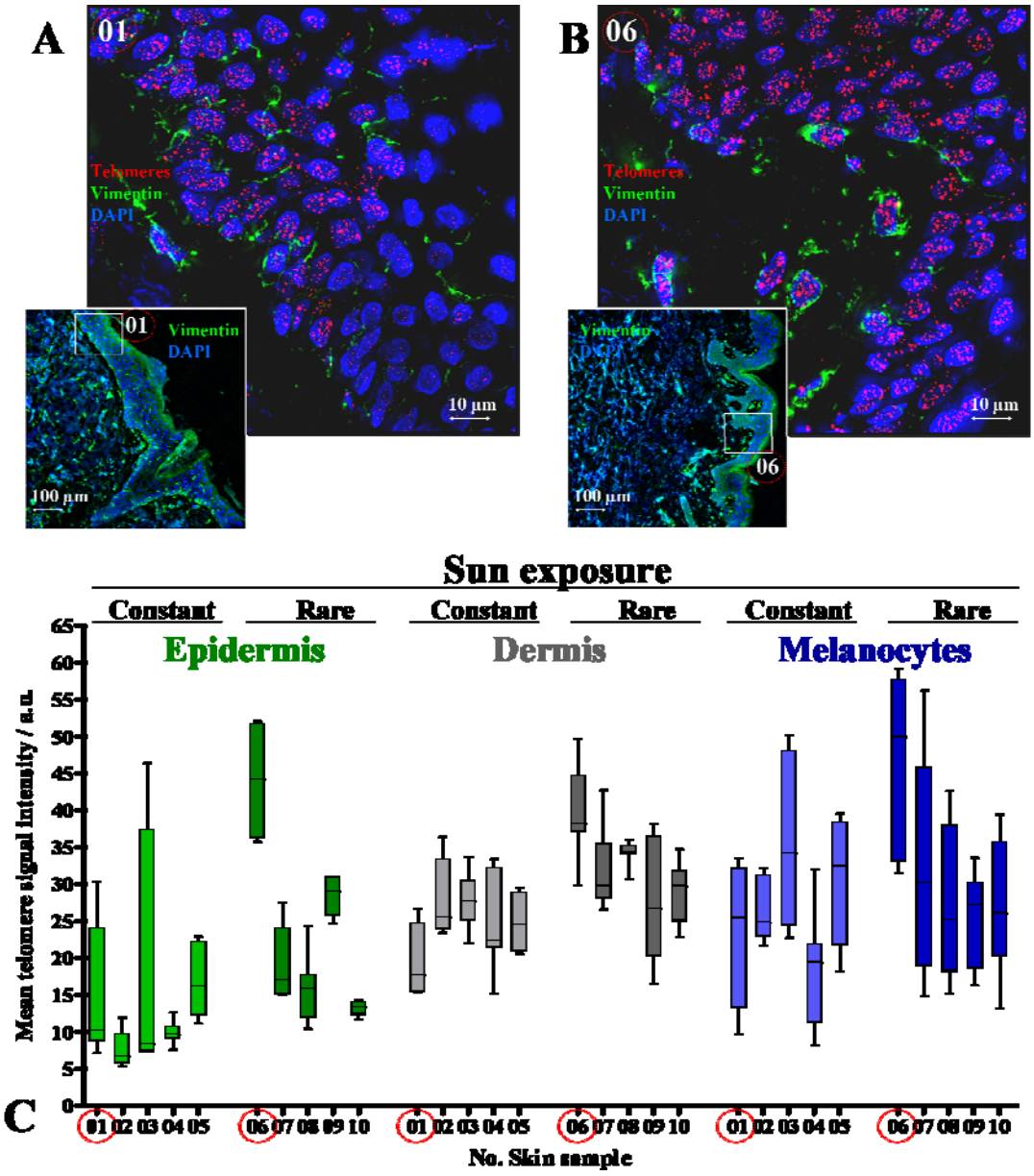

Figure 27: High intrapersonal variations and shorter telomeres in the sun exposed skin versus non-exposed skin. A) Skin from the sun-exposed donors (number 01 in the graph C) is stained for telomeres (red), vimentin (dermal fibroblasts and all non-keratinocytes in green), and DAPI (nuclei in blue). Note the accelerated telomere shortening and on average weaker telomere signals than in the **B)** region from a non-exposed skin (sample number 06 in the graph C). Inserts in A) and B) represents parts of the analysed skins visualized at low magnification (10x objective) and rectangle indicates the position of the regions shown in higher magnification above. **C)** Box plot of the mean telomere signal intensities (TSIs) measured in 7 different regions of the skin sections from the each skin sample. TSIs were determined for keratinocytes (green), dermis (gray) and melanocytes (blue) from the constantly sun exposed skins (containing CRBCs) (number of samples 01-05), and from rarely exposed skins (with no CRBCs) (samples 06-10).

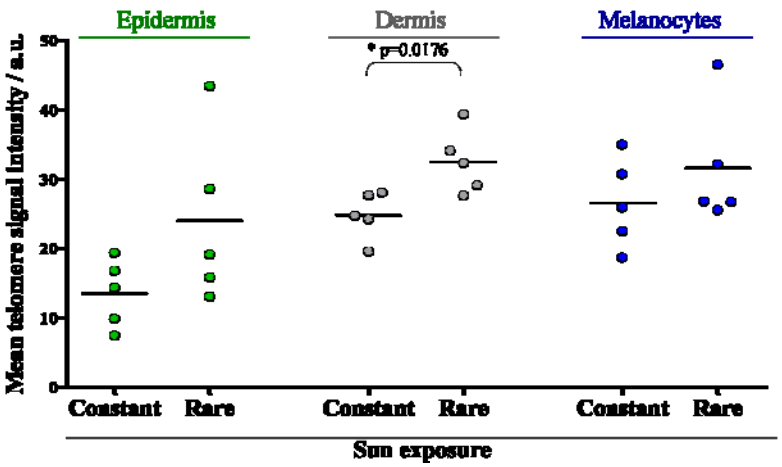

Figure 28: Difference in the telomere length in sun exposed skin versus nonexposed skin. Each dot on the graph represents the mean telomere signal intensity in one skin sample in keratinocytes (green), dermis (gray) and melanocytes (blue) from the sun exposed skin, and from the rarely exposed skins. Note the high variation within each group due to interpersonal differences and the small size of sample (5 donors only per group), nevertheless there is a tendency for longer telomeres in the non-exposed group in the keratinocytes and melanocytes, and significant difference in telomere length in dermis (nonpaired t test, $\alpha<0.05$, *$p<0.05$).

Intriguingly, all 5 exposed samples contained parts of, or complete hair follicles (HFs), which enabled additional analysis of deeper parts of the epidermis. The regression slopes of telomere lengths were determined for each HF. Slopes differed between samples indicating different rates of telomere shortening in different sun-exposed skins. Moreover, as the UV damage was measured in each sample as an average number of CRBCs, it allowed to determine whether there was a correlation between the telomere length regression closer to the surface of the skin and the rate of UV damage. As is it obvious from the figure 29, a strong correlation was determined for keratinocytes. The stronger the UV – damage was, the shorter were telomeres closer to the surface of the skin. Similar results were determined for dermis and melanocytes, although regression was less significant. The most extensive telomere shortening was observed in the sun-exposed sample with the multiple CRBCs, thus with the highest damage.

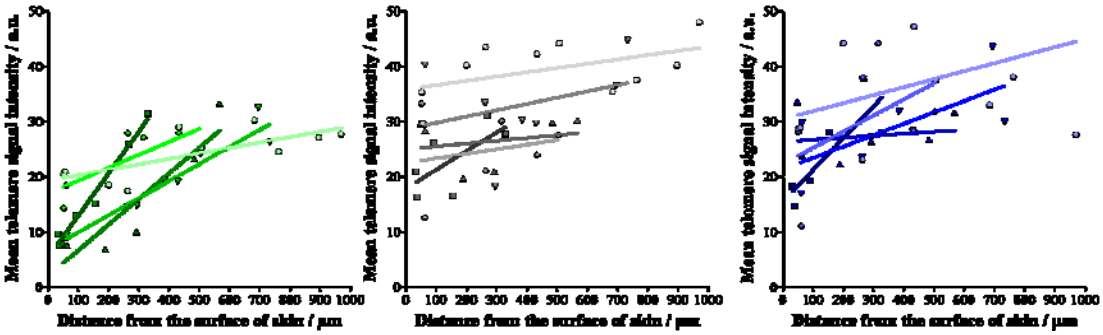

Figure 29: Graphic presentation of the decrease in telomere length closer to the skin surface in **A) keratinocytes** of 5 hair follicles from the sun exposed skin. Note that the different regression slopes are proportional to the amount of damage indicated as the number of CRBCs. Similar correlation was observed for the **dermis** **B)** and the **melanocytes** **C)** although it was less significant then in keratinocytes.

3.2.10 Acute UV exposure and telomere length

Can we prove that UV exposure is causal for accelerated telomere erosion? Since skin from chronically UV-exposed donors showed a significant telomere shortening we asked whether UV radiation is able to cause telomere shortening. To answer this question we established a collaboration with Dr. Annegret Kuhn, DKFZ, Heidelberg, who had access to lupus erythematosus patients and healthy donors who, with ethic approval, were irradiated with a single dose of UV-A and B, or in some cases only one of two as indicated in the table 4. All together 16 different patients were included, 8 of which were lupus, and 8 healthy donors. Skin biopsies were obtained from 2 or 3 different time points up to 14 days after irradiation as described (Kuhn, 2006) and 7µm thick skin cryosections were analysed for telomere lengths.

We did not observe any difference in average telomere length between lupus patients and healthy donors, but the variation between the 8 Lupus patients was significantly higher than between the 8 healthy donors. Interestingly, similar variations in telomere length were not observed in the dermis and melanocytes on the day 1 after radiation (for simplicity only the 1st and 3rd day are shown in figure 30A).

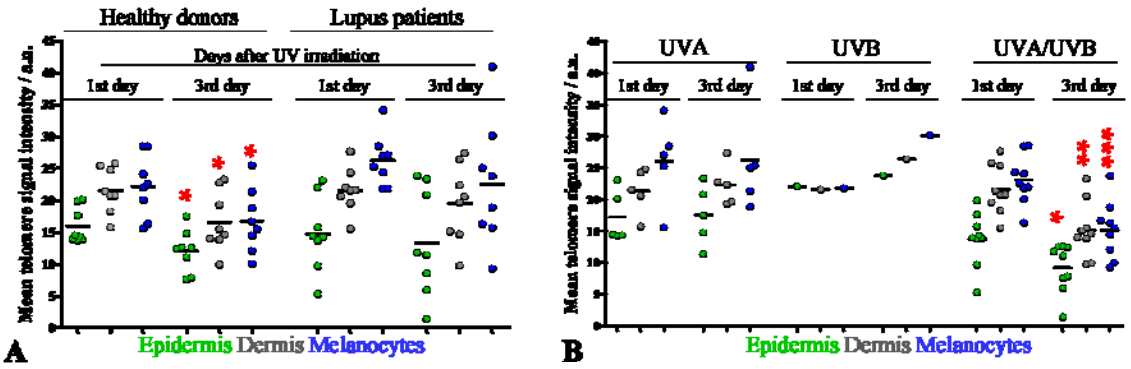

Figure 30: A) Telomere length of UV irradiated skin of Lupus patients slightly differed from that in healthy donors. Average telomere signal intensity (TSI) was measured in keratinocytes, dermis and melanocytes of each donor on day 1 and on day 3 after UV irradiation (UVR). Note that the average TSI is similar in the epidermis of healthy versus Lupus donors. However, the variation of TSI between the Lupus patients is bigger than between the healthy donors (F test, $p=0.0326$, $\alpha<0.05$). **B) Rapid telomere shortening in the skin 3 days after UVA/UVB irradiation.** Five donors irradiated with the UVA on average do not have reduced telomere length on 3rd day when compared with the first day. Only one sample is irradiated with the UVB. Note that the TSI decline is strongest in ten samples irradiated with the combination of UVA and UVB, and this accounts for the epidermis, dermis and in melanocytes. Significance of difference in mean telomere signal intensities between day 1 and day 3 is indicated (non-paired t test, $\alpha<0.05$, *$p<0.05$, **$p<0.01$, ***$p<0.001$)

Another important question was whether different UV irradiation types can differently influence the telomere length. Interestingly, five samples that were irradiated with the UVA on their average did not show decrease telomere length when compared day 3 versus day 1 post irradiation. A significant decline was, however, observed after a combinatory radiation UVA/UVB in the epidermis, dermis and melanocytes. For UVB only one sample from one Lupus patient was analysed for telomere length and here we observed an increase in telomere signal intensity 3 days after irradiation (figure 30B, for simplicity only 1st and 3rd day are shown). How relevant this is, remain to be seen.

From all 16 donors, samples from two or three time points were available for the first 3 days after irradiation. Therefore, we analysed the telomere length regression within first 3 days and determined clear tendency towards telomere length decline in keratinocytes of 13 out of 16 samples (note the negative slope in the table 4). A similar tendency was observed for dermis and melanocytes as it can be observed on the graph of representative four donors (figure 31). If samples from other time points (day 5 to 14) were available, they were also analysed for telomere length and compared with the day 1 as indicated in table 4.

Table 4: Mean telomere signal intensity in keratinocytes from 16 different patients irradiated with UV light.

Patients health	Mean telomere signal intensity in epidermis							Type of UV irradiation	Slope in first 3 days
	Days after UV irradiation								
	day 1	day 2	day 3	day 5	day 6	day 10	day 14		
Healthy	13.73	12.19	7.56**					UVA-UVB	-3.085
	14.2	12.86	12.53					UVA-UVB	-0.835
	13.84		12.49		19.6***			UVA-UVB	-0.675
	17.57		11.04**		11.02*			UVA-UVB	-3.265
	13.9		12.38		15.86			UVA-UVB	-0.76
	19.81		7.81***		6.45***			UVA-UVB	-6
	14.43	13.95	17.45					UVA	1.51
	20.06	17.6	14.74**					UVA	-2.66
Lupus	15.71		11.73					UVA-UVB	-1.99
	5.27	1.91**	1.35*					UVA-UVB	-1.96
	9.65	4.75**	5.92					UVA-UVB	-1.865
	13.64		8.53**					UVA or UVB	-2.555
	14.19		23.28**	15.47				UVA (day 1 and 3), UVA-UVB (day 5)	4.545
	23.08		20.81			16.59**		UVA (day 1 and 3), UVA-UVB (day 10)	-1.135
	14.34		11.37				12.35	UVA (day 1 and 3), UVB (day 14)	-1.485
	21.99	14.74***	23.8					UVB	0.905

*Mean telomere signal intensity was measured in different regions of two serial sections from the each patient and for the each time-point. For simplicity, only epidermis is shown in the table. Samples from the 2nd and the 3rd time-point were compared with the sample from the day 1, and statistical significance of difference in mean telomere signal intensities was determined with the unpaired t-test (*p<0.05, **p<0.01, ***p<0.001, α<0.05).

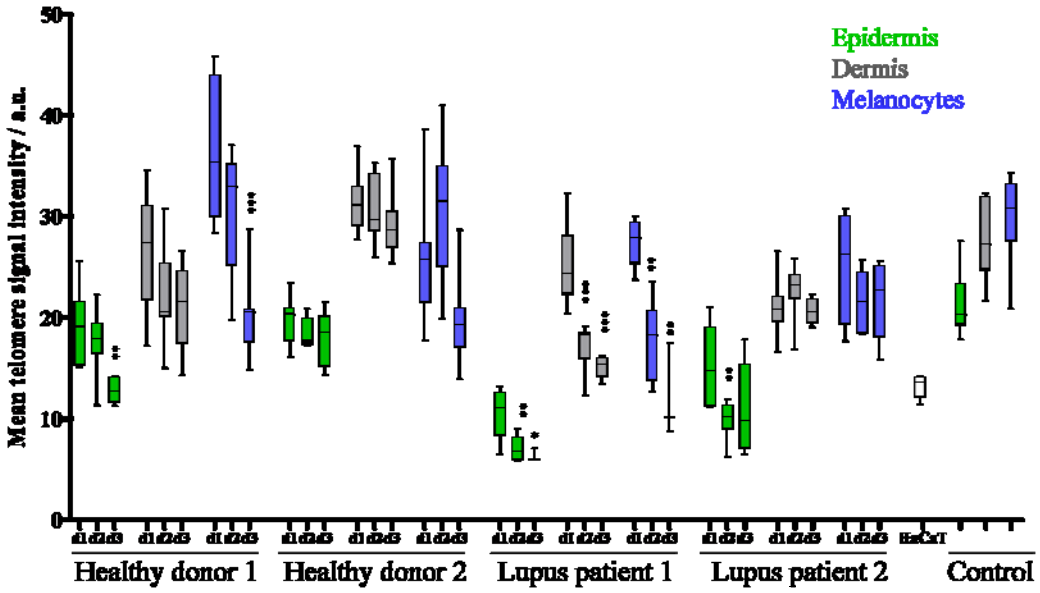

Figure 31: Acute UV irradiation causes telomere shortening within first 3 days after irradiation. In two representative healthy, and two Lupus patients mean telomere signal intensity was measured in 7 different regions of 2 serial sections from each donor, and for each time point. Days after irradiation are indicated with d1, d2, d3. Telomeres were measured in keratinocytes, dermis, and in melanocytes. Note the significance of telomere shortening day 2 or 3 when compared to day 1 of the three donors, and a clear tendency towards telomere length regression within first 3 days in all donors and cell types. HaCaT cell line with telomere length of 4 kb, and sun protected human skin ~8 kb were used as controls. Asterisks indicate the result of non-paired t test (α<0.05, *p<0.05, **p<0.01, ***p<0.001).

Unexpectedly, significantly longer telomeres were identified in samples from two time points in two donors out of a total 30 samples from different time points of 16 donors. Since all results were confirmed with consecutive sections, hybridisation artefacts can largely be excluded. However, we can not exclude higher intrapersonal differences in telomere length of some donors; even if telomeres were shortened therefore, due to high variation in telomere length the influence of irradiation would not be detected.

The sensitivity to UV damage can also differ between different donors, and could explain why in some donors only slight telomere shortening was observed, while in others UV caused extreme telomere shortening.

To check whether there is a difference in the overall UV damage between the donors, we analysed samples from 4 donors for the presence of UV induced DNA double-strand breaks. We stained skin sections from different time points for 53BP1 and γH2AX proteins, which localize to sites of DNA double-strand breaks. Interestingly, samples with increased telomere shortening within the first 3 days after irradiation also showed many more 53BP1 and γH2AX co-localized foci, and much stronger γH2AX nuclear staining of large number of cells. Figure 32 shows the part of the skin stained for 53BP1 and γH2AX from a non irradiated control skin (A and A'), a donor with non-significant telomere length decline (B and B'), and a donor with accelerated telomere shortening within the first 3 days post irradiation (C and C'). As the patients were treated in the same way with the same UVA/UVB dose, were of the same skin type, and the sections were stained and visualized at the same time and with the same conditions, we have to postulate that the observed differences are likely due to non-skin type-dependant differences in sensitivity to UV-light.

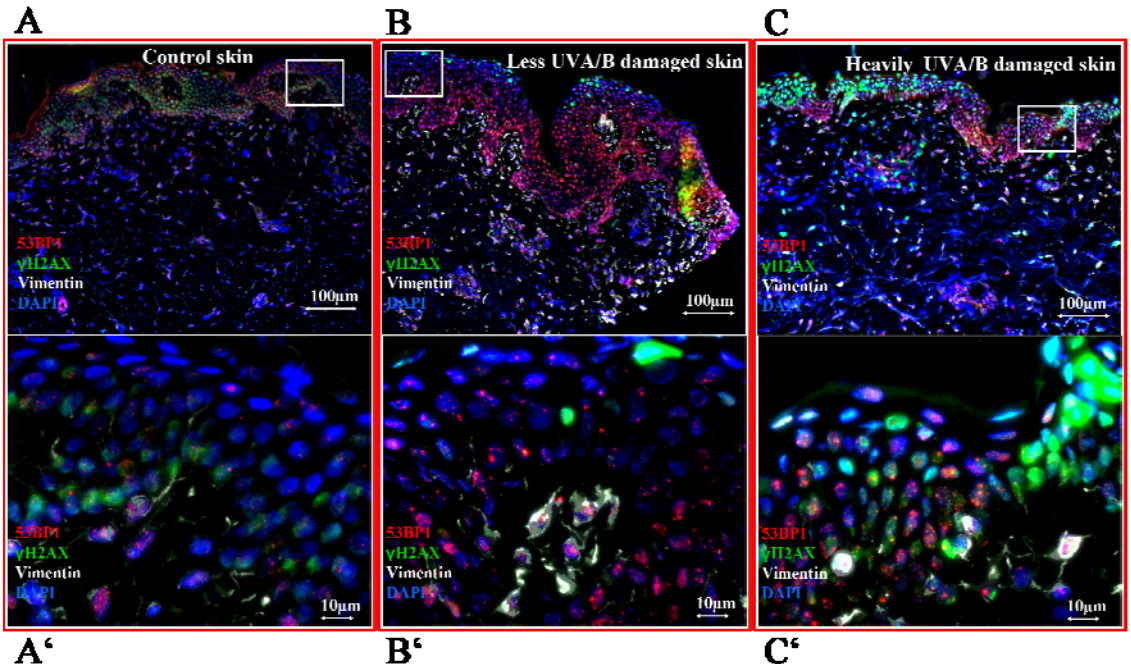

Figure 32: Different sensitivity on UV radiation, in two patients. The control skin and two skins from the day 1 after UVA/UVB irradiation were stained for 53BP1 (red) and γH2AX (green). More 53BP1 and γH2AX co-localized foci with stronger intensity, and much stronger γH2AX expression in more cells is obvious on the right panel, when compared with the middle panel, and especially when compared with the left – control skin from intermittently sun exposed 31 year old female trunk. 100µm bar is indicated on upper images that were acquired at low magnification (10x objective), and 10µm bar is marking lower set of images (63x objective, Z-projected 3D image).

3.2.11 Telomere erosion in human epidermis proximal to wounds

3.2.11.1 Telomeres in epidermis are shorter proximal to chronic wounds

Chronic wounds are regions of the skin constantly exposed to damage through e.g. bacterial infiltrations, or oxidative damage due to constant inflammation. To investigate how this would relate to telomere shortening we analysed four skin samples with chronic wounds, and compared them with the healthy skin from the same patients, both kindly supplied by Dr. Sabine Emig, Dermatology, Köln. A clear telomere erosion was observed in the epidermis of four samples; telomeres were shorter proximally to the wound. Interestingly, telomeres were not only shorter in those keratinocytes that were directly in the wounded area, but also in keratinocytes that were 2-3 mm distant from the wound edge. Only further away telomere length was again comparable to that of the normal skin from the same patient. Telomere shortening was accompanied with increased thickness of the epidermis, indicating an abnormal proliferation in the wound margins. Surprisingly, we did not find any telomere shortening in the dermis. On the contrary, in one sample telomeres in dermis were even longer in the region proximal to

the chronic wound. Mosaic images of a pair of the healthy skin (figure 33A), and skin with the chronic wound (figure 33B), as well as quantification of telomere length is shown in the figure 33C. The data from all four samples are summarised in figure 34.

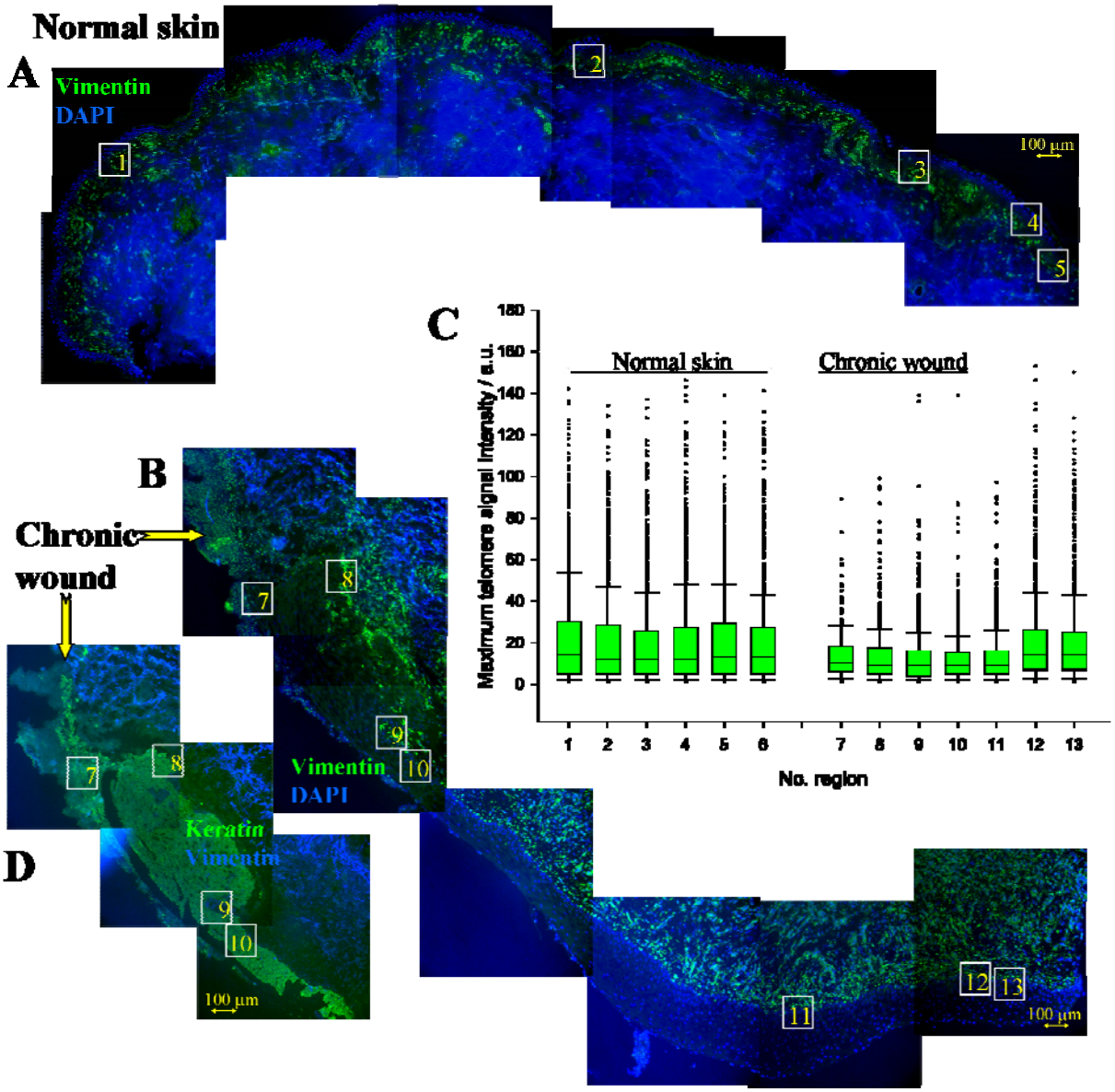

Figure 33: Telomere erosion in human epidermis proximal to chronic wound A) Mosaic image of normal human skin stained for vimentin (dermis in green), and DAPI (nuclei in blue). **B)** Mosaic image of the part of chronic wound and its neighbouring skin stained for vimentin (dermis in green), and DAPI (nuclei in blue). **C)** Box plot of the maximum telomere signal intensities in the epidermis of the normal skin (areas number 1 to 6), and in the skin from the same patient but proximal to the chronic wound (areas 7 to 13). Note that the telomeres in the close proximity of the chronic wound (areas 7 to 11) are much shorter then those distant from the wound (areas 12 and 13), or those from the normal skin. **D)** Image of the wound area taken from serial sections, and stained for pan-keratin (epidermis in green), vimentin (dermis in blue) to verify the epidermal origin of the analysed skin. All images are captured with the 10x objective, composed into a mosaic, labelled with 100 µm scale bars, and marked with rectangles that indicate the positions of regions that were quantified for telomere signal intensity by capturing images with higher magnification (63x objective).

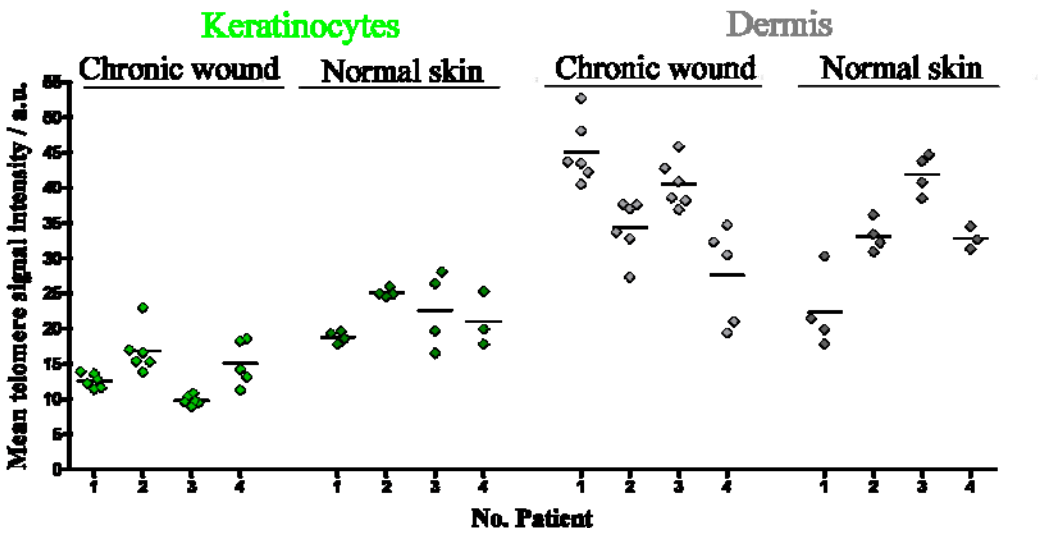

Figure 34: Telomeres are shorter in keratinocytes, but not in the dermis of chronic wounds compared to normal skin from the same patient;
Each dot on the graph represents the mean telomere signal intensity in one region of the skin section in keratinocytes (green), and in dermis (gray). Patients are indicated with numbers 1-4. Note the clear tendency of longer telomeres in keratinocytes of normal skin as compared to keratinocytes in or close to the wound area, while no difference are seen in fibroblast with the exception of sample ID 1.

3.2.11.2 Telomeres are less shortened proximally to acute wounds

To investigate whether short term damage can also cause telomere shortening, we additionally analysed acute skin wounds. The important difference between chronic and acute wounds is the inflammatory phase of the wound healing, which is abnormally prolonged in chronic wounds, while it only lasts until fifth day after acute wounding. As inflammatory cells produce reactive oxygen species which could be responsible for local tissue damage this may cause telomere shortening and thus a certain effect on telomere length may also be seen in acute wounds. Unfortunately, such tissue samples are rare and we were only able to analyse one sample from a day 1 wound, and two samples from day 5 wounds. The samples are kindly provided by Dr. Sabine Werner, ETH, Zürich. One example of day 5 wound is shown in figure 35. Telomere length from the one day-old wound did not differ from the surrounding skin. Small differences were observed on day 5 after wounding on both wounds. The telomeres were shorter around wound edges where re-epithelialisation took place and this correlated with an increased number of what appeared to be inflammatory cells in the surrounding dermis. In the neighbouring normal skin there were no signs of inflammation, the epidermis was not hyperplastic and telomere length in the epidermis was slightly increased. Interestingly, telomere length in dermis was also not decreased proximally to the acute wound (figure 35D). The data from three acute wounds are summarised in figure 36.

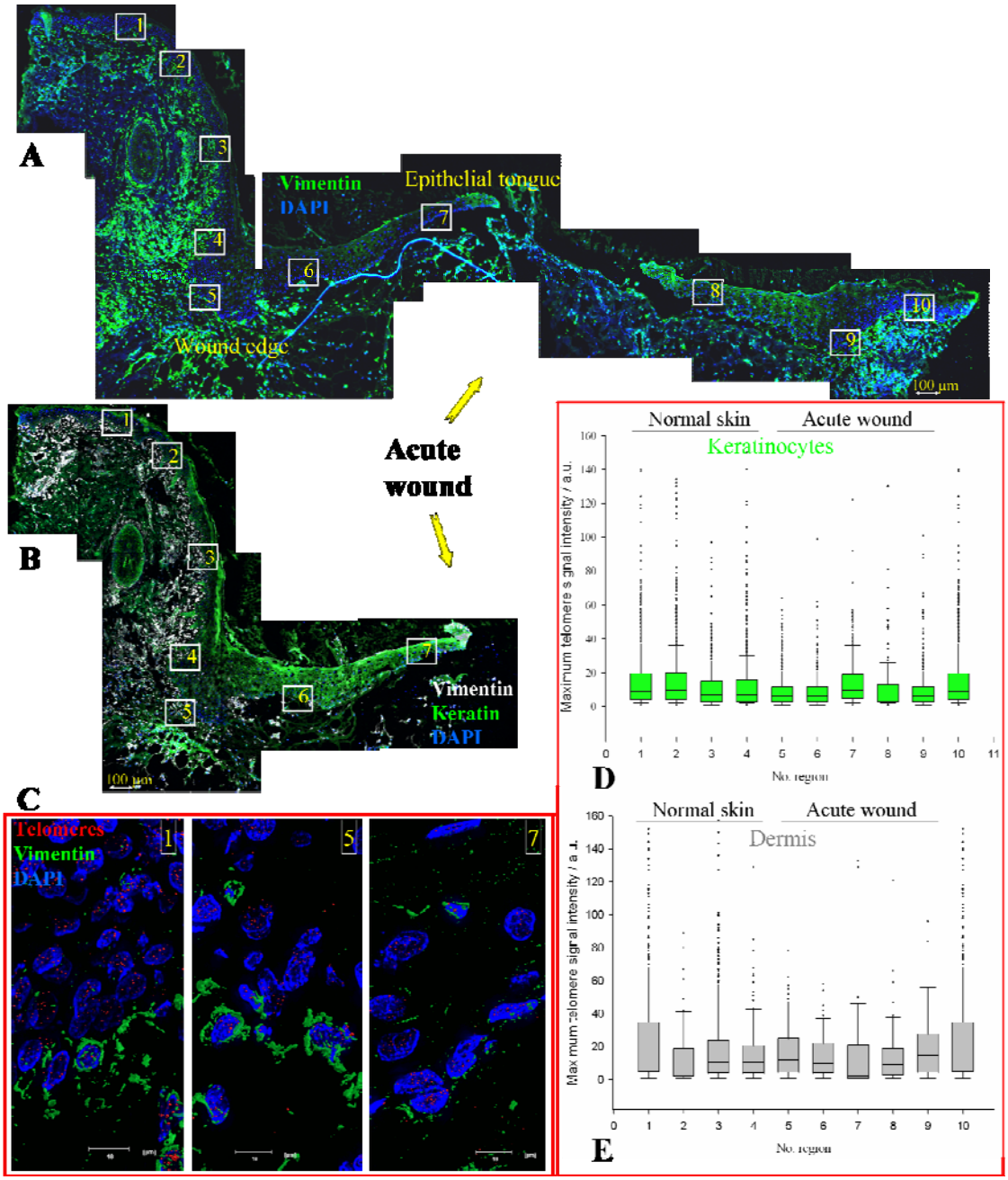

Figure 35: Minimal telomere length erosion in human skin proximally to acute wound.
A) Mosaic image of the section through the acute wound and its neighbouring skin stained for vimentin (dermis in green), and DAPI (nuclei in blue). **B)** Image of the acute wound from the serial section stained for vimentin (dermis in gray) and pan-keratin (epidermis in green) to specifically mark the keratinocytes. All images are captured with the 10x objective, composed into a mosaic, labelled with 100 µm scale bars, and marked with rectangles that indicate positions of regions that were quantified for telomere signal intensities by capturing images at higher magnification (63x objective). **C)** Examples of 3 regions used for quantification are visualized in 3D: a normal skin distant from the wound (left panel), part of the wound edge (middle panel), part of the epithelial tongue cowering the wound (right panel). The numbers of the regions are indicated in the mosaic image. **D)** and **E)** Box plot of the maximum telomere signal intensities in the epidermis and dermis of the normal skin distant from the wound (areas on the mosaic and in the graph are the same - number 1 to 4, and 10), and in the acute wound (areas 5 to 9). Note that the telomeres in the close proximity of the acute wound are not much shorter then those distant from the wound, and that there is no difference in telomere length in dermis.

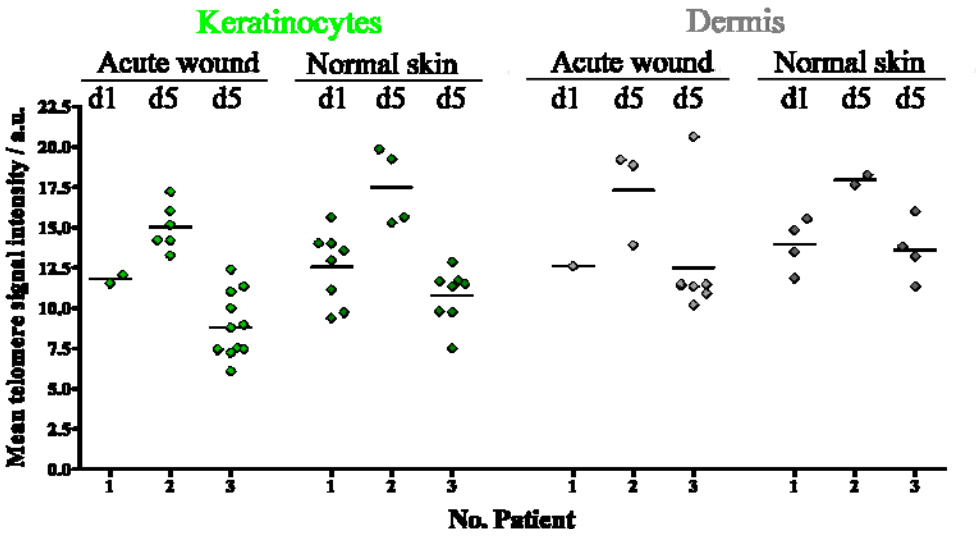

Figure 36: Telomere length is slightly reduced in keratinocytes, but not in the dermis of acute wounds compared to the neighbouring normal skin from the same patient. Each dot on the graph represents the mean telomere signal intensity in one region of the skin section in keratinocytes (green), and in dermis (gray). Patients are indicated with numbers 1-3, and days after wounding with d1, and d5. Note the weak tendency to have longer telomeres in keratinocytes of normal skin as compared to keratinocytes from the wound area, and no difference in fibroblast.

3.3 Telomere length may be a novel stem cell marker

The skin is constantly exposed to UV, wounding, and other types of insults, thus, has to be able to renew its damaged tissue integrity. Renewal capacity of the epidermis is maintained through a population of long-lived stem cells interspersed through the basal layer of the epidermis. Despite the fact that it is long known that stem cell exist, their identity is still elusive. A number of markers are described, however none is specific for stem cells in human epidermis (reviewed in Kaur, 2006). Since stem cells are supposed to only rarely proliferate and are slowly cycling, the successor cells, the so called transit amplifying cells (TACs) are the ones that proliferate more quickly and after 4 to 6 divisions are destined to differentiate. Thus, since stem cells and TACs have a different replication history, telomere length may vary with the stem cells having longer telomeres than the TACs.

3.3.1 Telomere length varies in the basal layer of the epidermis

To test whether telomere length may be a stem cell marker we analysed 18 skin samples of different aged donors for telomere length in the individual cells of the basal layer. One example of the back skin of 81 years old male is presented in figure 37.

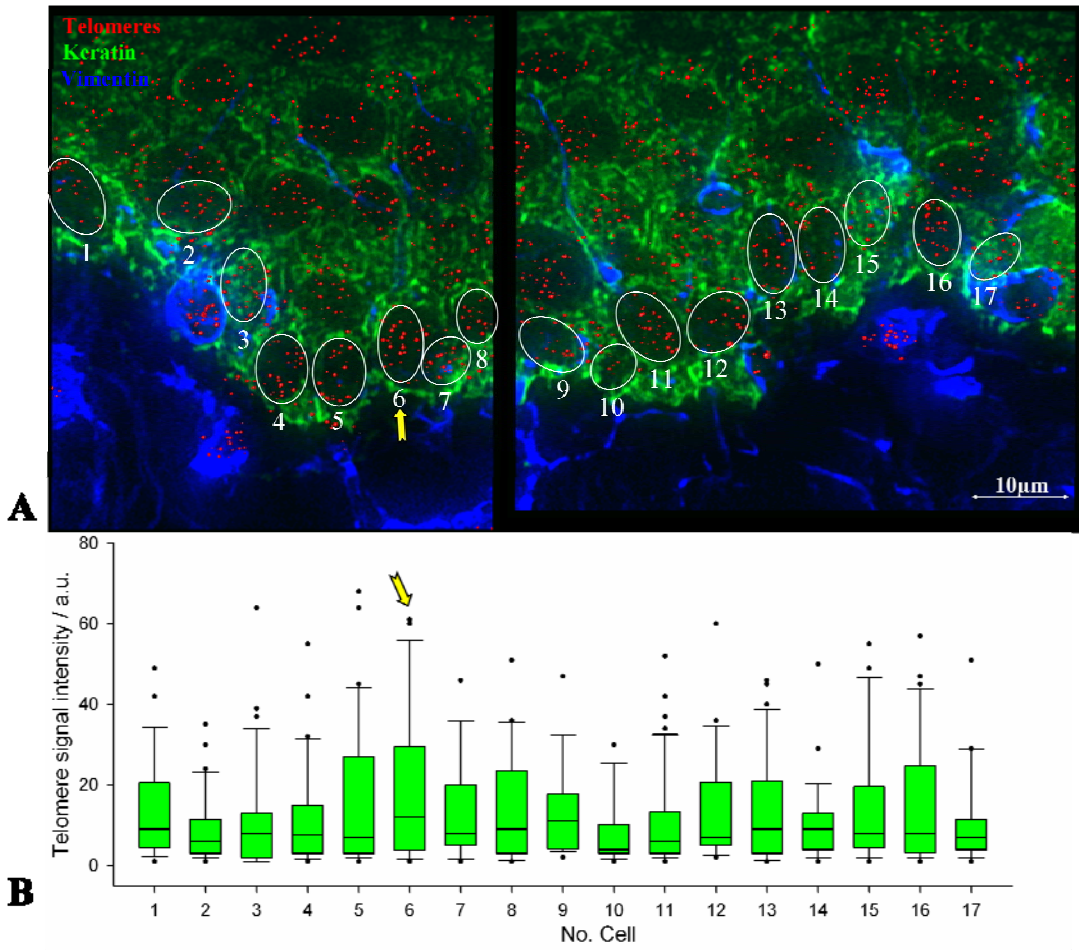

Figure 37: Telomere length varies between cells in the basal layer of the back skin of an 81 years old male. A) Skin sections were stained for keratin (green) and vimentin (blue) and the telomeres hybridized with a telomere-specific PNA probe (in red). Individual cells of the basal layer, which were analysed for telomere signal intensity, are encircled. **B)** Graphic presentation of telomere signal intensities of keratinocytes from the basal layer, demonstrating that telomere length varies between cells; the cell with the longest telomeres in this region is indicated with the yellow arrow.

In all skin samples telomere lengths varied between cells, with only a few cells showing "very long" telomeres. In samples with relatively long telomeres, the difference in telomere length between cells with "very long" telomeres and the other cells in the basal layer was generally less pronounced (figure 38A-C). In regions where telomeres were on average shortest it was easiest to identify cells with longest telomeres as they clearly differed in telomere length from the other cells (figure 38E, F). There

were also some exceptions for regions where on average telomeres were long in the analysed region, but the cells with longest telomeres could still easily be identified (figure 38D). Variations in telomere length between cells appeared rather region- and donor- then age-dependent.

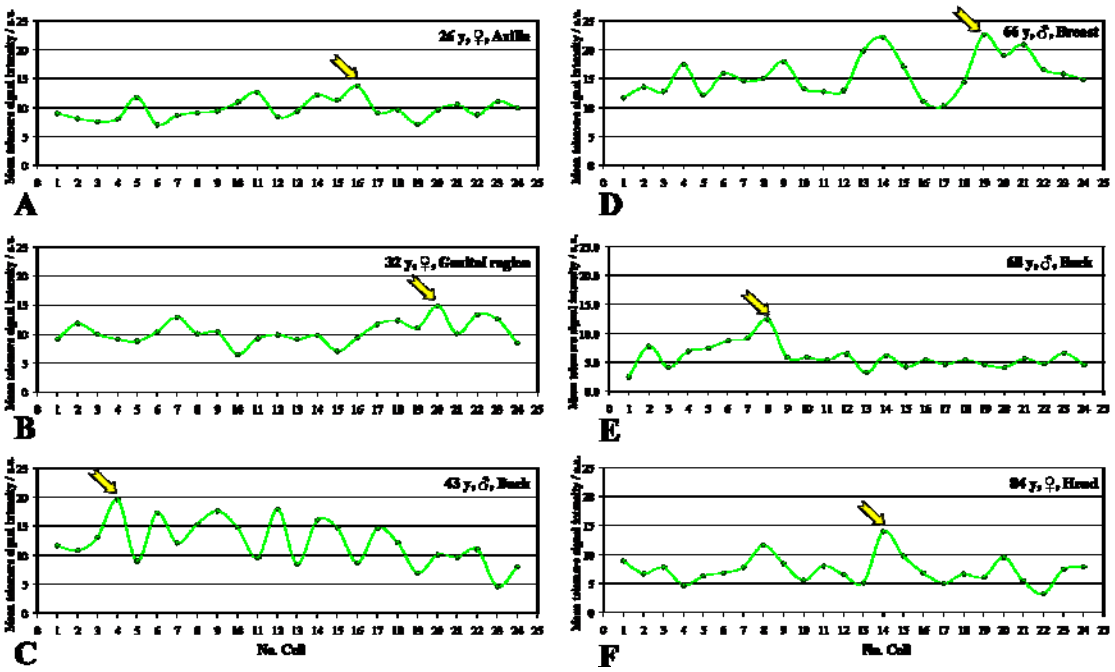

Figure 38: Variations in telomere length between cells in the basal layer differ between different regions in different skin samples. Six examples of different variations in telomere length: **A)** to **C)** cells with longest telomeres can be distinguished from other cells in the basal layer, but the difference is not extreme, **D)** to **F)** cells with longest telomeres can easily be identified as they strongly differ from other cells in the basal layer. Note that telomeres are on average shortest in E) and F). Cells with longest telomeres are labelled with arrows. For simplicity, only one cell is labelled per graph (per analysed region) although more peaks could often be identified. Age (y), gender (♂, ♀) and skin site are indicated on each graph.

To determine the distribution of the cells with longest telomeres in the epithelial tissue we analysed 19 consecutive sections from 84 years old female head skin. On each section, the same region was identified, images were captured and aligned, and telomere signal intensities were measured for all cells in the basal layer. The size of the skin region was approximately 140µm x 200µm, and it included 667 cells from the basal layer. Results are presented in the form of 3-dimensional graph representing the epidermal tissue with the peaks (colour) indicate the position of 8 % of cells with longest telomeres (figure 39). This demonstrated that if the cells with longest telomeres are stem cells they are distributed throughout the epidermis as single cells in a pattern that as present appears rather random.

Interestingly, in the same skin there was a region with longer telomeres, which was present within the first 8 skin sections. As the images of serial sections 9 to 19 were captured with a slight shift to the left, the region with longer telomeres was no longer visualized and in the graph this area only appears at the upper right borders.

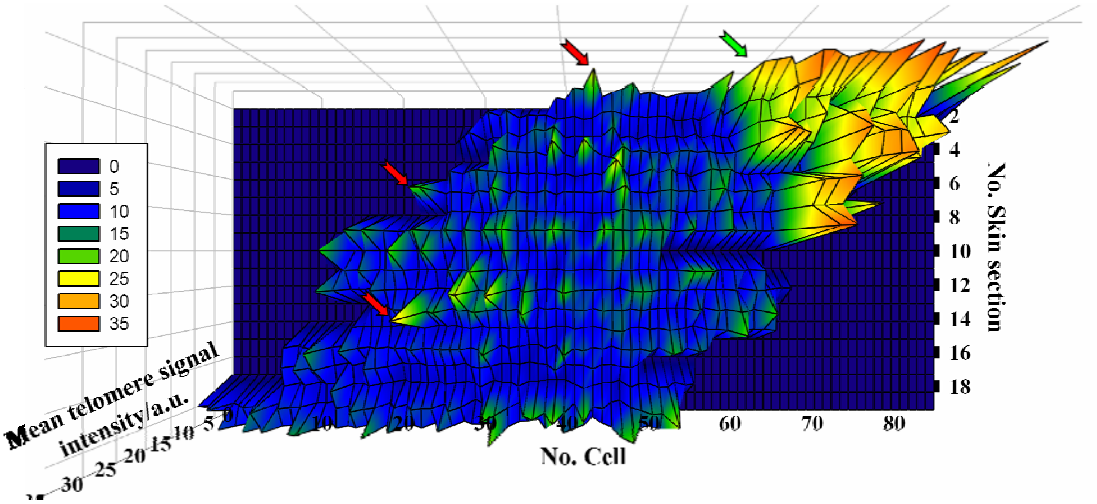

Figure 39: Distribution of cells with longest telomeres appears random in the skin. Nineteen consecutive skin sections were stained for telomeres and for vimentin to distinguish non-keratinocytes. The same region on each section was analysed for telomere signal intensities (TSI) in keratinocytes of the basal layer. Measured values were aligned and presented in the form of 3-dimensional graph where the height of peaks indicates the mean TSI in the each cell. Note the region with much longer telomeres present within first 8 sections (green arrow). Also note the randomly distributed cells with long telomeres (highest peaks) in the region of the skin with shorter telomeres (for simplicity only three cells are indicated with the red arrow). Dark blue regions without peaks on left and on the right do not contain cells.

3.3.2 Cells with long telomeres are not only located in areas of the potential stem cell marker MCSP

To further identify the localisation of the cells with longest telomeres within the epidermis we used a marker, melanoma chondroitin sulphate proteoglycan (MCSP) that is supposed to mark the areas of stem cell locations. In human rete ridge-rich epidermis, MCSP is localized to the upper part of the rete ridges and marks a distinct group of cells (Legg et al., 2003). Since MCSP is one of the most discrete markers, we used it here to ask whether and how basal cells with longest telomeres would co-localize.

To determine would this also be the location of the cells with the longest telomeres all skin sections were immunostained for MCSP at the same time with the same conditions, and microscopy was performed with the same settings within a few days to obtain the most quantifiable and comparable results. 2d images of the whole section were taken

with low magnification (10x objective) and combined to a mosaic image to determine the staining pattern for the entire skin sample. In addition, various regions were visualized in 3D at higher magnification (63X objective) (figure 40A).

The same sections were then re-stained for telomeres and all centromeres. During the FISH procedure all the immunostaining was lost. However, in six different skin samples 27 regions could be relocated and visualized and the same cells could be analysed for telomere length. For these samples we asked whether cells that strongly expressed MCSP differ in telomere length from those cells with weak MCSP expression. In 12 out of 27 regions we found tendency that MCSP expressing cells have on average longer telomeres but the difference was not statistically significant. We also found that cells with longest telomeres expressed MCSP in 12 regions out of 27, but in the other 15 regions cells with longest telomeres were not positive for MCSP or the staining was very weak and close to the treshold.

Five regions of the 84 years old female head skin are shown in figure 40B. Region number 3 is also presented in figure 40A, and marked on the graph in figure 40B with the ellipse. There was a weak tendency that MCSP expressing cells had in average longer telomeres in all five regions in the skin but the difference was not statistically significant. Concerning individual cells with the longest telomeres, in two out of five regions (No. 1, and 3 on the graph in figure 40B) they also expressed high level of MCSP. The cell with longest telomeres in the region number 3 is indicated with the arrow on the graph, and on figure 40A. However, in the other three regions (No. 2, 4, and 5) cells with longest telomeres were less MCSP positive or were not stained at all. Thus, these data suggest that there is no clear correlation between cells with longest telomeres and strong MCSP expression.

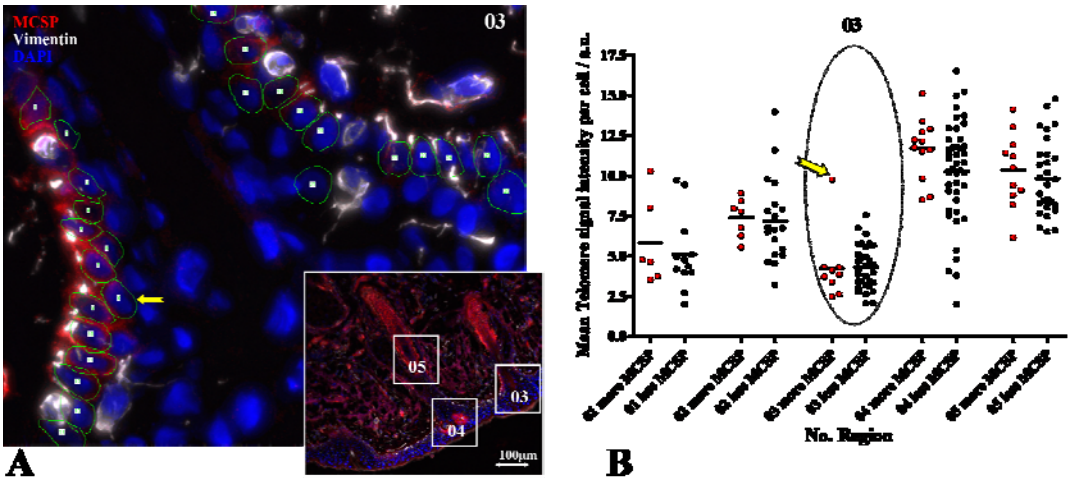

Figure 40: Correlation of telomere length and MCSP in the skin from 84 years old female; *in silico* cell sorting on more and less MCSP expressing.
A) Image of the 84 years old female skin immunostained for MCSP (red), vimentin (gray), and nuclei were stained with DAPI (blue) visualized with the high resolution (63x objective) as a Z-projection of 3D image. Each cell is marked with the ROI (green) used for quantification of integrated density of MCSP staining. Insert presents low magnification of the skin (10x objective), that is marked with rectangles indicating positions of 3 regions out of 5 in this skin sample where we quantified telomere signals in individual cells. Rectangle number 3 presents the localization of the image A). The scale is indicated with the bar. The same skin section is restained for telomeres. Cell with longest telomeres is labelled with arrow. **B)** Dot plot of the correlation of telomere signal intensity and MCSP staining; note that the each cell is presented with one dot. Cells within each of five regions in the graph are sorted in two subgroups; the one with strong MCSP staining (red dots on the graph B) and the rest of the basal keratinocytes in that region (black dots). Mean telomere lengths are indicated as black horizontal lines. Dashed ellipse marks the region of the skin No. 3, which is visualized in the panel A).

3.3.2.1 Distribution of CA-IX and MCSP in the skin

It was recently proposed that hypoxia characterised the stem cell niche (Gustafsson et al., 2005). One marker characterising hypoxia is carbonic anhydrase IX (CA-IX). Interestingly, in skin sections CA-IX and MCSP frequently but not always coo-localize in the upper part of the rete ridges (Muffler, unpublished results).

However, from the previous studies it was not clear whether both proteins indeed always co-localize and thus whether CAIX may be a better marker for the stem cell niche.

To address this question we next compared the expression of CAIX and MCSP using high resolution microscopy. Skin samples from 16 different-age donors and different body sites (indicated in table 5) were immunostained for both proteins and analyzed by deconvolution microscopy. As described above, MCSP was generally expressed at the top of the rete ridges and, if present, a strong expression was also seen in the hair follicles (figure 41). CAIX showed a similar distribution, being present at the top of the

rete ridges. However, the two proteins were not necessarily co-expressed by the same cells; in fact staining pattern was rather exclusive for one or the other in some regions. When co-expressed, MCSP expression was restricted to the basal cells while CA-IX expression was also be detected in suprabasal cells (figure 42A). Furthermore, in the hair follicles, this discrimination is even more obvious. The number of cells per region but also the regions that stained positive for MCSP or CA-IX differed between samples largely differed from sample to sample and did not seem to correlate with age, body site or gender. In the hair follicles, CAIX expression was most prominent in the upper parts while MCSP was strongly expressed in the lower parts (figure 41B and 41C). Some co-localisation was seen in the middle part of the hair follicle.

Despite the heterogeneous distribution, three basic staining patterns (expression of both proteins) could be established:

1. On the top of rete ridges only- if no HF were present (6 of 16 samples, figure 41A)
2. In both, on top of rete ridges and in HF if HF were present (6 of 16, figure 41C).
3. In rete ridge deficient skin only in HF (4 of 16, figure 41B)

Table 5: Characterization of MCSP or CA-IX staining in different skin samples

No. Donor	Age / years	MCSP Staining*	CA9 Staining*	Gender	Staining pattern**	No. hair follicles	Body site
1	25	4	4	m	R.R. and H.F.	2	Buttock
2	26	4	3	f	R.R.	0	Axilla
3	31	3	5	f	R.R.	0	Stomach
4	32	3	2	f	H.F.	2	Genital
5	41	3	4	f	R.R.	0	Unknown
6	43	3	2	m	R.R. and H.F.	3	Back
7	46	3	2	m	R.R.	0	Back
8	50	3	5	m	R.R.	0	Back
9	66	2	3	m	R.R. and H.F.	2	Breast
10	71	2	2	m	H.F.	3	Temple
11	71	5	3	m	R.R. and H.F.	1	Back
12	72	4	3	Unknown	R.R. and H.F.	1	Neck
13	72	2	3	Unknown	R.R.	0	Unknown
14	72	2	1	m	H.F.	3	Nose
15	81	4	3	m	R.R. and H.F.	1	Back
16	84	2	1	f	H.F.	3	Unknown

* MCSP and CA-IX staining was semi-quantified with numbers 1 to 5, where 1 determines the smallest number of cells and regions, and weakest intensity of staining, while 5 represents the strongest staining and largest number of cells and regions stained.
** Strong MCSP and CA-IX staining was present on the top of rete ridges (R.R.), in different parts of hair follicles (H.F.), or in both; R.R. and H.F.

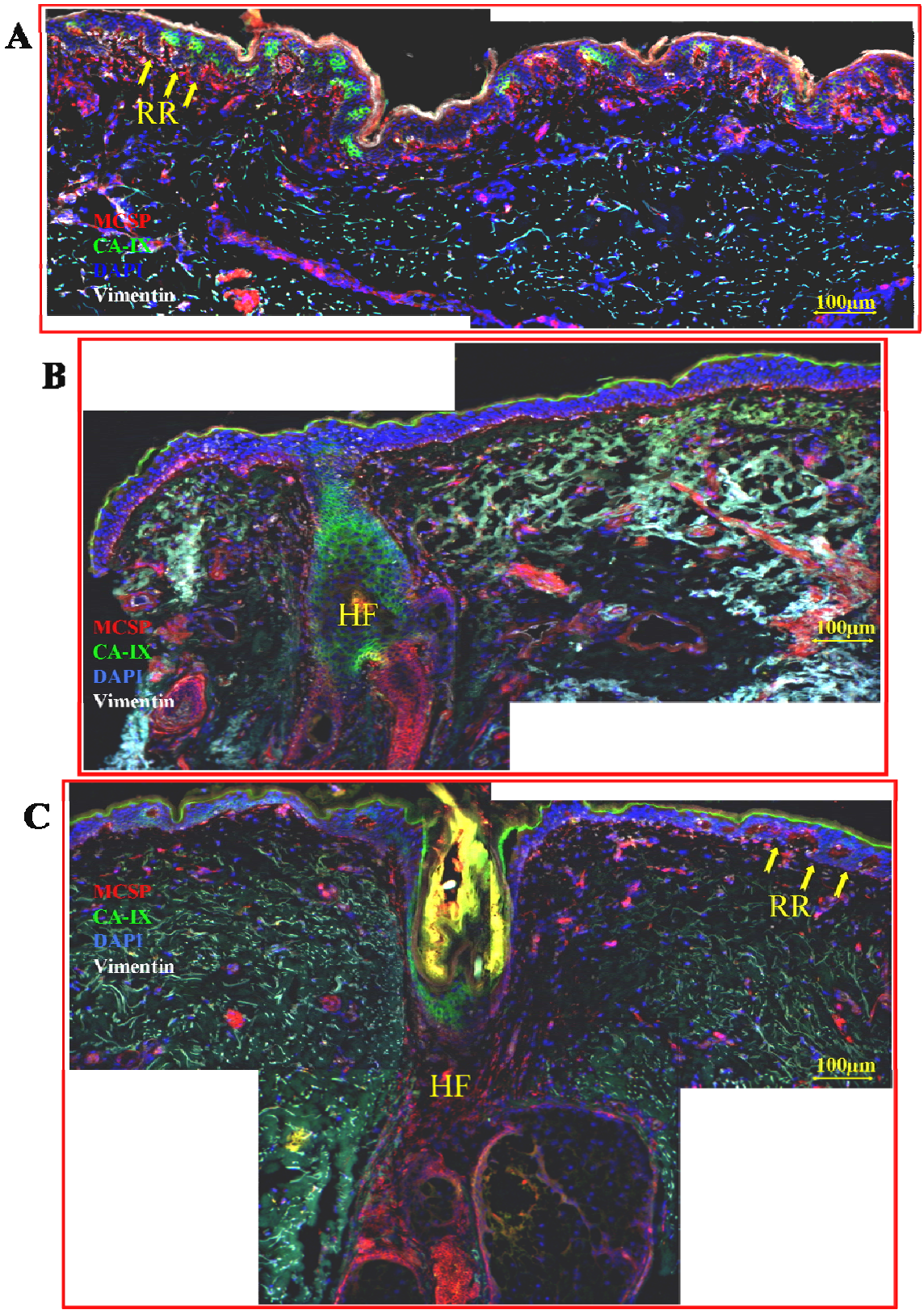

Figure 41: Three basic staining patterns of MCSP and CA-IX. Staining was present on **A)** the top of rete ridges (RR) only - if there were no hair follicles (HF), but if there are no rete ridges than in HF only **B)**, or finaly in both; on top of RR and in the HF **C)**. Scale is indicated as well as hair follicles and for simplicity only some rete ridges are marked with arrows.

3.3.2.2 Telomeres are not necessarily longer in the cells expressing CA-IX

To determine whether CA-IX rather than MCSP may mark the stem cell niche we next compared the average telomere lengths in cells that were strongly CA-IX-stained with cells that were expressing less CA-IX.

Reinvestigating 27 regions in the same 6 skin samples already investigated for MCSP expression, we found that only in 6 regions there is a tendency that cells expressing CA-IX have on average longer telomeres. In 10 of 27 analysed regions telomeres were on average even shorter in cells expressing CA-IX. Nevertheless, in other 10 of 27 regions individual cells that had longest telomeres in the region were stined for CA-IX, and 6 of those 10 were also MCSP positive. An example is head skin from 84 years old female shown in figure 42.

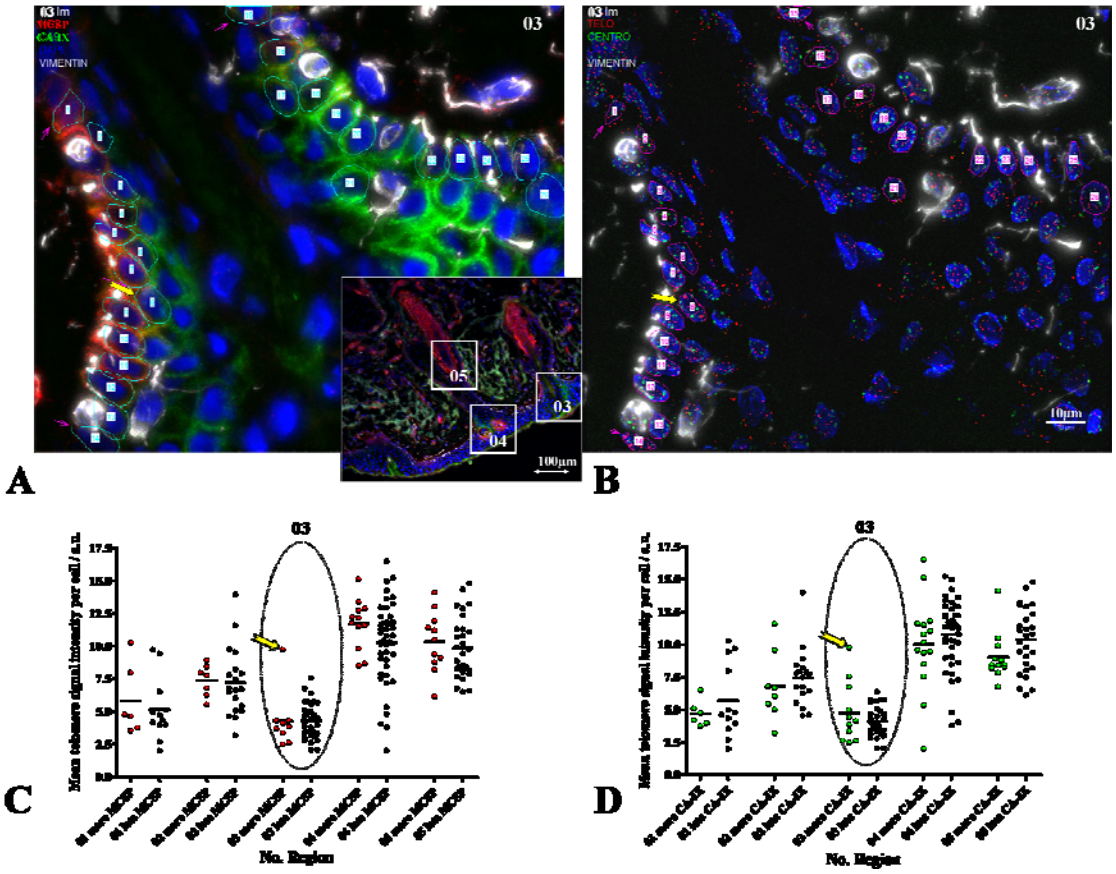

Figure 42: Correlation of telomere length, MCSP and CA-IX; cell sorting on more and less MCSP and CA-IX expressing. A) Image of the 84 years old female skin immunostained for MCSP (red), CA-IX (green), vimentin (gray), and nuclei were stained with DAPI (blue) visualized with the high resolution (63x objective) as a Z-projection of 3D image on one plane. Insert presents small magnification of the skin (10x objective), that is marked with rectangles indicating positions of 3 regions out of 5 in this skin sample where we quantified telomere signals in individual cells. Rectangle number 3 presents the localization of the image A). The scale is indicated with the bar. Each cell is marked with the ROI (pink) used for quantification of integrated density of CA-IX and MCSP staining **B)** The same skin section is restained for telomeres (red) and all centromeres (green foci). Cell with the longest telomeres is marked with yellow arrow, both on images A) and B), and graphs C) and D)). **C)** Dot plot of the telomere and MCSP staining correlation, and **D)** of telomere and CA-IX staining; note that the each cell is presented with one dot. Cells within each of five regions in the graph are sorted in two subgroups; the one with strong MCSP staining (red dots on the graph C) or strong CA-IX (green dots on the graph D) and the rest

of the basal keratinocytes in that region (black dots). Dashed ellipses mark the region of the skin No. 3, wich is visualized in the panels A), and B).

Region number 3 is visualised in figure 42A and 42B, and marked with elipses in figures 42C and 42D where each cell is presented with a dot, and the average telomere signal intensities are shown as horisontal lines. In the region 3 there was a tendancy to have on average longer telomeres in cells expressing CA-IX (figure 42D). However, in other 4 regions analysed in this skin sample telomeres were on average shorter in CA-IX positive cells. Interestingly, as we performed double-labelling for CA-IX and MCSP, we found that the cell with longest telomeres in the region number 3 was positive for both markers (yellow arrow in figure 42A, 42B, 42C, and 42D). Arguing for MCSP rather than CAIX

Similar MCSP and CA-IX staining pattern as well as correlation with telomere length, was also observed in other 5 skin samples that were analysed. Another example is 66 years old male breast skin (figure 43), where the CA-IX, and MCSP staining, and the ratio of telomere and centromere integrated density was quantified and presented for the each cell of the basal layer (figure 43C). This type of the graphical presentation shows that cells with strongest CA-IX or MCSP staining are not necessarily ones with the longest telomeres. Cells No. 19 and 21 for example, (marked with yellow arrow on the figure 43C) have the longest telomeres in the analysed region of the skin; the cell No. 21 was stained for MCSP, but the cell No. 19 was not MCSP or CA-IX positive at all. Thus, it was clear that cells with longest telomeres can be in the same time positive for one or both of these two proposed epidermal stem cell markers, but they do not have to necessarily correlate.

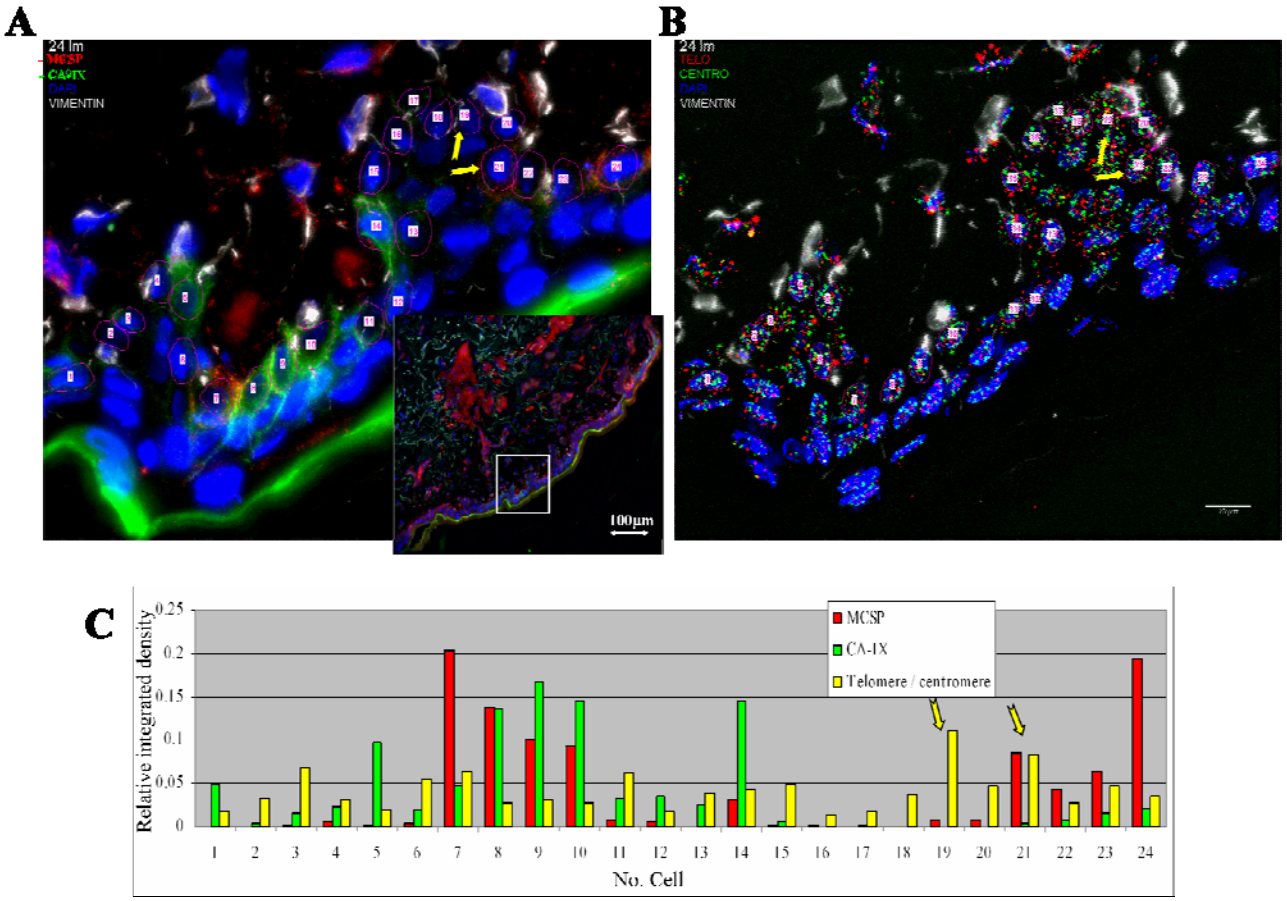

Figure 43: Correlation of telomere length with MCSP and with CA-IX expression pattern in the basal layer of 66 years old male breast skin. A) Image of the skin stained for MCSP (red), CA-IX (green), vimentin (gray), and nuclei (blue). The region is visualized at high magnification (63x objective) in 3D and all layers were projected on one plane**.** Each cell is marked with the ROI used for quantification of integrated density of CA-IX and MCSP staining. The insert is image of the same region acquired with 10x objective with the rectangle indicating position of the region in A) and B). The scale is indicated with the bar. **B)** The same skin section is re-stained for telomeres (red) and all centromeres (green), and the same region as in A) is visualized again as the z-projection of the 3D image. Each nucleus is labelled with the ROI (pink) that is used for telomere and centromere signals quantification, and arrows indicate 2 cells with longest telomeres (yellow arrows on the images and on the graph). **C)** Graphical presentation of the relative integrated density of CA-IX, and MCSP staining, (which is proportional to the expression of the protein by the analyzed cell), and relative ratio of telomere and centromere integrated density (comparable to telomere length) of each cell.

3.3.3 Telomeres are on average longer in label retaining cells of 58 days old Organotypic co-cultures

In a parallel project, a model for human epidermal stem cells was developed that allows the identification of the stem cells by their ability to only rarely proliferate. Because of this, cells that are labelled with a DNA marker (iodo-deoxyuridine, IUdR)

maintain this label while all cells that rapidly proliferate loose this label (Bickenbach, 1981; Muffler et al., subm.). For this, human keratinocytes are grown in Organotypic co-cultures (OTCs) where they establish a normal epidermis. During the early phase of tissue development the proliferating cells are labelled with IUdR (Muffler et al., subm.). Thereafter, tissue maintenance is performed without label. During this chase period the label is lost in most cells. Only those cells that establish as stem cells remain as label-retaining cells (LRCs).

Assuming that the cells with longest telomeres in the epidermis *in situ* are the stem cells, and assuming that only these cells can re-establish as stem cells in OTCs then all LRCs should have the longest telomeres. If all cells can re-establish as "stem cells", we should not find a positive correlation between telomere length and LRC.

To address this, we performed in situ telomere length analyses on OTCs that were pre-evaluated for the presence of LRCs. The parallel study had shown that within a chase period of 4 weeks the number of labelled was significantly reduced, leaving 1% to 2 % of LRCs in the basal layer of the epidermis (Muffler et al., subm). Therefore, OTCs have been labelled for 2 weeks and further evaluated after a 4- and 6-week chase period, respectively.

In the 4-week chase analysis, 18 regions with LRCs were identified. The relative telomere length for each region was measured in LRCs as well as in the neighbouring cells of the basal layer and compared with the relative amount of IUdR labelling in cells. Comparison of telomere length of the heavily labelled (LRCs) cells versus those that only contained little or no label in all individual regions, is summarized in figure 45. From this study no clear correlation could be drawn between longest telomeres and LRCs. There was a tendency that LRCs have longer telomeres, however, the general distribution of telomere lengths in the LRCs was in the same range as that of the non-LRCs. Accordingly evaluation of statistical significance using the Pearson test gave a $p=0.0590$ ($\alpha<0.05$). Interestingly, when individual regions are analysed separately in 7 of 18 regions we found LRCs with longest telomeres within each of those regions.

Investigating epithelia after 6-weeks chase period, the number of LRCs was further reduced (Muffler et al., subm.) suggesting that after 4 weeks not all heavily labelled cells were indeed LRCs. We, therefore, next analysed 8 regions that contained altogether 13 LRCs (<1% of all basal cells). In three out of the 8 regions we identified one LRC per region that was strongly stained for IUdR, while much weaker or no staining was present in surrounding cells. In the other five regions there were more than

one LRC per region. One example is presented in figure 44. In this region, three (number 5 to 7) cells were heavily labelled and, interestingly, the cell in the middle (marked with an arrow) had the longest telomeres. From this it is intriguing to speculate that the cell with the longest telomeres in a region is the stem cells and that the two neighbouring cells are descendents that just start to proliferate, thus are now acting as transit amplifying cells. In line with this interpretation, we observed a strong tendency and accordingly a statistically significant correlation for the LRCs to have the longest telomeres in regions that had been analysed in OTCs chased for a 6-week-period (Pearson test of correlation, $p=0.001$, $\alpha<0.05$).

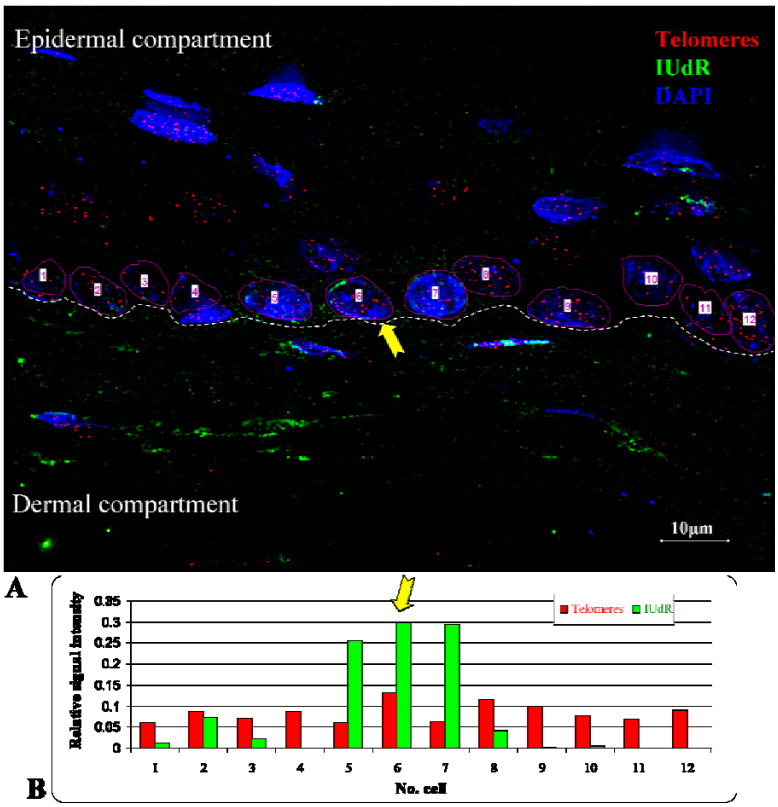

Figure 44: Telomeres are longer in label retaining cells of 58 days old 3D-OTC A) Image of the small region of 58 days old 3D-OTC stained for telomeres (red), IUdR label retain (green), and nuclei DAPI counterstaining (blue) visualized with the high resolution (63x objective) as a z-projection of 3D image on one plane. Each nucleus in the basal layer is marked with the ROI (pink) used for quantification of relative mean telomere signal intensity, and relative integrated density of IUdR staining, which is presented in the graph **B)**. Cell with the longest telomeres that retained the most of the IUdR label is marked with the yellow arrow, in both, the image and the graph. Dashed line on the image approximates the position of the basement membrane, and the scale bar is indicated.

Finally, and as a control we compared a 42-day-old OTCs labelled overnight with Bromodeoxyuridine (BrdU). In this case those cells that are replicating during this phase incorporate BrdU and thus labelling provides a measure for active proliferation. As

summarized in figure 45, we did not find any significant correlation between BrdU staining and telomere length (Pearson test of correlation, p=0.4368, α<0.05). In one case also a cell with the longest telomeres was BrdU-positive. Since we know that also the 58-day-old LRCs can proliferate (Muffler et al., subm.), we cannot exclude that this cell was a long-term LRC. However, since we analysed only 7 regions with 75 cells in total, it remain to be seen how relevant this is as more regions and OTCs sections would have to be analysed.

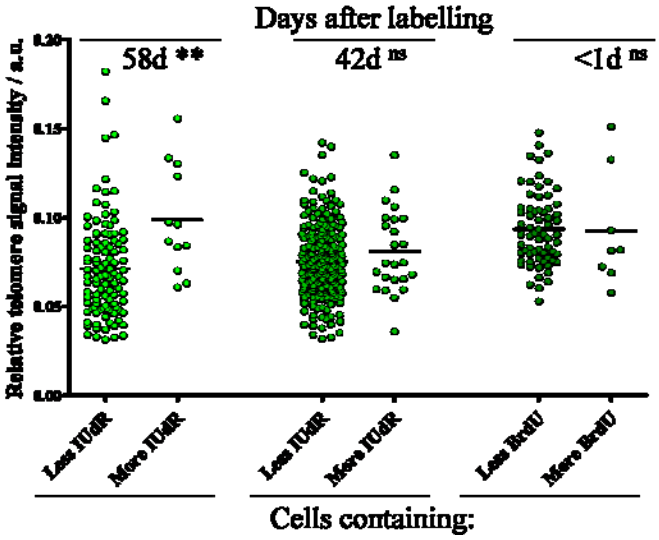

Figure 45: Telomeres are on average longer in the label retaining cells (LRCs) 58 days after labelling than 42 days, or when labelled overnight at the very end of culturing. Cells from the basal layers of 3D-OTC are presented as green dots and grouped in 3 groups; on the left are cells from the 3D-OTCs 58 days after labelling with IUdR, in the middle there are cells from 3D-OTCs 42 days after labelling, and on the right cells from control 42-day-old 3D-OTCs that were labelled with BrdU overnight. Each group is divided in two groups – in cells with more and cells with less (or no) label. Note that the non-paired t-test show significant difference in telomere length only between LRCs and other less IUdR positive cells 58 days after labelling (** p<0.01, α<0.05, ns – non-significant).

4. Discussion

4.1 Cell cycle dependent 3D distribution of telomeres

Telomeres play a significant role in the maintenance of genomic integrity as they form protective caps that guarantee chromosomal stability. Telomeres are also involved in chromosomal localization in the nuclear space. By having established a new *in situ* technique to determining the 3D distribution of the telomeres several novel and unexpected results could be established.

It was recently shown for mouse and human lymphocytes that the organisation and distribution of the telomeres is cell cycle-dependent. Weierich *et al*. (2003) reported on differences in telomere distribution in mouse and human G0 lymphocytes; in mouse nuclei, the telomeres were located preferentially at the nuclear periphery while in human lymphocytes most telomeres were located in the nuclear interior. Another study on human and mouse lymphocytes reported on a rather relaxed telomere distribution throughout the nucleus in G0/G1 and S phases while the telomeres aligned to a telomeric disc in the centre of the nucleus as cells progress into the late G2 (Chuang *et al*., 2004).

Using adherently growing human cells which were characterized by a more flattened ellipsoid nucleus we now show that telomeres in the interphase nuclei were localized in the interior and rarely at the periphery. Similar to study from Weierich *et al*. (2003) during interphase we found most of the telomeres enclosed by the DAPI stained chromatin, and only a minor population of the telomeres seemed to face towards the nuclear envelope. Comparable to Chuang *et al*. (2004) during the progression through the cell cycle from G1 to G2 we observed a non-random and dynamic telomeric organization resulting in a formation of more densely packed telomeric disk in G2. However, our spatial distribution seems to slightly differ as telomeres became more loosely distributed during different phases of mitosis. Thus, this telomere kinetics was similarly characteristic of different cell types such as keratinocytes and fibroblasts, our data suggest that the pattern established here in general accounts for adherently growing cells. The reason for this different behaviour may well be due to the more flattened ellipsoid nucleus that may limit the movement of the telomeres. Whether this is also of consequence for chromosomal movement is still elusive.

During mitosis the cells are more rounded up and this correlates with the described relaxation in telomere distribution, as well as with chromosome movement being most widely distributed in the z-axe during the formation of metaphase plate and separation of chromatides in early anaphase. Therefore, cell cycle and the growth behaviour, and possibly other factors like cell type- and probably species-specific organization of chromatin could explain differences in telomere distribution observed in previous studies (Chuang *et al*., 2004; Weierich *et al*., 2003). For example, in adherently growing keratinocytes and fibroblast we detected far less then 40% of telomeres associated with the edge of the nucleolus as it was described for the murine dorsal root ganglion cells (Billia and de Boni, 1991). A very specific telomere distribution was described for gonads during spermatogenesis. Here, the chromosomes form the bouquet and the telomeres are clustered at one side of the meiotic cell. It was shown there that the distribution is of great importance for the function since the fast and efficient homologous pairing and finally recombination between homologs depended on this telomere clustering (reviewed in Harper *et al*., 2004).

Thus, all this demonstrates that differences in telomere organisation exist between adherently and non-adherently growing cells. Whether only the nuclear space is responsible for these differences remains elusive. However, it suggests that this non-random distribution is highly regulated and of functional importance.

4.1.1 Constitutive expression of *c-myc* correlates with the presence of telomeric aggregates (TAs) throughout the cell cycle

While in general telomeres appeared to be localized individually, previous studies have shown that telomeres can interact with each other and temporal associations of telomeres were observed in normal and immortalized cell types (Nagele *et al*., 2001; Molenaar *et al*., 2003). Telomeric associations were also described to occur due to critically shortened and dysfunctional telomeres which can result in a formation of end-to-end fusions and the subsequent genetic instability (Autexier and Greider, 1996; Wan *et al*., 1999) caused by chromosome breakage-fusion-bridge cycle (McClintock, 1941; Haber and Thorburn, 1984).

A different type of associations was recently described in a collaborative study of the Boukamp and May laboratories. They showed that telomeres can aggregate in

some human and mouse tumours in a way that even distribution of telomeres throughout the nucleus can be distorted. Such telomeric aggregates are characterized by a much larger volume than normal non-overlapping and non-aggregated telomeres (Chuang *et al*., 2004). In agreement with continuation of this work, it was shown that *c-myc* deregulation can cause remodelling of the 3D nuclear organization of telomeres and chromosomes, which could create spatial conditions that initiate genomic instability (Louis *et al*., 2005). I was observed that cycles of telomeric aggregate formation in interphase nuclei, accompanied with chromosomal rearrangements, are directly proportional to the duration of *c-myc* deregulation.

Here we demonstrated that telomeric aggregates are present in HaCaT-myc cells that constitutively express c-Myc transcription factor, an oncogene known to contribute to genomic instability. We also confirm that the presence of TAs can interfere with the overall telomere organization by causing a more irregular distribution. Most importantly, we found TAs at all phases of mitosis suggesting that TAs are rather stable complexes that are obviously not dissociated during replication. Furthermore, being present during segregation of the chromosomes during anaphase suggests that those chromosomes that are grouped by the TAs are likely segregated together to one daughter cell. This is also supported by the finding that in some telophase cells as well as in new daughter nuclei only one part is carrying a TA. As a consequence this results in an uneven distribution of the chromosomes between the two daughter cells, causing gain in one and loss of chromosomes in the other. Thus, TAs may represent an attractive model to explain numerical chromosomal aberrations.

Previous time-lapse experiments have demonstrated that it is a common feature of individual telomeres to temporarily interact with each other (Molenaar *et al*., 2003), and also in our analyses we observed telomeres that were in a very close vicinity, however, the telomeric aggregates of HaCaT-myc cells were much more complex in a shape and size. Thus, although not yet firmly proven, these findings indicate that i) the TAs reported previously (Chuang *et al*., 2004) and described here for the HaCaT-myc cells, differ from those associations occurring with the general movement of the telomeres and ii) that they are highly stable structures that are maintained also throughout mitosis.

4.1.2 Matrin 3 could be involved in the formation of telomere aggregates

To approach the mechanisms of TA formation we assumed that some of the telomere binding proteins may be disregulated due to constitutive expression of *c-myc* in HaCaT-myc cells. We, therefore, performed 2D gel electrophoresis from nuclear extracts from HaCaT (without TAs) and HaCaT-myc cells (with TAs). Thereby, we identified 30 proteins that were differentially expressed. Besides some unrelated keratins we found Matrin 3, a nuclear matrix protein that was significantly reduced in in the HaCaT-myc extracts. There are no reports that Matrin 3 is directly or indirecty interacting with telomeres. However, some studies suggested an important role of highly of Matrin 3 in chormatin organisation (Belgrader *et al*., 1990). Therefore, destabilised Matrin 3 expression could have important influence on telomere distribution. Matrin 3 is a salt-resistant proteinaceous nuclear structure that as part of the nuclear matrix could be isolated from interphase cell (Berezney and Coffey, 1974; reviewed in Berezney, 2002). Using this approach to biochemically characterize the protein in the HaCaT-myc cells and si-RNA to reduce Matrin 3 in the parental HaCaT cells (without TAs) and determine its functional consequence on TA formation are planned to further elucidate the role of this most promising candidate.

4.2 Telomere length regulation in human skin

The formation of TAs was correlated with the deregulated *c-myc* expression in HaCaT-myc keratinocytes and in some tumour cells, however, it was not correlated with the telomere length. TAs could be identified in cells with longer as well as in those with shorter telomeres, therefore supporting our hypothesis that TA formation is a telomere-length-independent mechanism of chromosomal instability (reviewed in Boukamp *et al*., 2005).

A different mechanism, which also involves telomeres, is telomere-length-dependent mechanism of genomic instability. It was proposed that stabile telomere length guarantees protective capping of chromosomes and genomic integrity, while telomere shortening up to the critical length can cause telomere dysfunction and result in the formation of chromosomal end-to-end fusions (Autexier and Greider, 1996; reviewed in Shay and Wright, 2005). Since we did not identify TAs in parental HaCaT keratinocytes nor in normal skin, we asked whether telomere shortening can occur in

the skin *in vivo*. Therefore, we analysed telomere length regulation in normal human skin.

4.2.1 Minimal age dependant decline of telomere length

Telomere length in the normal skin was analyzed in four studies so far and all of them have shown an age-associated telomere shortening. However, there was a big differences in the rate of telomere shortening in different reports. Friedrich *et al*. (2000) demonstrated an average reduction of 75 bp/year, while a recent study from Sugimoto *et al*. (2006), which is also the one with the most skin samples, showed that both the epidermis and the dermis have an age-associated telomere loss of 9 and 11 bp/years, respectively.

In agreement with this previous results from our laboratory based on Southern blot-dependent terminal restriction fragment length (TRFL) of telomeres confirmed these results and provided a calculated loss of 25 bp/year (Krunic *et al*., in revision). The here presented *in situ* 3D telomere length analysis on tissue sections further substantiated the low rate of age-dependent telomere loss in the epidermis. Investigating skin from 15 different age donors (2-90 years) originating from various parts of body as well as 9 different donors (age of 32 to 77 years) which derived from the upper side of the both hands from each donor, showed an only weak regression which was comparable to that reported by Sugimoto *et al*. (2006). Taking into consideration that the epidermis constantly proliferates with a regeneration rate of about four weeks and the age-related decline in the skin during a lifetime would be on average less than 2 kb, this loss appears very minor and can only be explained by the fact that the epidermal keratinocytes express telomerase (Härle-Bachor and Boukamp, 1996) and that this telomerase is able to minimize replication-dependent telomere loss (Krunic *et al*., in revision). Starting from >10 kb, telomere length would on average still be 8 kb after a life span of 100 years. Thus, telomeres would still be much longer than the about 6 kb found in senescent fibroblasts *in vitro* (Figueroa *et al*., 2000) or the critical telomere length of 0-2 kb, which was proposed by Allsopp and Harley (1995) making the biological relevance of telomere shortening questionable for the epidermal aging process.

4.2.2 Differentiation and telomere length

Work from the Boukamp laboratory showed that during differentiation telomerase is turned off (Harle-Bachor and Boukamp, 1996; Bickenbach *et al*., 1998; Rosenberger, 2007). Keratinocytes migrate from the proliferative basal layer of epidermis through several suprabasal layers where they undergo a continuous process of differentiation terminated in the formation of dead horn squames. To determine how this would affect telomere length regulation, *in situ* studies were performed that allowed to dissect the epidermis into basal, suprabasal and upper layers.

In most samples (10/14) telomere quantification revealed highly comparable values in all three compartments. In the 4 samples only smaller differences were observed when telomere length was either slightly decreased (3/14) or even increased (1/14) in suprabasal layers when compared with the basal layer. However, in most samples telomere length was not altered, which clearly demonstrates that telomere erosion is dependent on replication. Thus, if changes occur these should only be seen within the basal layer where the proliferatively active cells are located but not in the suprabasal layers where the cells no longer proliferate but are replication-arrested and differentiate. From this it is tempting to speculate that non-proliferative, differentiated keratinocytes have their chromosomal ends secured and tightly "locked". More intense studies are now needed to determine whether differences exist in telomere constitution in proliferating *versus* differentiating cells and whether specific combinations of proteins are associated with the telomeres during the differentiation process.

4.2.3 Telomeres are shorter in keratinocytes as compared to the dermal fibroblasts and melanocytes

Despite the fact that fibroblasts are telomerase-deficient it was noted recently that when measuring TRFL of telomeres from dermis *versus* epidermis of the same skin the dermal fibroblasts had longer telomeres than the epidermal keratinocytes (Sugimoto *et al*., 2006). Similar observations were reported for cells isolated from oral mucosa (Kang *et al*., 2002). With our novel *in situ* approach we not only confirmed this unexpected finding but additionally show that also melanocytes, which make ~10% of the basal layer of the epidermis, had longer telomeres than the keratinocytes. Thus, using deconvolution based Q-FISH on interphase cells combined with immunostaining

gave comparable results to the well established TRFL measurements – confirming the quality of the meaurements. In addition, however, it provided the possibility to analyse a given tissue in much more detail and in relation to its normal organisation.

Accordingly, we compared telomere length in the epidermal keratinocytes, dermal fibroblasts, and intraepidermal melanocytes. The latter could be easily identified as they are the only vimentin-positive cells in the epidermis. Interestingly, these studies demonstrated that both fibroblasts and melanocytes always showed longer telomeres than the keratinocytes and most importantly, that they had very similar telomere length and with that a very similar age-dependent regression slope. Thus, although these cells are of different embryonic origin - melanocytes differentiate from melanoblasts that migrate from the neural crest, fibroblast are of mesenchymal origin – they behave very similar in respect to age-dependent telomere length regulation. A reason for this unexpected regulation could be that both cell types are only proliferatively active during embryonic development. In the adult organism they hardly proliferate and, therefore, replication-dependent telomere loss can be neglected. In keratinocytes, on the other hand, epithelial cells of ectodermal origin proliferate constantly. If not counteracted by telomerase, this would lead to a significant loss as it is seen when keratinocytes are grown in culture (Krunic *et al*., in revision). Instead, despite being somewhat shorter, they show a rather similar regression slope as the other two cell types. This suggests that for the keratinocytes the high rate of proliferation during early development is too extensive for telomerase to be able to counteract and hinder telomere loss. However, after birth the rate of telomere loss is minimal and despite ongoing, though steady state proliferation this loss can be minimized by the telomerase activity expressed by the keratinocytes.

A second unexpected result was that in a given skin the telomere length - either shorter or longer (in relation to other skin samples) – was similar for all three cell types. This suggested the importance of genetic determinants of the respective telomere length as it was already described for other tissues (Slagboom *et al*., 1994). Thus, one hypothesis would be that the variation between individuals observed in our tissue sample collection may be due to differences in the originally inherited telomere length.

4.2.4 Accelerated telomere erosion in discrete areas of human epidermis

A different interpretation could also come from our finding that some specimens from similar locations of the same donor (upper part of the right and left hand), as well as different regions of the same tissue specimen exhibited significant differences in telomere lengths, a fact that could not be explained by inheritance.

Unexpectedly, we observed significant differences in telomere lengths in some samples when analysing skin from the upper part of the left and right hand from the same donor. Since was not characteristic for all samples a general site-to-site variation in telomere length, i.e. different genetically determined telomere lengths at different body sites, appeared unlikely. Instead, the most likely explanation would be that these variations are due to differences in proliferation rate as caused by repeated trauma (e.g. wounding) or by extrinsically induced damage. Most importantly and again something that can only be identified by *in situ* analysis, we even identified extreme telomere loss in very small intra-epidermal areas.

The most dramatic difference was seen in six skin samples. Within an otherwise "normal" epidermis, i.e. epidermis with normal telomere length, we found smaller regions (from 20 to 40 basal cells in diameter) where the telomere length was strongly reduced. Interestingly, accelerated telomere erosion was restricted to the keratinocytes while the melanocytes and the dermal fibroblasts showed similarly strong telomere signal intensities in these as in the unaltered areas. To confirm that this finding was not an artefact, we performed a number of controls: co-hybridisation with the centromere 7 specific PNA probe, counting the number of signals per cell, and hybridisation on the next serial section. Quantification of the mean centromere intensity showed no significant difference in the hybridisation efficiency between cells with short and those with long telomeres. Also counting the total number of telomeres showed no difference indicating that "all" telomeres were present. All this strongly argued against an artefact but instead points to a very important aspect, namely accidental accelerated telomere loss.

Interesting in this context is also the fact that the same short telomeres were seen in all basal and suprabasal cells of that region. This has two major implications. This drastic effect can nor be due to a higher proliferation rate of only some basal cells and second it must have occurred in a stem cell. If damage occurs in a proliferating, so-called transit amplifying cell or in a differentiating cell, the "damage" is only passed on

to a few daughter cells and these are lost after one epidermal regeneration cycle (about 4 weeks). Instead all cells have the same telomere length and this length is obviously maintained throughout further regeneration. Therefore, "damage" must have occurred in a stem cell, the only cell that is maintained in the basal layer for long term.

Thus, besides an inter-personal variations, telomere length in the epidermis and dermis in some samples varied strongly between different though largely equivalent sites of the same person. Even more so, intra-epidermal sites were present where telomeres were on average 5 or even more times shorter than in their direct neighbourhood. Since it is proposed that critically short telomeres elicit telomere dysfunction (Autexier and Greider, 1996; Hemann *et al*., 2001), this accelerated telomere loss may well contribute to genomic instability. Furthermore, since the cell that is primarily hit is a stem cell that is maintained in the epidermis also further on, it is tempting to suggest that such regions have to be considered as early stages of skin carcinogenesis (reviewed in Boukamp 2005).

4.2.5 Accelerated telomere erosion correlates with the p53 expression and formation of 53BP1 foci

Normal cells detect potential DNA damage by activating a signal cascade through the p53 tumour suppressor protein (Finlay *et al*., 1989). Based on this, p53 is regarded as "the guardian of the genome" (Lane, 1992), as it initiates a program of cell cycle arrest, cellular senescence or apoptosis (rewieved in Harris and Levine, 2005). Signalling through the p53 is also known to occur due to experimental disruption of the telomere loop structure, or in the presence of oligonucleotides homologous to the telomere overhang sequence, which are proposed to mimic exposure of the 3' telomere overhang (reviewed in Kosmadaki and Gilchrest, 2004). Interestingly, when investigating the p53 status in our skin sections, we found that regions of the skin with accelerated telomere loss were also those with strong p53 expression. Moreover, quantification of the mean telomere length and the total amount of p53 protein in the same cells strongly suggest that the regulation of p53 expression is correlated with the telomere length - the shorter the telomeres were the more p53 was expressed. When telomeres are on average shorter there is a higher probability that one of the telomeres would be critically short and therefore dysfunctional (Hemann, 2001).

To confirm that telomeres do get dysfunctional in regions with accelerated telomere loss, we in addition analysed the 3D distribution of small telomeric signals in respect to p53 binding protein 1 (53BP1) foci. 53BP1 was described to be an important part of a DNA damage repair complex, it co-localizes with chromatin regions surrounding the sites of DNA double strand breaks (DSBs) (Ward *et al*., 2003). It was also described that 53BP1 can recognize dysfunctional telomeres, and 53BP1 foci were found to co-localize with telomeres in baboon skin biopsies originating from older animals (Jeyapalan *et al*., 2007). We now show that, similarly to p53 staining, p53BP1 foci signals are strongest in cells with shortest telomeres. In addition, 3D visualization in regions with accelerated telomere shortening clearly revealed co- localization of 53BP1 foci with telomeres in a number of cells, which was previously described to be a sign of dysfunctional telomeres (Takai *et al*., 2003). This further substantiates that some telomeres are uncapped and behave like DSBs thus demonstrating dysfunctional telomeres in these particular regions.

4.2.5.1 Regions with accelerated telomere loss are relatively frequent in human skin

Having found a good correlation between strong p53 expression and 53BP1 co-localizing with short telomeres which argued for a potential telomere length-dependant mechanism of genomic instability, we used this to determine the frequency of such regions in skin samples from different age donors by using immune-staining for p53. In the 30 skin samples analyzed 10 samples contained one or more p53-positive regions. Since the average length of the skin sections was only ~1 cm, i.e. only a minimal part of the skin, this implicates that the number of such "micro-lesions" is likely to be very high. This is also suggested from a study which determined p53-positive cells in the skin and showed that they often represented cells with mutated p53 (Jonason *et al*., 1996). Actually, the authors found on average 40 p53 expressing cells per cm^2 and proposed a positive correlation of p53-expressing regions in the epidermis with sun exposure. We confirmed that correlation by grouping the skin samples according to their potential sun exposure which revealed that the p53 stained regions occurred mostly in intermittently and continuously exposed skin (9/23). In the rarely sun exposed group only one out of 7 skin samples had detectable p53 stained regions. Different from their findings, however, we found a strong tendency for an increased number of p53-positive patches with increasing age. The reason for this may be that the range of our sample

collection was wider (7-90 years) and more equally distributed and that we could include 5 samples from donors >80 years and strongly support our hypothesis that these patches are UV-induced and increase in number with increased life span. Furthermore, our study suggests that the p53-positive patches are also characterized by short and potentially dysfunctional telomeres, thus could contain genomically instable cells.

4.2.5.2 Significance of p53 mutation and shortened telomeres in the epidermis

Possible explenation for p53 expressing regions in the epidermis is the mutation of p53, which was described for skin carcinomas (Einspahr *et al*., 1997, reviewed in Boukamp, 2005). A high rate of p53 mutations was also described for normal skin where the p53-positive regions were first identified (Jonason *et al*., 1996). Most importantly, 50% of the p53-expressing regions contained mutated protein, and it was proposed that p53 mutations are likely required for the development of clonal populations, i.e. the p53-positive regions. The authors even argued that due to technical limitations one may underestimate the true number and that more then 50% of the clones may contain p53 mutations. Some other reports propose that p53 mutations occur later in cancer development (Gorgoulis *et al*., 2005; Bartkova *et al*., 2003). They propose that the earliest stage of cancer development could be associated with DNA replication stress (as occurs in preneoplastic lesions), which leads to DSBs, genomic instability and selective pressure for p53 mutations. Although the telomere attrition was finally proposed to contribute to DSB formation, activation of the checkpoint and genomic instability (Gorgoulis *et al*., 2005), *in situ* measurement of telomere length was not performed.

We show that telomeres are shortened in p53 stained regions, however, we do not have information on eventual mutations in p53 gene. If the p53 is mutated in p53 stained regions of normal skin it could together with shortened telomeres initiate genomic instability. If the p53 would be active (wild type) it would in low levels favour growth arrest, whereas in higher levels it would override this default pathway and trigger apoptosis (Laptenko and Prives, 2006). Growth arrest may provide selective pressure for p53 inactivation which could again, in combination with shortened telomeres, lead to increase in genomic instability. Thus, p53 stained regions with shortened telomeres already fulfil important traits of early skin cancer lesions. We have to conclude that in normal skin and particularly aged skin a number of “early stage skin

cancer" lesions exist and that damage-dependent accelerated telomere loss is one crucial step for the development of these lesions.

4.2.6 Telomere length heterogeneity as a consequence of UV damage

Since the above studies demonstrated that telomere shortening had occurred at distinct sun exposed skin sites and correlated with defined signs of damage (p53 up-regulation, 53BP1 foci formation), we hypothesised that also the telomere length heterogeneity seen in the different age donors may at least in part be due to damage-dependent accelerated telomere erosion.

4.2.6.1 Telomere DNA sequence is prone to UV damage

UV irradiation is a well-known extrinsic insult that induces a variety of clinical features such as benign, premalignant, and malignant neoplasms in the skin. It is known that UVB exposure induces cyclobutane pyrimidine dimers (CPDs) and (6-4) photoproducts and that both, UVA and UVB, can induce oxidative stress (reviewed in Ichihashi, 2003). CPDs are more often present at thymine-thymine (TT), but can also be at thymine-cytosine (TC) and cytosine-/cytosine (CC) sites, while oxidative stress is frequently damaging guanine (G) rich sequences - especially at the GGG sites - where 8-oxoguanine (8-oxoG) is formed. Since the telomeric sequence is 5'…TTAGGG…3', and the complementary 3'…AATCCC…5' repeats, the telomere could be extremely sensitive and damage could occur principally all along the telomere. Furthermore, UV-dependent oxidative stress is also inducing single- and double-strand breaks and also these could occur at the telomeric DNA with the consequence of UV irradiation leading to telomere shortening. In line with this it was reported that UVA can cause a dose dependent telomere shortening in WI-38 human cultured fibroblasts (Oikawa *et al*., 2001). Nevertheless, direct proof that the UV damage can cause telomere shortening in the skin *in situ* was not shown so far.

4.2.6.2 Chronic sun exposure cause telomere shortening in the skin

During our study on telomere lengths in the different skin samples we also had skin samples from two individuals who, because of their profession, were heavily UV-exposed - a sailor and a farmer. Interestingly, both showed extremely short telomeres in

their epidermis. The skin section from the sailor contained a hair follicle (HF). Measuring telomere lengths along this HF demonstrated a steady telomere elongation with continuous distance from the surface. Since it suggested that UV radiation may have contributed to telomere shortening by affecting particularly the most exposed (outer) parts of the epidermis, we also measured telomere length at different depths from the surface in HF from skin where telomere shortening in the epidermis was not as extreme as seen in the sailor skin. Nevertheless, we found in two thirds of the samples (15 of 21) a positive correlation between telomere signal intensity and distance from the surface. Even in the dermal fibroblasts and melanocytes, despite the fact that both have in general longer telomeres than the keratinocytes, we observed a similar increase in telomere length with distance from the surface. In addition, we investigated different parts of the rete ridges (RRs), the structures that interconnect epidermis and dermis and because of which some parts of the epidermis are close to the surface (top of the rete RR) and some parts are further away (bottom of the rete ridges) and thus should be protected from UV damage. Indeed, in some of the deeper RRs we found significantly longer telomeres than at the bottom part, substantiating our hypothesis that constant UV exposure is the most crucial factor for telomere shortening in the epidermis.

While the above studies only provided indirect evidence for UV radiation contributing to telomere erosion in a significant manner, we could confirm the relevance for UV-dependent damage by analysing skin from 5 donors who had a history of chronic exposure to UV radiation and where UV-dependent damage was confirmed by the presence of cyclobutane pyrimidine dimers (CPDs). CPD-retaining basal cells (CRBCs) were counted in each of five samples to determine the average level of UV damage. They were compared with 5 UV protected skin samples without detected CRBCs. Even though the sample size was relatively small (five in each group), this study provided some important results. First, telomeres were clearly shortened in the sun-exposed skin, in dermis, keratinocytes and in melanocytes. Second, we also found strong correlation of the level of damage (number of CRBCs), and the rate of telomere shortening closer to the surface of HFs. So far there is only one study published on the influence of sun exposure on telomere length in skin. Using Southern blot-dependent TRFL analysis Sugimoto *et al*. (2006) reported that telomere lengths in the epidermis did not differ between 24 sun-exposed and 76 sun-protected samples. Comparing sun-exposed *versus* sun-protected skin from the same donor in 6 different patients, they even found telomere elongation in 5 of the sun-exposed samples and concluded that

extensive sun exposure causes telomere elongation. This latter is in strong contrast to our data. When measuring the overall telomere length we found an obvious difference in the two samples derived from the sailor and the farmer, i.e. in individuals who are professionally exposed to sun light continuously and these were characterized by significantly shortened telomeres. Furthermore, when measuring individual areas with particular emphasis on "close to sun" *versus* "more distant from sun" we observed shorter telomeres in sun-exposed areas more frequently.

The reason for this discrepancy is presently unclear. However, for all techniques that require larger amounts of tissue for e.g. DNA – irrespective of the fact that the Southern blot technique in itself does not allow very precise measurements (>1kb deviation)- and do not allow *in situ* analysis, may easily be miss leaded. Furthermore, we have found a wide variation in telomere length between donors and most importantly between different sites of the same donor and also this could influence the results. Therefore, more detailed studies would be required to prove the role of UV on telomere lengths regulation.

4.2.6.3 Acute UVA/UVB irradiation can cause telomere shortening in the skin

To address this, we studied the direct consequence of UV radiation on telomere length by investigating telomere length in 16 skin samples - 8 were derived from Lupus erythematosus patients and 8 from healthy donors - that were irradiated with a single dose of UVA and/or UVB and biopsies were taken from the irradiated area at different time points.

Comparing the overall telomere length, there was no obvious difference between the Lupus patients *versus* healthy donors. There only appeared to be a higher interpersonal variation in the epidermis of the Lupus patients. So far, telomere length was measured before only in Lupus leukocytes where a disease-dependent telomere shortening was described (reviewed in Rus and Via, 2001). As Lupus is an autoimmune disease, it may not be surprising that the chronic immune stimulation resulted in an accelerated telomere shortening, in particular since leucocytes are generally prone to telomere shortening, e.g. also during aging (Frenck *et al*., 1998; Krunic *et al*., in revision).

Concerning the UV-dependent telomere length regulation, we found telomere loss in both sample collections. On average, telomere length and the rate of telomere shortening due to UV irradiation appeared the same in Lupus *versus* healthy donors.

Therefore, we felt confident to combine the data derived from the altogether 16 samples. Different as expected from the study reported by Sugiomto *et al*. (2006), we observed rapid telomere shortening as a consequence of radiation with a combination of UVA and UVB. Thus, these data further substantiate our hypothesis that UV radiation (sun exposure) is responsible for accelerated telomere erosion in human skin. Since telomere shortening is a very rapid process, major telomere shortening occurred within the first days after irradiation, it can only be explained by UV radiation causing formation of DSBs followed by breakage of the telomeres.

A less clear decline was seen after UVA or UVB only. Interestingly and with all caution because of the small sample number, our data do not allow on attributing this to a specific UV source since both UVA and UVB alone were less effective. ROS, as induced by UVA radiation, are known to cause breaks in G-rich sequences, which makes telomeric DNA 5 to 10-fold more assailable than non-telomeric DNA (Oikawa and Kawanishi, 1999; von Zglinicki *et al*., 2000). Thus, telomeres should be optimal substrates for UVA radiation. On the other hand, UVA-induced ROS depend on the up-to-now unknown nuclear sensitizers, which may not be always present at the telomeres. UVA radiation, therefore, may not account for rapid telomere erosion (Wischermann *et al*., subm.).

A further argument for telomere breakage as a cause of UV-dependent telomere shortening is the fact that four samples that were in addition investigated for 53BP1 and γH2AX, two markers for DNA DSBs (Schultz *et al*., 2000) showed a positive correlation. 53BP1 was described to be important part of a DNA damage repair, it becomes hyperphosphorylated after radiation and co-localizes with phosphorylated γH2AX in megabase regions surrounding the sites of DSBs (Ward *et al*., 2003). We observed that those samples with extreme telomere shortening had more 53BP1 and γH2AX co-localized foci and much stronger γH2AX expression in more cells than samples with only minor telomere shortening. Thus despite the same UVA/ UVB treatment and similar skin types, the damage response obviously differs. The reason for this is presently still unclear. But this may also be the reason for the high interpersonal variation in telomere lengths seen in the different-age individuals (see before).

In summary, we conclude that telomeres can shorten in the epidermis as a consequence of the chronic sun exposure. The rate of telomere shortening may not necessarily be proportional to the amount of UV damage but may be dependent on as yet undetermined factors which can differ between different individuals.

4.2.7 Telomeres are shortened in keratinocytes proximally to chronic wounds

Besides UV, other common insults affect the skin. These include infectious agents but also the immune response. Similar to UV, activated phagocytes in the tissue produce reactive nitrogen NO and oxygen O_2^- species (ROS), which cause a formation of 8-oxodG and directly damages any DNA that has a high guanine content as is the telomere sequence $(TTAGGG)_n$. Accordingly, it was shown in *in vitro* experiments that oxidative stress and ROS can damage DNA and shorten telomeres (Oikawa and Kawanishi, 1999; von Zglinicki *et al*., 1995). It is well known that ROS are a major burden for chronic wounds, either coming from infectious agents, hypoxia, or the constant immune response (Khodr and Khalil, 2001; Moseley *et al*., 2004). Telomeres in chronic wounds, therefore, should suffer from constant telomere shortening.

While the actual wound is a fibrin-rich granulation tissue with numerous inflammatory cells, thus, not very meaningful in respect to stress-dependent telomere regulation, we analyzed the skin in immediately adjacent to the wound. We had the chance to compare four skin samples with chronic wounds with healthy skin from the same patients. Interestingly, we did not find any telomere shortening in the dermis. On the contrary, in one sample telomeres of the dermal fibroblasts were even longer in the region proximal to the wound. Although this is in contrast to what we would have expected, another group reported on similar findings. Having isolated fibroblasts from chronic wounds and healthy skin from the same donors, they did not find signs of senescence, including telomere shortening in the fibroblasts originating from the chronic wounds (Stephens *et al*., 2003). Due to our advantage of being able to investigate *in situ* the different parts of the sections, and the different cell types individually, however, we found a clear difference in telomere length in keratinocytes proximal to the chronic wound. Interestingly, telomeres were not only shorter in those keratinocytes that were directly in the wound, but also in those regions of the epidermis that were even 2-3 mm distant from the wound edge telomere length was still reduced. Here, telomere shortening was accompanied by hyperproliferation, as obvious from the increased thickness of the epidermis. In the epithelial tongues that partly covered the wounds we did not detect additional shortening. As proliferation is not present in the epithelial tongue, but only at the wound edge (Bartkova *et al*., 2003), this further supports the requirement for proliferation to see telomere shortening. If telomeres break, this will only be detectable after replication in the daughter cells. Thus accelerated

telomere erosion is the consequence of an concerted action between damage on telomeres and cell divisions.

In the same regions we also observed strong infiltration of inflammatory cells, indicated by the high number of vimentin-positive cells - many more than were present in the uninvolved skin. As inflammatory cells are responsible for oxidative stress and the telomeric sequence is prone to damage by reactive oxygen species, we propose that in chronic wounds telomere shortening occurs in the keratinocytes as a direct consequence of the oxidative damage in combination with an increased proliferation rate.

4.2.7.1 Telomere length is slightly reduced in the epidermis of acute wounds

The important difference between chronic and acute wounds is that in acute wounds the inflammatory phase is restricted to the first five days of the wound healing process while in chronic wounds this process is continuing. To investigate whether short term exposure to ROS in the acute wounds would also cause telomere shortening we had the chance to analysed telomere length in one 1-day-old wound sample and two 5-day-old wound samples. Telomere length in the keratinocytes from the 1-day-old wound did not differ from that of the surrounding skin. However, a slight reduction in telomere length was observed in the wound edges of the two 5-day-old wounds. Since telomeres were only shortened at the wound edges but not in the surrounding epidermis, and since inflammation with high numbers of monocytes and macrophages is present from the second to the fifth day after wounding in the wound area but not in the surrounding skin, also this shortening was likely mediated by the oxidative stress caused by the inflammatory cells. Interestingly, telomere length in dermis was unaffected by this and similar in length irrespectively of the distance from the wound. Whether this is because fibroblasts are less sensitive to ROS or that different from the keratinocytes they do proliferate less still needs to be elucidated.

Taken together, despite the fact that only a very small number of samples could be analyzed, our data provide evidence that the stress of skin wounding has an effect on telomere length. While telomere shortening may only be minimal in acute wounds it seems to be of significance in chronic wounds. From this it is tempting to speculate that telomeres may finally reach a length where they no longer promote proliferation. Thus

one reason for the non-healing chronic wounds may indeed be telomere exhaustion and thus senescence of the keratinocytes.

4.3 Stem cells and telomere length in the skin

The skin is constantly exposed to UV radiation, wounding, and other types of insults, thus, has to keep the renewal capacity through the lifetime to be able to repair eventual damage of tissue integrity. Another important requirement is genomic stability during lifetime, therefore, telomeres should not be significantly shortened as it could result in the critical telomere length and chromosomal end-to-end fusions (Autexier and Greider, 1996). In all studies described so far, telomere length was investigated in the entire epidermis and we could show that the overall telomere length did not decrease significantly with age, i.e. with constant replication. Despite the fact that keratinocytes are telomerase-positive and thus telomerase could minimize telomere erosion, there also could be an alternative explanation. It is well accepted that the constant epidermal renewal depends on a population of long-lived stem cells (SCs). These are located in the basal layer of the epidermis. The stem cells themselves are believed to only proliferate rarely, while their daughter cells, the so called transit amplifying cells (TACs) are the ones that proliferate more rapid. However, also these cells only proliferate 4 to 6 times before they enter a differentiation pathway that finally terminates in dead horn squames; meaning that the cells are lost and do not further account for the overall telomere length. Since telomere loss is replication-dependent and if telomerase is not active, telomeres in stem cells should thus be longer than in the more rapidly proliferating stem cells.

4.3.1 Cells with “very long” telomeres are present in the basal layer of the epidermis

We found variations of the telomere length within the epidermal basal layer in all 18 skin samples (from different-age donors) tested. Interestingly, in some regions of different skin samples where telomeres were on average longer, the difference in telomere length between the cells of the basal layer was generally less pronounced. In those regions where telomeres were on average shorter it was easier to identify cells with “very long” telomeres as they more clearly differed in telomere length from the

other cells. Most importantly, in each sample there were only a few cells showing "very long" telomeres. Unfortunately, and despite of >30 years of epidermal stem cell research, no markers exist that are specific for human interfollicular epidermal stem cells and thus allow to unequivocally identify them (reviewed in Kaur, 2006). Therefore, we presently can not prove that these cells are indeed the stem cells. However, the likelihood that telomeres in these cells were maintained due to their rare proliferation is high.

Similar as the nature of the stem cells also their localisation in the human interfollicular epidermis is still unknown and rather controversially discussed. Various markers that stained different clusters of cells within the human epidermal basal layer were described, however, none of them could be used to identify only the stem cells (reviewed in Kaur, 2006). One marker, melanoma chondroitin sulphate proteoglycan (MCSP) is specific for the upper part of the rete ridges only (Legg *et al*., 2003). To more specifically define the location of the cells with the longest telomeres, we, therefore, investigated for co-expression of MCSP in 27 different regions of six different skin samples. To our surprise, we found tendency that MCSP expressing cells have on average longer telomeres in 44% (12/27) of regions, however, the difference was not statisticaly significant. In 12 regions out of 27 we even identified individual cells with longest telomeres that were stained positive for MCSP, however, in most of the regions (15/27) they were not MCSP positive.

From this we have to conclude that the cells with the "very long" telomeres are not restricted to a specific region but are present throughout the basal layer of the epidermis. Furthermore, MCSP is supposed to promote SCs clustering as it was shown that it has a role in promoting cohesiveness of keratinocytes (Legg *et al*., 2003). However, irrespective of whether colocalized with MCSP or not we did not find any clusting of cells with "very long" telomeres. They always appeared as individual cells and randomly distributed. If these are the stem cells our study strongly supports the work by Ghazizadeh and Taichman (2005) which were the first to show that in human epidermis the stem cells are distributed all along the basal layer.

The rather random distribution of the cells with "very long" telomeres in the basal layer of the skin was also confirmed by reconstructing an entire part of the tissue. For this 19 consecutive sections from one skin sample were analyzed for telomere length by identifying in each section the same region and reconstructing a two-dimensional distribution pattern. This approach allowed insight into telomere length of

each individual cell in the whole region of approximately 140µm x 200µm. Also this analysis did not provide evidence for any particular distribution and demonstrated that about 8 % of the analysed basal cells contained "very long" telomeres. This demonstrated that, if these cells are indeed the stem cells, they are distributed throughout the epidermis as single cells in a pattern that at present appears rather random.

4.3.1.1 Very long telomeres are not restricted to hypoxic areas

It was recently proposed that hypoxia promotes the undifferentiated cell state in various stem and precursors cell populations as it blocked neuronal and myogenic differentiation in a Notch-dependent manner (Gustafsson *et al*., 2005). Furthermore, evidence was provided that hypoxia promotes maintainance of human hematopoietic and mouse embryonic stem cells (Cipolleschi *et al*., 1993; Covelo *et al*., 2006). It, therefore, seemed reasonable that stem cells were located in hypoxic areas. Since hypoxia is characterized by induction of the hypoxia-survival gene carbonic anhydrase IX (CA-IX), localization of CA-IX expression in the skin may indicate position of the stem cells. When we localized and quantified the expression of CA-IX and correlated this with the telomere length of the individual cells of the basal layer of the epidermis, we did not find any tendency for longer telomeres in the CA-IX expressing cells. On the contrary, in 10 of 27 regions from 6 different skin samples telomere lengths was on average even slightly reduced. However, in 37% (10/27) of regions individual cells with longest telomeres were stained for CA-IX. Therefore, similar as described for MCSP, a few cells with "very long" telomeres were expressing the CA-IX. However, the majority of cells with "very long" telomeres were not located in CA-IX -positive areas. If these cells are indeed stem cells our data suggest that neither MCSP not CAIX specifically mark the stem cell niche in human interfollicular epidermis.

Interestingly, MCSP and CA-IX are expressed in the same region of the skin, namely at the top of the rete ridges (Muffler, unpublished results). Having performed double- labelling for CA-IX and MCSP, we found a similar distribution, often being present at the top of the rete ridges. However, high resolution microscopy revealed that the two proteins were not necessarily always co-expressed by the same cells; in fact staining pattern was quite exclusive for one or the other in some regions. If they were co-expressed, MCSP expression was restricted to the basal cells while CA-IX

expression was detected in suprabasal cells as well. In the interfollicular epidermis the number and size of the regions on the skin sections that were stained with one or another marker, and also the level of co-localization of two markers varied significantly between different samples. The largest difference was in the hair follicles (HFs): CA-IX expression was most prominent in the upper parts of the hair follicle, while MCSP was strongly expressed in the lower parts, with some co-localisation in the middle.

In some skin samples without rete ridges (in 4 out of 16 skin samples), on the other hand, there were no MCSP or CA-IX-stained regions in the interfollicular epidermis. This strongly argues that the expression of both proteins is conformation-dependent. Accordingly, these two markers can not be indicative for the stem cell niche as stem cells are also present in rete ridge-poor or –deficient skin.

Finally and as a side aspect, this study demonstrated the importance of precisely identifying the staining pattern of the potential stem cell markers on various skin samples before using them for further isolation procedures. For example, the staining for MCSP and/or CA-IX markers was not present only in IFE. The strongest intensity was detected in HFs. If epidermal stem cells are isolated from the skin sample and selected according to high expression of MCSP and/or CA-IX, Fluorescence activated cell sorting could easily result in an enriched population of HF cells. Since it is as yet unclear – though implicated from mouse skin studies that HF and IFE stem cells differ - incorrect conclusions could be drawn on the nature and characteristics of the IFE stem cells.

4.3.2 Telomeres are on average longer in label-retaining cells

One of the characteristics of stem cells is that they only rarely proliferate and because of this, cells that are labelled with a DNA marker, as Bromo-deoxyuridine (BrdU), maintain this label while all cells that rapidly proliferate loose the label (Bickenbach, 1981). Unfortunately, human skin can not be labelled thus all respective studies were performed with mice (reviewed in Fuchs, 2007). Only recently a human model was established in the Boukamp laboratory that allows to establish label-retaining cells in long-term 3D Organotypic co-cultures (3D-OTC) (Stark et. al., 2006, Muffler *et al*., subm.). During the early phase of tissue development the proliferating cells are labelled with Iodo-deoxyuridine (IUdR). Thereafter, tissue regeneration is performed without further labelling. During this chase period the label is lost in those

cells that proliferate. Only cells that do not proliferate and thus behave like stem cells remain as label-retaining cells (LRCs). While it could be shown with this model that keratinocytes that had been propagated in conventional monolayer cultures were able to re-establish a stem cell hierarchy, the kind of cell from which this stem cell hierarchy establishes is still elusive. Two hypothesis exist: first, stem cells are genetically defined and thus only these cells can function as stem cells and re-establish themselves in the proper environment, the stem cell niche. Second, stem cells are determined by the stem cell niche, and thus stem cell is a functional term, allowing also non-stem cells to revert back into a stem cell state.

Having established that in the epidermis *in situ* a small population with long telomeres exists and assuming that this is the stem cell population, one possibility to address this question was to evaluate the telomere lengths in the LRCs. Assuming that the cells with longest telomeres in the epidermis *in situ* are the stem cells, and assuming that only these cells can re-establish as stem cells in OTCs then all LRCs should have the longest telomeres. If all cells can re-establish as "stem cells", we should not find a positive correlation between telomere length and LRC.

We now demonstrate that after a chase period of 4-weeks there was a slight tendency that LRCs had longer telomeres. Furthermore, in 7 of 18 regions we found LRCs with longest telomeres within each of those regions. After a chase period of 6-weeks, however, there was a strong tendency and accordingly a statistically significant correlation for LRCs to have the longest telomeres. These findings have two major implications. First, a 4-week-chase period is not sufficient to eliminate all labelled cells that are not true LRCs. Accordingly, the number of heavily labelled cells decrease from 2.8% to 0.9% during this time period (Muffler *et al*., subm.). In agreement with that, also some transit amplifying cells are still heavily labelled. These proliferated and loose the label during the following two weeks, leaving only the stem cells as LRCs after 6 weeks. Second, since most of the LRCs are the cells with the longest telomeres, we have to conclude that the cells with "very long" telomeres in the epidermis *in situ* are the stem cells and that these cells establish themselves as stem LRCs/stem cells in the OTCs. So likely, these cells are genetically defined and obviously maintain their "nature" also during *in vitro* propagation.

However, on the same section we could localize regions with on average longer telomeres that contained cells without label. Therefore, the telomere lengths distribution was similar as in the epidermis *in situ*, where regional differences in telomere length

exist. Those differences in the skin could, as proposed above, originate from different exposure to proliferative stress and/or external damage, e.g. whether the stem cells derived from more UV-exposed parts or protected parts of the epidermis. An extreme example would be the regions with accelerated telomere shortening that we observe in some samples, where extensively damaged stem cell obviously produce an entire region of cells with shorten telomeres. Since we found "very long" telomeres in all parts of the epidermis it appears, therefore, tempting to stress the importance of the location of the stem cell niche in the intact skin, as the most crucial determinant for the telomere length of the stem cells also after isolation and further propagation.

Taken together, there are individual cells with long telomeres in the basal layer of the epidermis. These can but do not necessarily have to co-localize with the proposed stem cell marker MCSP or with potential areas of hypoxia as indicated by CAIX staining. Instead, our data suggest that these cells are distributed in an unrestricted though not jet well defined manner throughout the basal layer of the epidermis. Interestingly, also in OTCs the long-lasting LRCs are the cells with longest telomeres, suggesting that the longest telomeres indeed mark the stem cells in human epidermis *in situ* and that these cells establish themselves as stem cells (LRCs) in the OTCs.

5. References

5 References

Allsopp RC, Harley CB (1995) Evidence for a critical telomere length in senescent human fibroblasts. Exp Cell Res 219:130-136

Autexier C, Greider CW (1996) Telomerase and cancer: revisiting the telomere hypothesis. Trends Biochem Sci 21:387-391

Bachor C, Bachor OA, Boukamp P (1999) Telomerase is active in normal gastrointestinal mucosa and not up-regulated in precancerous lesions. J Cancer Res Clin Oncol 125:453-460

Bartkova J, Gron B, Dabelsteen E, Bartek J (2003) Cell-cycle regulatory proteins in human wound healing. Arch Oral Biol 48:125-132

Bartkova J, Horejsi Z, Koed K, Kramer A, Tort F, Zieger K, Guldberg P, Sehested M, Nesland JM, Lukas C, Orntoft T, Lukas J, Bartek J (2005) DNA damage response as a candidate anti-cancer barrier in early human tumorigenesis. Nature 434:864-870

Belgrader P, Dey R, Berezney R (1991) Molecular cloning of matrin 3. A 125-kilodalton protein of the nuclear matrix contains an extensive acidic domain. J Biol Chem 266:9893-9899

Berezney R, Coffey DS (1974) Identification of a nuclear protein matrix. Biochem Biophys Res Commun 60:1410-1417

Berezney R (2002) Regulating the mammalian genome: the role of nuclear architecture. Adv Enzyme Regul 42:39-52

Bickenbach JR (1981) Identification and behavior of label-retaining cells in oral mucosa and skin. J Dent Res 60 Spec No C:1611-1620

Bickenbach JR, Vormwald-Dogan V, Bachor C, Bleuel K, Schnapp G, Boukamp P (1998) Telomerase is not an epidermal stem cell marker and is downregulated by calcium. J Invest Dermatol 111:1045-1052

Billia F, de BU (1991) Localization of centromeric satellite and telomeric DNA sequences in dorsal root ganglion neurons, in vitro. J Cell Sci 100 (Pt 1):219-226

Blackburn EH, Gall JG (1978) A tandemly repeated sequence at the termini of the extrachromosomal ribosomal RNA genes in Tetrahymena. J Mol Biol 120:33-53

Blackburn EH (1992) Telomerases. Annu Rev Biochem 61:113-129

Blackburn EH (2005) Telomeres and telomerase: their mechanisms of action and the effects of altering their functions. FEBS Lett 579:859-862

Bose B, Agarwal S, Chatterjee SN (1990) Membrane lipid peroxidation by UV-A: mechanism and implications. Biotechnol Appl Biochem 12:557-561

Boukamp P, Petrussevska RT, Breitkreutz D, Hornung J, Markham A, Fusenig NE (1988) Normal keratinization in a spontaneously immortalized aneuploid human keratinocyte cell line. J Cell Biol 106:761-771

Boukamp P, Popp S, Krunic D (2005) Telomere-dependent chromosomal instability. J Investig Dermatol Symp Proc 10:89-94

Boukamp P (2005) UV-induced skin cancer: similarities--variations. J Dtsch Dermatol Ges 3:493-503

Boukamp P, Mirancea N (2007) Telomeres rather than telomerase a key target for anti-cancer therapy? Exp Dermatol 16:71-79

Brinkley BR, Brenner SL, Hall JM, Tousson A, Balczon RD, Valdivia MM (1986) Arrangements of kinetochores in mouse cells during meiosis and spermiogenesis. Chromosoma 94:309-317

Broccoli D, Young JW, de Lange T (1995) Telomerase activity in normal and malignant hematopoietic cells. Proc Natl Acad Sci U S A 92:9082-9086

Cerezo A, Kalthoff H, Schuermann M, Schafer B, Boukamp P (2002) Dual regulation of telomerase activity through c-Myc-dependent inhibition and alternative splicing of hTERT. J Cell Sci 115:1305-1312

Chuang TC, Moshir S, Garini Y, Chuang AY, Young IT, Vermolen B, van den DR, Mougey V, Perrin M, Braun M, Kerr PD, Fest T, Boukamp P, Mai S (2004) The three-dimensional organization of telomeres in the nucleus of mammalian cells. BMC Biol 2:12

Cipolleschi MG, Dello SP, Olivotto M (1993) The role of hypoxia in the maintenance of hematopoietic stem cells. Blood 82:2031-2037

Covello KL, Kehler J, Yu H, Gordan JD, Arsham AM, Hu CJ, Labosky PA, Simon MC, Keith B (2006) HIF-2alpha regulates Oct-4: effects of hypoxia on stem cell function, embryonic development, and tumor growth. Genes Dev 20:557-570

de Lange T (2002) Protection of mammalian telomeres. Oncogene 21:532-540

de Lange T (2005) Shelterin: the protein complex that shapes and safeguards human telomeres. Genes Dev 19:2100-2110

Einspahr J, Alberts DS, Aickin M, Welch K, Bozzo P, Grogan T, Nelson M (1997) Expression of p53 protein in actinic keratosis, adjacent, normal-appearing, and non-sun-exposed human skin. Cancer Epidemiol Biomarkers Prev 6:583-587

Engelhardt M, Kumar R, Albanell J, Pettengell R, Han W, Moore MA (1997) Telomerase regulation, cell cycle, and telomere stability in primitive hematopoietic cells. Blood 90:182-193

Ermler S, Krunic D, Knoch TA, Moshir S, Mai S, Greulich-Bode KM, Boukamp P (2004) Cell cycle-dependent 3D distribution of telomeres and telomere repeat-binding factor 2 (TRF2) in HaCaT and HaCaT-myc cells. Eur J Cell Biol 83:681-690

Figueroa R, Lindenmaier H, Hergenhahn M, Nielsen KV, Boukamp P (2000) Telomere erosion varies during in vitro aging of normal human fibroblasts from young and adult donors. Cancer Res 60:2770-2774

Finlay CA, Hinds PW, Levine AJ (1989) The p53 proto-oncogene can act as a suppressor of transformation. Cell 57:1083-1093

Frenck RW, Jr., Blackburn EH, Shannon KM (1998) The rate of telomere sequence loss in human leukocytes varies with age. Proc Natl Acad Sci U S A 95:5607-5610

Friedrich U, Griese E, Schwab M, Fritz P, Thon K, Klotz U (2000) Telomere length in different tissues of elderly patients. Mech Ageing Dev 119:89-99

Fuchs E (2007) Scratching the surface of skin development. Nature 445:834-842

Fusenig NE, Worst PK (1975) Mouse epidermal cell cultures. II. Isolation, characterization and cultivation of epidermal cells from perinatal mouse skin. Exp Cell Res 93:443-457

Gerstein AD, Phillips TJ, Rogers GS, Gilchrest BA (1993) Wound healing and aging. Dermatol Clin 11:749-757

Ghazizadeh S, Taichman LB (2005) Organization of stem cells and their progeny in human epidermis. J Invest Dermatol 124:367-372

Gorgoulis VG, Vassiliou LV, Karakaidos P, Zacharatos P, Kotsinas A, Liloglou T, Venere M, Ditullio RA, Jr., Kastrinakis NG, Levy B, Kletsas D, Yoneta A, Herlyn M, Kittas C, Halazonetis TD (2005) Activation of the DNA damage checkpoint and genomic instability in human precancerous lesions. Nature 434:907-913

Goukassian DA, Gilchrest BA (2004) The interdependence of skin aging, skin cancer, and DNA repair capacity: a novel perspective with therapeutic implications. Rejuvenation Res 7:175-185

Greider CW (1996) Telomere length regulation. Annu Rev Biochem 65:337-365

Griffith JD, Comeau L, Rosenfield S, Stansel RM, Bianchi A, Moss H, de Lange T (1999) Mammalian telomeres end in a large duplex loop. Cell 97:503-514

Gustafsson MV, Zheng X, Pereira T, Gradin K, Jin S, Lundkvist J, Ruas JL, Poellinger L, Lendahl U, Bondesson M (2005) Hypoxia requires notch signaling to maintain the undifferentiated cell state. Dev Cell 9:617-628

Haber JE, Thorburn PC (1984) Healing of broken linear dicentric chromosomes in yeast. Genetics 106:207-226

Harle-Bachor C, Boukamp P (1996) Telomerase activity in the regenerative basal layer of the epidermis inhuman skin and in immortal and carcinoma-derived skin keratinocytes. Proc Natl Acad Sci U S A 93:6476-6481

Harley CB, Futcher AB, Greider CW (1990) Telomeres shorten during ageing of human fibroblasts. Nature 345:458-460

Harper L, Golubovskaya I, Cande WZ (2004) A bouquet of chromosomes. J Cell Sci 117:4025-4032

Harris SL, Levine AJ (2005) The p53 pathway: positive and negative feedback loops. Oncogene 24:2899-2908

Hastie ND, Allshire RC (1989) Human telomeres: fusion and interstitial sites. Trends Genet 5:326-331

Hayflick L, Moorhead PS (1961) The serial cultivation of human diploid cell strains. Exp Cell Res 25:585-621

Hayflick L (2000) The illusion of cell immortality. Br J Cancer 83:841-846

Hemann MT, Strong MA, Hao LY, Greider CW (2001) The shortest telomere, not average telomere length, is critical for cell viability and chromosome stability. Cell 107:67-77

Hiyama E, Hiyama K (2007) Telomere and telomerase in stem cells. Br J Cancer 96:1020-1024

Hodes RJ (1999) Telomere length, aging, and somatic cell turnover. J Exp Med 190:153-156

Houghtaling BR, Cuttonaro L, Chang W, Smith S (2004) A dynamic molecular link between the telomere length regulator TRF1 and the chromosome end protector TRF2. Curr Biol 14:1621-1631

Ichihashi M, Ueda M, Budiyanto A, Bito T, Oka M, Fukunaga M, Tsuru K, Horikawa T (2003) UV-induced skin damage. Toxicology 189:21-39

Jeyapalan JC, Ferreira M, Sedivy JM, Herbig U (2007) Accumulation of senescent cells in mitotic tissue of aging primates. Mech Ageing Dev 128:36-44

Jonason AS, Kunala S, Price GJ, Restifo RJ, Spinelli HM, Persing JA, Leffell DJ, Tarone RE, Brash DE (1996) Frequent clones of p53-mutated keratinocytes in normal human skin. Proc Natl Acad Sci U S A 93:14025-14029

Kang MK, Swee J, Kim RH, Baluda MA, Park NH (2002) The telomeric length and heterogeneity decrease with age in normal human oral keratinocytes. Mech Ageing Dev 123:585-592

Karlseder J, Broccoli D, Dai Y, Hardy S, de Lange T (1999) p53- and ATM-dependent apoptosis induced by telomeres lacking TRF2. Science 283:1321-1325

Kaur P (2006) Interfollicular epidermal stem cells: identification, challenges, potential. J Invest Dermatol 126:1450-1458

Kawanishi S, Hiraku Y, Oikawa S (2001) Mechanism of guanine-specific DNA damage by oxidative stress and its role in carcinogenesis and aging. Mutat Res 488:65-76

Kawanishi S, Oikawa S (2004) Mechanism of telomere shortening by oxidative stress. Ann N Y Acad Sci 1019:278-284

Khodr B, Khalil Z (2001) Modulation of inflammation by reactive oxygen species: implications for aging and tissue repair. Free Radic Biol Med 30:1-8

Klobutcher LA, Swanton MT, Donini P, Prescott DM (1981) All gene-sized DNA molecules in four species of hypotrichs have the same terminal sequence and an unusual 3' terminus. Proc Natl Acad Sci U S A 78:3015-3019

Konishi T, Kagan V, Matsugo S, Packer L (1991) UV induces oxy- and chromanoxyl free radicals in microsomes by a new photosensitive organic hydroperoxide, N,N'-bis(2-hydroperoxy-2-methoxyethyl)- 1,4,5,8-naphtalene-tetra-carboxylic-diimide. Biochem Biophys Res Commun 175:129-133

Kosmadaki MG, Gilchrest BA (2004) The role of telomeres in skin aging/photoaging. Micron 35:155-159

Kupsch JM, Tidman N, Bishop JA, McKay I, Leigh I, Crowe JS (1995) Generation and selection of monoclonal antibodies, single-chain Fv and antibody fusion phage specific for human melanoma-associated antigens. Melanoma Res 5:403-411

Lane DP (1992) Cancer. p53, guardian of the genome. Nature 358:15-16

Laptenko O, Prives C (2006) Transcriptional regulation by p53: one protein, many possibilities. Cell Death Differ 13:951-961

Lavker RM, Sun TT (1982) Heterogeneity in epidermal basal keratinocytes: morphological and functional correlations. Science 215:1239-1241

Legg J, Jensen UB, Broad S, Leigh I, Watt FM (2003) Role of melanoma chondroitin sulphate proteoglycan in patterning stem cells in human interfollicular epidermis. Development 130:6049-6063

Leigh IM, Lane B, Watt MW (1994) *The Keratinocyte Handbook* (Cambridge Univ.

Press, Cambridge, U.K.).

Lindsey J, McGill NI, Lindsey LA, Green DK, Cooke HJ (1991) In vivo loss of telomeric repeats with age in humans. Mutat Res 256:45-48

Louis EJ (2002) Are Drosophila telomeres an exception or the rule? Genome Biol 3:REVIEWS0007

Louis SF, Vermolen BJ, Garini Y, Young IT, Guffei A, Lichtensztejn Z, Kuttler F, Chuang TC, Moshir S, Mougey V, Chuang AY, Kerr PD, Fest T, Boukamp P, Mai S (2005) c-Myc induces chromosomal rearrangements through telomere and chromosome remodeling in the interphase nucleus. Proc Natl Acad Sci U S A 102:9613-9618

Lundblad V, Blackburn EH (1993) An alternative pathway for yeast telomere maintenance rescues est1- senescence. Cell 73:347-360

Manuelidis L (1994) Genomic stability and instability in different neuroepithelial tumors. A role for chromosome structure? J Neurooncol 18:225-239

McClintock B (1941) The Stability of Broken Ends of Chromosomes in Zea Mays. Genetics 26:234-282

McEachern MJ, Krauskopf A, Blackburn EH (2000) Telomeres and their control. Annu Rev Genet 34:331-358

Mergny JL, Helene C (1998) G-quadruplex DNA: a target for drug design. Nat Med 4:1366-1367

Molenaar C, Wiesmeijer K, Verwoerd NP, Khazen S, Eils R, Tanke HJ, Dirks RW (2003) Visualizing telomere dynamics in living mammalian cells using PNA probes. EMBO J 22:6631-6641

Moroi Y, Hartman AL, Nakane PK, Tan EM (1981) Distribution of kinetochore (centromere) antigen in mammalian cell nuclei. J Cell Biol 90:254-259

Moseley R, Hilton JR, Waddington RJ, Harding KG, Stephens P, Thomas DW (2004) Comparison of oxidative stress biomarker profiles between acute and chronic wound environments. Wound Repair Regen 12:419-429

Müller HJ (1938) The remaking of the chromosomes. *The Collecting Net*, 13: 181-195.

Nagele RG, Velasco AQ, Anderson WJ, McMahon DJ, Thomson Z, Fazekas J, Wind K, Lee H (2001) Telomere associations in interphase nuclei: possible role in maintenance of interphase chromosome topology. J Cell Sci 114:377-388

Nakamura K, Izumiyama-Shimomura N, Sawabe M, Arai T, Aoyagi Y, Fujiwara M, Tsuchiya E, Kobayashi Y, Kato M, Oshimura M, Sasajima K, Nakachi K, Takubo K (2002) Comparative analysis of telomere lengths and erosion with age in human epidermis and lingual epithelium. J Invest Dermatol 119:1014-1019

Nakayama H, Kato H, Okajima H, Yasumoto S (1998) [Telomerase activity in the uterine cervix and the uterine body]. Nippon Rinsho 56:1305-1309

Neumann AA, Reddel RR (2002) Telomere maintenance and cancer -- look, no telomerase. Nat Rev Cancer 2:879-884

Nishiyama A, Dahlin KJ, Stallcup WB (1991) The expression of NG2 proteoglycan in the developing rat limb. Development 111:933-944

Notaro R, Cimmino A, Tabarini D, Rotoli B, Luzzatto L (1997) In vivo telomere dynamics of human hematopoietic stem cells. Proc Natl Acad Sci U S A 94:13782-13785

Ogura R, Sugiyama M, Nishi J, Haramaki N (1991) Mechanism of lipid radical formation following exposure of epidermal homogenate to ultraviolet light. J Invest Dermatol 97:1044-1047

Oikawa S, Kawanishi S (1999) Site-specific DNA damage at GGG sequence by oxidative stress may accelerate telomere shortening. FEBS Lett 453:365-368

Oikawa S, Tada-Oikawa S, Kawanishi S (2001) Site-specific DNA damage at the GGG sequence by UVA involves acceleration of telomere shortening. Biochemistry 40:4763-4768

Olovnikov AM (1971) [Principle of marginotomy in template synthesis of polynucleotides]. Dokl Akad Nauk SSSR 201:1496-1499

Olovnikov AM (1973) A theory of marginotomy. The incomplete copying of template margin in enzymic synthesis of polynucleotides and biological significance of the phenomenon. J Theor Biol 41:181-190

Parkinson GN, Lee MP, Neidle S (2002) Crystal structure of parallel quadruplexes from human telomeric DNA. Nature 417:876-880

Patrick MH, Snow JM (1977) Studies on thymine-derived UV photoproducts in DNA--II. A comparative analysis of damage caused by 254 nm irradiation and triplet-state photosensitization. Photochem Photobiol 25:373-384

Petrini S, Tessa A, Stallcup WB, Sabatelli P, Pescatori M, Giusti B, Carrozzo R, Verardo M, Bergamin N, Columbaro M, Bernardini C, Merlini L, Pepe G, Bonaldo P, Bertini E (2005) Altered expression of the MCSP/NG2 chondroitin sulfate proteoglycan in collagen VI deficiency. Mol Cell Neurosci 30:408-417

Phillips K, Dauter Z, Murchie AI, Lilley DM, Luisi B (1997) The crystal structure of a parallel-stranded guanine tetraplex at 0.95 A resolution. J Mol Biol 273:171-182

Rabl C (1885) Uber Zelltheilung. *Morphol. Jahrbuch* 10, pp. 214–330.

Raymond E, Soria JC, Izbicka E, Boussin F, Hurley L, Von Hoff DD (2000) DNA G-quadruplexes, telomere-specific proteins and telomere-associated enzymes as potential targets for new anticancer drugs. Invest New Drugs 18:123-137

Renzing J, Hansen S, Lane DP (1996) Oxidative stress is involved in the UV activation of p53. J Cell Sci 109 (Pt 5):1105-1112

Rosenberger S, Thorey IS, Werner S, Boukamp P (2007) A novel regulator of telomerase. S100A8 mediates differentiation-dependent and calcium-induced inhibition of telomerase activity in the human epidermal keratinocyte line HaCaT. J Biol Chem 282:6126-6135

Rota M, LeCapitaine N, Hosoda T, Boni A, De AA, Padin-Iruegas ME, Esposito G, Vitale S, Urbanek K, Casarsa C, Giorgio M, Luscher TF, Pelicci PG, Anversa P, Leri A, Kajstura J (2006) Diabetes promotes cardiac stem cell aging and heart failure, which are prevented by deletion of the p66shc gene. Circ Res 99:42-52

Rufer N, Brummendorf TH, Kolvraa S, Bischoff C, Christensen K, Wadsworth L, Schulzer M, Lansdorp PM (1999) Telomere fluorescence measurements in granulocytes and T lymphocyte subsets point to a high turnover of hematopoietic stem cells and memory T cells in early childhood. J Exp Med 190:157-167

Rus V, Via CS (2001) Telomeres, telomerase, and lupus: the long and short of it. Clin Immunol 99:195-197

Sansone P, Storci G, Giovannini C, Pandolfi S, Pianetti S, Taffurelli M, Santini D, Ceccarelli C, Chieco P, Bonafe M (2007) p66Shc/Notch-3 interplay controls self-renewal

and hypoxia survival in human stem/progenitor cells of the mammary gland expanded in vitro as mammospheres. Stem Cells 25:807-815

Scherthan H (2001) A bouquet makes ends meet. Nat Rev Mol Cell Biol 2:621-627

Schultz LB, Chehab NH, Malikzay A, Halazonetis TD (2000) p53 binding protein 1 (53BP1) is an early participant in the cellular response to DNA double-strand breaks. J Cell Biol 151:1381-1390

Shay JW, Wright WE (2005) Senescence and immortalization: role of telomeres and telomerase. Carcinogenesis 26:867-874

Slack JM (2000) Stem cells in epithelial tissues. Science 287:1431-1433

Slagboom PE, Droog S, Boomsma DI (1994) Genetic determination of telomere size in humans: a twin study of three age groups. Am J Hum Genet 55:876-882

Smith FW, Feigon J (1992) Quadruplex structure of Oxytricha telomeric DNA oligonucleotides. Nature 356:164-168

Stark HJ, Boehnke K, Mirancea N, Willhauck MJ, Pavesio A, Fusenig NE, Boukamp P (2006) Epidermal homeostasis in long-term scaffold-enforced skin equivalents. J Investig Dermatol Symp Proc 11:93-105

Stephens P, Cook H, Hilton J, Jones CJ, Haughton MF, Wyllie FS, Skinner JW, Harding KG, Kipling D, Thomas DW (2003) An analysis of replicative senescence in dermal fibroblasts derived from chronic leg wounds predicts that telomerase therapy would fail to reverse their disease-specific cellular and proteolytic phenotype. Exp Cell Res 283:22-35

Sugimoto M, Yamashita R, Ueda M (2006) Telomere length of the skin in association with chronological aging and photoaging. J Dermatol Sci 43:43-47

Takai H, Smogorzewska A, de Lange T (2003) DNA damage foci at dysfunctional telomeres. Curr Biol 13:1549-1556

Taylor RS, Ramirez RD, Ogoshi M, Chaffins M, Piatyszek MA, Shay JW (1996) Detection of telomerase activity in malignant and nonmalignant skin conditions. J Invest Dermatol 106:759-765

Tumbar T, Guasch G, Greco V, Blanpain C, Lowry WE, Rendl M, Fuchs E (2004) Defining the epithelial stem cell niche in skin. Science 303:359-363

Van Ziffle JA, Baerlocher GM, Lansdorp PM (2003) Telomere length in subpopulations of human hematopoietic cells. Stem Cells 21:654-660

van Steensel B, Smogorzewska A, de Lange T (1998) TRF2 protects human telomeres from end-to-end fusions. Cell 92:401-413

Vaziri H, Dragowska W, Allsopp RC, Thomas TE, Harley CB, Lansdorp PM (1994) Evidence for a mitotic clock in human hematopoietic stem cells: loss of telomeric DNA with age. Proc Natl Acad Sci U S A 91:9857-9860

Venkatesan RN, Price C (1998) Telomerase expression in chickens: constitutive activity in somatic tissues and down-regulation in culture. Proc Natl Acad Sci U S A 95:14763-14768

Vink AA, Roza L (2001) Biological consequences of cyclobutane pyrimidine dimers. J Photochem Photobiol B 65:101-104

von Zglinicki T, Saretzki G, Docke W, Lotze C (1995) Mild hyperoxia shortens telomeres and inhibits proliferation of fibroblasts: a model for senescence? Exp Cell Res 220:186-193

von Zglinicki T, Serra V, Lorenz M, Saretzki G, Lenzen-Grossimlighaus R, Gessner R, Risch A, Steinhagen-Thiessen E (2000) Short telomeres in patients with vascular dementia: an indicator of low antioxidative capacity and a possible risk factor? Lab Invest 80:1739-1747

Vourc'h C, Taruscio D, Boyle AL, Ward DC (1993) Cell cycle-dependent distribution of telomeres, centromeres, and chromosome-specific subsatellite domains in the interphase nucleus of mouse lymphocytes. Exp Cell Res 205:142-151

Wan TS, Martens UM, Poon SS, Tsao SW, Chan LC, Lansdorp PM (1999) Absence or low number of telomere repeats at junctions of dicentric chromosomes. Genes Chromosomes Cancer 24:83-86

Ward IM, Minn K, Jorda KG, Chen J (2003) Accumulation of checkpoint protein 53BP1 at DNA breaks involves its binding to phosphorylated histone H2AX. J Biol Chem 278:19579-19582

Watson JD (1972) Origin of concatemeric T7 DNA. Nat New Biol 239:197-201

Watt FM (2002) The stem cell compartment in human interfollicular epidermis. J Dermatol Sci 28:173-180

Webb A, Li A, Kaur P (2004) Location and phenotype of human adult keratinocyte stem cells of the skin. Differentiation 72:387-395

Weierich C, Brero A, Stein S, von HJ, Cremer C, Cremer T, Solovei I (2003) Three-dimensional arrangements of centromeres and telomeres in nuclei of human and murine lymphocytes. Chromosome Res 11:485-502

Weng NP, Levine BL, June CH, Hodes RJ (1995) Human naive and memory T lymphocytes differ in telomeric length and replicative potential. Proc Natl Acad Sci U S A 92:11091-11094

Weng NP (2002) Regulation of telomerase expression in human lymphocytes. Springer Semin Immunopathol 24:23-33

Wlaschek M, Scharffetter-Kochanek K (2005) Oxidative stress in chronic venous leg ulcers. Wound Repair Regen 13:452-461

ya-Grosjean L, Dumaz N, Sarasin A (1995) The specificity of p53 mutation spectra in sunlight induced human cancers. J Photochem Photobiol B 28:115-124

Yanez GH, Khan SJ, Locovei AM, Pedroso IM, Fletcher TM (2005) DNA structure-dependent recruitment of telomeric proteins to single-stranded/double-stranded DNA junctions. Biochem Biophys Res Commun 328:49-56

Yokoyama Y, Takahashi Y, Shinohara A, Lian Z, Xiaoyun W, Niwa K, Tamaya T (1998) Telomerase activity is found in the epithelial cells but not in the stromal cells in human endometrial cell culture. Mol Hum Reprod 4:985-989

Yui J, Chiu CP, Lansdorp PM (1998) Telomerase activity in candidate stem cells from fetal liver and adult bone marrow. Blood 91:3255-3262

Zalensky AO, Allen MJ, Kobayashi A, Zalenskaya IA, Balhorn R, Bradbury EM (1995) Well-defined genome architecture in the human sperm nucleus. Chromosoma 103:577-590

Zhan Q, Carrier F, Fornace AJ, Jr. (1993) Induction of cellular p53 activity by DNA-damaging agents and growth arrest. Mol Cell Biol 13:4242-4250

6. Addendum

6. Addendum

Publications

Ermler S*, **Krunic D***, Knoch TA, Moshir S, Mai S, Greulich-Bode KM, Boukamp P (2004) Cell cycle-dependent 3D distribution of telomeres and telomere repeat-binding factor 2 (TRF2) in HaCaT and HaCaT-myc cells. Eur J Cell Biol 83:681-690

Boukamp P, Popp S, **Krunic D** (2005) Telomere-dependent chromosomal instability. J Investig Dermatol Symp Proc 10:89-94

Falkowska-Hansen B, Falkowski M, Metharom P, **Krunic D**, Goerdt S (2007) Clathrin-coated vesicles form a unique net-like structure in liver sinusoidal endothelial cells by assembling along undisrupted microtubules. Exp Cell Res 313:1745-1757

Krunic D*, Moshir S*, Greulich-Bode KM, Figueroa R, Cerezo A, Stammer H, Stark HJ, Gray SG, Vang Nielsen K, Hartschuh W, and Boukamp P Tissue context-regulated telomerase activity in human epidermis minimizes/counteracts age-dependent telomere loss.
Aging Cell – in revision

* Equal contribution

Age-dependent and genetic aspects of telomere length regulation

Damir Krunic, Karin M. Greulich-Bode, Sharareh Moshir, and Petra Boukamp

DKFZ, Dept. Genetics of Skin Carcinogenesis

Introduction:

Telomeres the ends of the chromosomes consist of (TTAGGG)n repeats and associated proteins and – due to loss of a number of repeats with each replication, the end-replication problem – are looked upon as the "mitotic clock" of cellular aging. When telomeres reach a critical length, cells stop to proliferate and senesce. Thus, telomeres are proposed to be key players in aging.

We were interested in investigating regulatory mechanisms which influence telomere length.

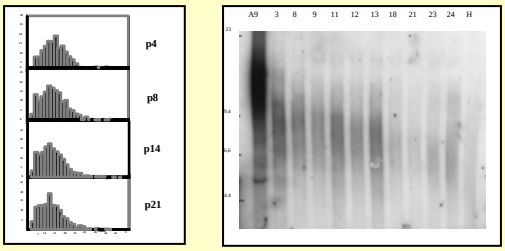

Figure 1: Q-FISH (left) and Southern blot (right) analysis revealed a decline in telomere length *in vitro* in fibroblasts from a juvenile donor due to the end replication problem, to the lack of telomerase and possibly additional mechanisms.

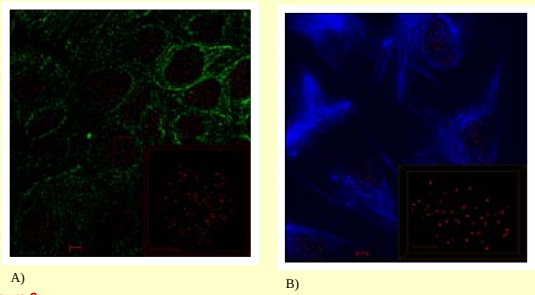

A) B)

C)

D)

Figure 2:
Combined IHC and FISH analysis displayed by 3D-reconstructed images of:
(A) in vitro cultured telomerase positive, immortal HaCaT cells,
(B) In vitro cultured primary telomerase negative fibroblasts,
(C+ D) cryosections of human skin from a young (C) (age 25) and an old (age 71) (D) donor.
NOTE: Telomeric DNA is shown in red, keratin in green and vimentin in blue.

Skin from:	Cell tipe	Telomere size / kb
7 years old mail	Keratinocytes	12.3
	Fibroblasts	13.2
25 years old mail	Keratinocytes	9.3
	Fibroblasts	9.6
71 years old mail	Keratinocytes	8.7
	Fibroblasts	10.8
86 years old femail	Keratinocytes	8.4
	Fibroblasts	11.2
Fibroblasts VH7 p 14		7.5
HaCaT myc		4.5

Table 1: 3D FISH telomere length (e.g. signal intensity) measurments displayed no significant telomere shortening in fibroblasts in old vs. young donors, while a significant decline was observed in keratinocytes within the same skin sections.
Immortalised HaCaT cells (telomere length constant ~ 4kb) and fibroblasts (p. 14, telomere length 7.5 kb) were used as controls.

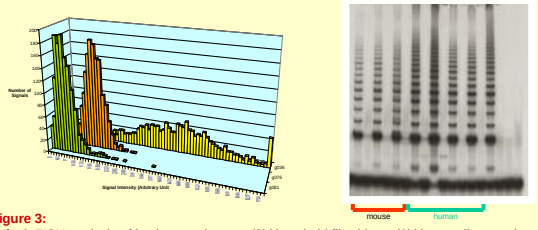

Figure 3:
Left: Q-FISH analysis of in vitro aged young (9kb) and old fibroblasts (6kb) as well as murine A9 cells (9-23kb): Murine cells in general have larger telomeres than human cells.
Right: TRAP assay of the parental A9 cells, A9 + chromosomes 15 or 3 respectively and the SCL cell lines, where these chromosomes were re-introduced: All cultured cells are telomerase positive (control: telomerase negative fibroblasts)

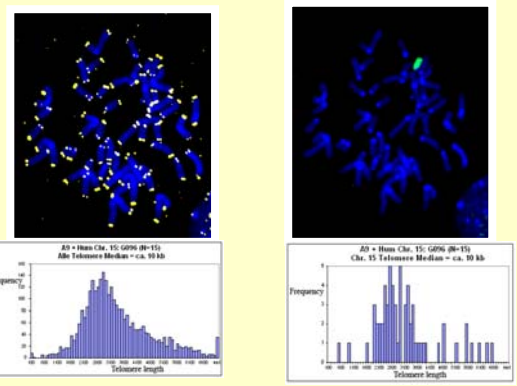

Figure 4:
Left: Metaphase spread of an A9 + human chromosome 15 cell hybridized with a CY3 labeled telomeric PNA probe.
Right: Image of the same metaphase after rehybridization with a spectrum green labeled human chromosome 15q probe.
Note that the telomere length in both cases is approx. 10kb

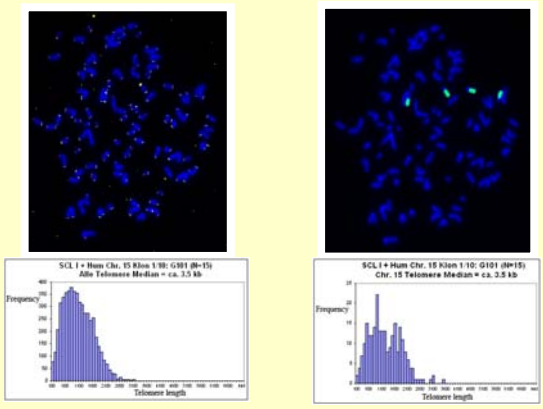

Figure 5:
Left: Metaphase spread of a SCL I + human chromosome 15 cell (clone 1/10) hybridized with a CY3 labeled telomeric PNA probe.
Right: Image of the same metaphase after rehybridization with a spectrum green labeled human chromosome 15q probe.
Note: Telomere length is in both cases approximately 3.5kb

	Chromosome 3 experiments		Chromosome 15 experiments	
Cell population	Telomere length population	Telomere length human Chr. 3	Telomere length population	Telomere length human Chr. 15
A9 (murine only)	11.24 kb		9.12 kb	
A9 + 3	11.13 kb	7.82 kb		
A9 + 15			10.12 kb	9.47 kb
SCL II + 3 (6/7)	5.14 kb	5.02 kb		
SCL II + 3 (4/7)	2.0 kb	3.12 kb		
SCL I + 15 (1/10)			3.16 kb	3.64 kb
SCL I + 15 (2/9)			3.93 kb	3.60 kb
Dipl. HaCaT	4 kb	3.57 kb	4 kb	3.67 kb

Table 2:
Telomere length analysis (Q-FISH) in hybrid cell lines and carcinoma cell lines containing additional human chromosomes 3 or 15, respectively. Diploid HaCaT cells served as standard for quantification purposes.
Note that the introduced chromosome quickly adapted to the mean telomere length of the host cells.

Results:

Our experiments revealed that there are several aspects that influence telomere length:

1) age-dependent (and proliferation-dependant) factors (*in vitro* and *in vivo*)
2) telomerase-activity (fibroblasts vs. HaCaT keratinocytes)
3) genetic, non-telomerase-dependant factors (A9 + human chromosome)
4) tissue specific aspects (3D FISH in skin sections)

Conclusion:

Taken together, all this demonstrates that telomere length regulation is a complex process, which is dependant on at least four different mechanisms. The 3D FISH investigations made it possible to study telomere length regulation *in situ* in resting cells as well as in tissue, which will lead to a better understanding of telomere length regulation *in vivo*.

Age-dependent aspects of telomere length regulation

Damir Krunic, Karin M. Greulich-Bode, Sharareh Moshir, and Petra Boukamp

DKFZ, Dept. Genetics of Skin Carcinogenesis

Introduction:

Telomeres, the ends of the chromosomes consist of (TTAGGG)n repeats and associated proteins. Due to loss of telomeric repeats with each replication (end-replication problem) telomere loss is thought to be the "mitotic clock" of cellular aging. When telomeres reach a critical length, cells stop to proliferate and senesce. Thus, telomeres are proposed to be key players in aging.
We have shown earlier that different from fibroblasts, human skin keratinocytes express telomerase. Thus, we aimed to determine how aging would effect telomere length in keratinocytes.

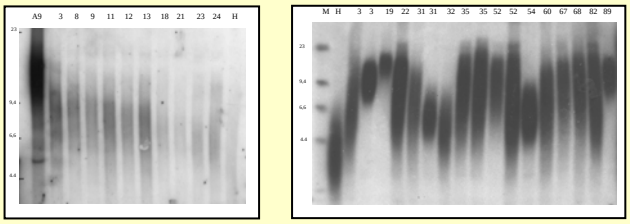

Figure 1: Southern blot analysis revealed a decline in telomere length *in vitro* in fibroblasts from a juvenile donor due to the end replication problem (left). Similar decline was not observed in keratinocytes from different aged individuals (right).

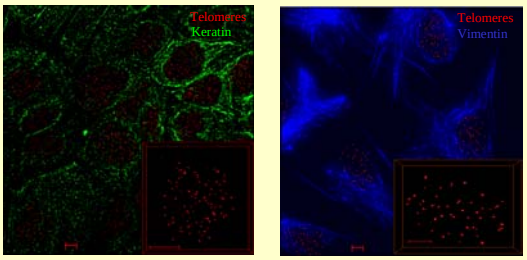

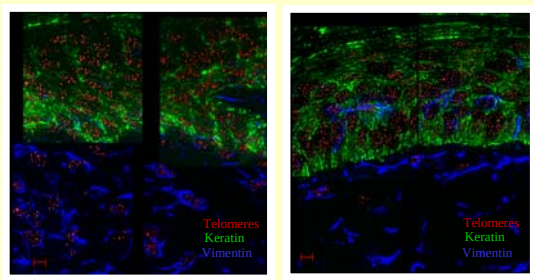

Figure 2:
Combined IHC and FISH analysis displayed by 3D-reconstructed images of:
(A) in vitro cultured telomerase positive, immortal HaCaT cells,
(B) In vitro cultured primary telomerase negative fibroblasts,
(C+ D) cryosections of human skin from a young (C) (age 25) and an old (age 71) (D) donor.

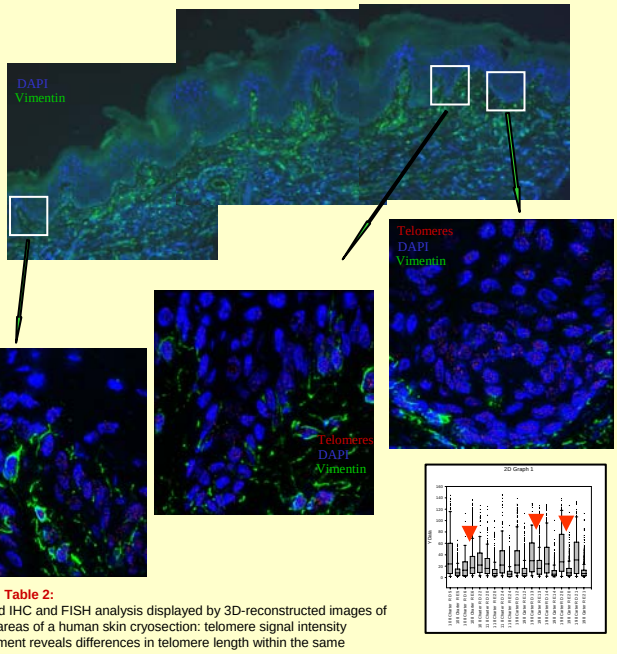

Figure 4; Table 2:
Combined IHC and FISH analysis displayed by 3D-reconstructed images of different areas of a human skin cryosection: telomere signal intensity measurement reveals differences in telomere length within the same epidermis.

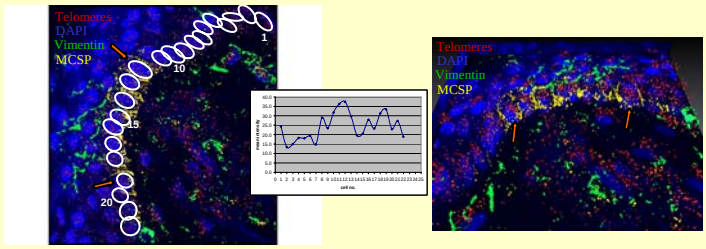

Figure 5: 3D FISH telomere length (signall intensity) measurement displayed differences within the basal layer of epidermis;
- telomere length varies from relatively short to very long
- cells with longest telomeres are among those also stained positive for MCSP (melanoma-associated chondroitin sulfate proteoglycan) a potential epidermal stam cell marker
- cells with shortest telomeres are outside of the "stem cell compartment". Short telomeres can be potentially hazardous as telomere length is important for genomic stability.

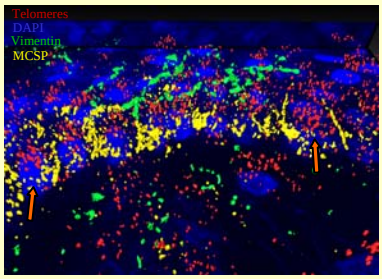

Age (years)	Mean telomere length epidermis (kb)	Mean telomere length dermis (kb)
2	10.0	11.6
7	8.7	9.8
25	8.5	8.9
49	7.2	7.7
31	6.8	8.5
31	8.3	8.7
43	6.3	8.6
41	7.5	8.1
50	8.2	8.1
71	8.6	10.8
81	8.1	9.4
86	5.7	8

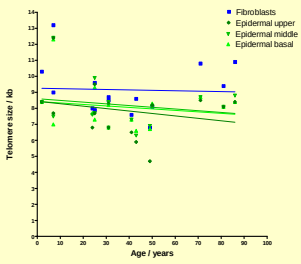

Table 1; Figure 3: 3D FISH telomere length (signal intensity) measurements displayed no significant telomere shortening in fibroblasts in old vs. young donors, while a certain decline was observed in keratinocytes in the same samples. Telomere length did not significantly differ from basal to suprabasal layers of the skin.
Immortalised HaCaT cells (4kb) and fibroblasts (p. 14, telomere length 7.5 kb) were used as controls.

Results:

Telomere length measurement in skin reveals that :
1) Dermal fibroblasts *in situ* show hardly any telomere shortening.
2) Kerationcytes do shorten but this decline is not statistically significant.
3) Telomere length is not shortened during differentiation.
4) However, telomere length varies at different sites.
5) Telomere length varies within the basal layer of the skin.
6) Cells with longest telomeres are within those group of cells stained positive for MCSP - a potential epidermal stam cell marker.

Conclusion:

We here show for the first time that 3D-reconstruction and measurement enabled us to get insight in telomere distribution and length *in situ.*
Additionally, since telomere length is well excepted as a marker for the "mitotic clock" of cells, this opens the opportunity for using our technique to identify the cells with particularly long telomeres, the potential epidermal stem cells.

Telomere length regulation in human skin

Damir Krunic*, Sharareh Moshir*, Charlotte Proby**, and Petra Boukamp*
*German Cancer Research Center, Dept. Genetics of Skin Carcinogenesis
** Centre for Cutaneous Research, London, UK

The Role of Telomeres and Telomerase in Cancer Research
December 6 - 9, 2007
San Francisco, California

Introduction:

Human skin is a tissue of major interest for aging research because the aging phenotype becomes easily detected by changes in texture (wrinkles) and whitening of the hair. Thus, various compounds are designed, to hinder or at least minimize the aging process, although the reason for these changes and the molecular details are still poorly understood. It is suggested that replication-dependent telomere loss contributes to the aging process because skin aging is associated with telomere loss. However, the epidermal keratinocytes are telomerase-positive and, therefore, should be protected against replication-dependent telomere loss. The dermal fibroblasts only proliferate rarely and, therefore, should also not suffer from major age-dependent telomere attrition. To test this hypothesis, we established *in situ* measurement of telomere length in interphase skin cells – *in situ* IQ-FISH, which is based on 3D deconvolution microscopy and immune labeling of different skin compartments.

Results:

Telomere length (TL) measurement in skin reveals that :

1) Age-dependent telomere decline is minimal in keratinocytes, fibroblasts and melanocytes.
2) Epidermal differentiation does not contribute to telomere decline.
3) Telomere length in skin can vary strongly between different sites of the same individual.
4) Accelerated telomere loss is seen in skin from chronically sun-exposed individuals.
5) Accelerated telomere loss can occur in discrete areas of epidermis.
6) Accelerated telomere loss strongly correlates with p53 and 53BP1 expression.
7) Acute UVA/UVB radiation causes telomere shortening in the skin.

Conclusion:

Taken together, this *in situ* study demonstrates that is not the life-long regeneration, and with that the age-dependent telomere loss that is deleterious for the skin. Instead, physical damage (UV radiation) can cause small areas of critically short telomeres that are likely susceptible to other insults. Since telomere shortening in those areas correlates with signs of "genomic instability" – p53 and 53BP1 – it may well contribute to early stages in skin cancer development.

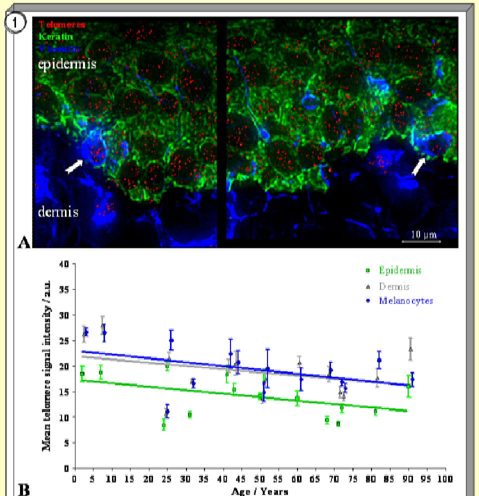

Figure 1: Minimal age-dependent decline determined by *in situ* IQ-FISH. A) Human skin section stained for keratin (epidermal keratinocytes, green), vimentin (fibroblasts in the dermis and melanocytes marked with arrows, blue) and telomeres, hybridized with a telomere-specific PNA probe (DAKO) (red). B) Graphic presentation of the mean telomere signal intensities of keratinocytes (green), melanocytes (blue), and dermal fibroblasts (grey) in skins from different-age donors. Note the minimal age-related telomere length decline in all cell types and generally shorter telomeres in the proliferating keratinocytes than in the non-proliferating melanocytes or dermal fibroblasts.

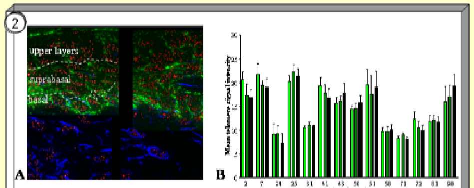

Figure 2: Epidermal differentiation does not contribute to telomere loss. A) Human skin stained for keratin (epidermis in green), vimentin (dermis in blue) and telomeres (telomere-specific PNA probe in red). The epidermis is divided by dotted lines into basal, suprabasal, and upper layers (as indicated). B) Graphic presentation of the mean telomere signal intensities and standard error of the mean in basal (light green), suprabasal (dark green), and upper layers (black) of the epidermis of different age donors.

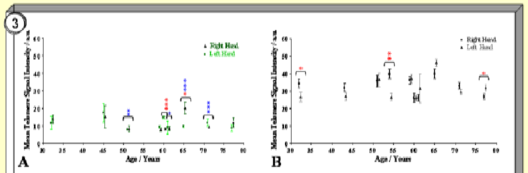

Figure 3: Intra-personal telomere length variations. Graphic presentation of the mean telomere signal intensities in skin samples from the upper part of the right and left hand of: A) epidermal keratinocytes and B) dermal fibroblasts. Note that the differences between telomere lengths (signal intensities) in samples from the left and right hand of the same donor can be statistically significant (*p=0.05, **p=0.01, ***p=0.001, *different variances – F test, *different length – T test). Donor age is indicated in the X-axis.

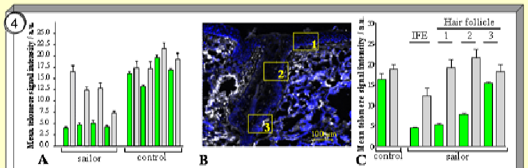

Figure 4: Chronic sun exposure can cause telomere shortening. : A) Graphic presentation of telomere signal intensities in sections from skin derived from a sailor and from the buttock of a 44 y-old control donor (epidermal keratinocytes in green and dermal fibroblasts in grey) in 4 different areas. Note the shorter telomeres in different areas of the sailor's epidermis B) Skin from the sailor showing a hair follicle (vimentin in grey, nuclei in blue). The numbered boxes mark the three areas measured for telomere signal intensities. C) Telomere signal intensities in control skin, the interfollicular epidermis and the three areas (1 to 3) of the sailor's hair follicle indicated in B.

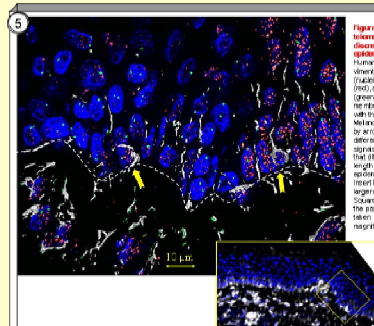

Figure 4: Accelerated telomere erosion in discrete area of human epidermis. Human skin stained for vimentin (gray), DAPI (nuclei in blue), telomeres (red), and centromeres (green). The basement membrane zone is indicated with the white dashed line. Melanocytes are pointed out by arrows. Note the extreme difference in telomere signals in the two areas and that differences in telomere length are restricted on epidermal keratinocytes. Insert below right shows the larger region of the skin. Square on the insert shows the position of the image taken at higher magnification.

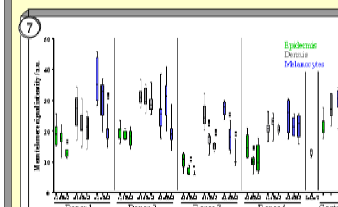

Figure 5: Acute UVA/UVB irradiation causes telomere shortening. In four representative donors mean telomere signal intensity was measured in keratinocytes, dermal fibroblasts, and in melanocytes. Days after irradiation are indicated as d1, d2, d3. Note the significance of telomere shortening day 2 or 3 when compared to day 1 (*) after irradiation. HaCaT cell line with telomere length of 4 kb, and sun protected human skin (~8 kb) were used as controls. (Non-paired t test, *p<0.05, **p<0.01, ***p<0.001)

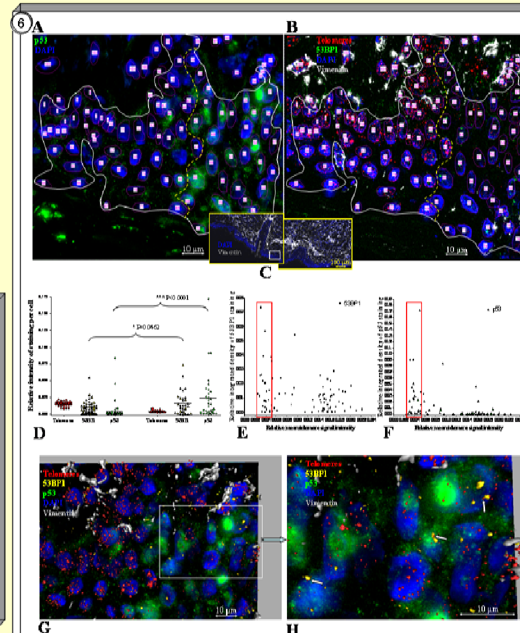

Figure 7: Correlation of accelerated telomere erosion with p53 and 53BP1.
A) p53 stained region (pseudo colored in green) of the epidermis with an accelerated telomere erosion B) The same skin section is re-stained for telomeres (red), 53BP1 (green foci), vimentin (dermal fibroblasts and all non-keratinocytes in gray), and DAPI (nuclei in blue). White line marks those keratinocytes that were further analyzed. The yellow dotted line separates the two groups of cells: those with normal telomere length (left side) and those with short telomeres (right side). C) Low magnification (10x objective) of the analyzed skin. The marked area indicates the position of the p53 stained region with short telomeres from A) and B). D) Dot plot of the quantified telomeres, p53, and 53BP1 staining intensities. Each dot represents one nucleus from A) and B). The left side of the plot represents cells with longer telomeres, significantly less 53BP1 foci, and much weaker p53 expression (on the left side of the image A) and B) also) when compared with cells from the right side of the plot (Mann Whitney test determined significance for the difference between medians) E) Dot plot representing the correlation of telomere and 53BP1 staining, and F) telomere and p53 staining. Note that the cells with shortest telomeres (marked with the red rectangle) are the ones with strongest 53BP1 foci and p53 expression. G) 3D visualization of the region with accelerated telomere shortening; telomeres (red), 53BP1 (yellow) and vimentin (gray) are visualized in 3D in front of projected image of p53 staining (green), and DAPI (blue). White rectangle indicates the region presented at higher magnification in image H) showing that the strong 53BP1 foci co-localize with the short telomeres (marked with white arrows).

3nd European workshop on:

Role of Telomeres and Telomerase in Cancer and Aging

Ladenburg, Germany 21.-23.11.2004

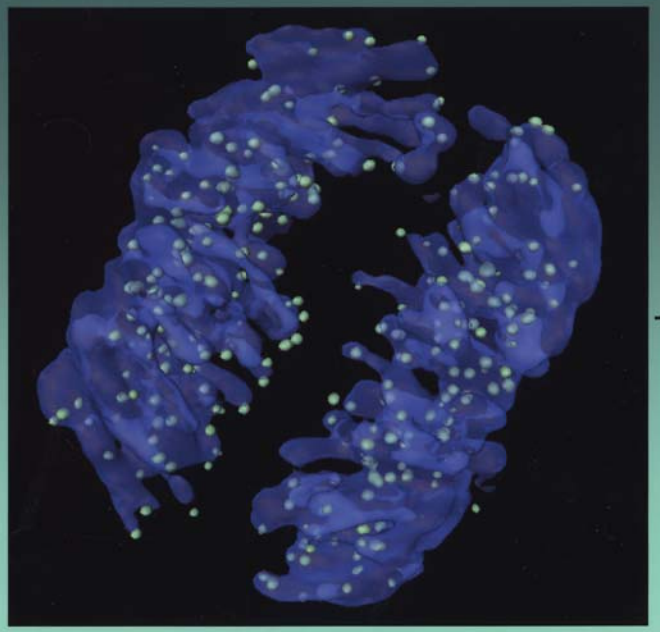

Organization:
Petra Boukamp,
DKFZ Heidelberg, Germany

Sponsored by:
Boehringer Ingelheim Stiftung